

# **RCA REVIEW**

*a technical journal*

**RADIO AND ELECTRONICS  
RESEARCH • ENGINEERING**

**VOLUME XVII**

**DECEMBER 1956**

**NO. 4**

RADIO CORPORATION OF AMERICA

DAVID SARNOFF, *Chairman of the Board*

FRANK M. FOLSOM, *President*

E. W. ENGSTROM, *Senior Executive Vice-President*

JOHN Q. CANNON, *Secretary*

ERNEST B. GORIN, *Vice-President and Treasurer*

---

RCA LABORATORIES

DOUGLAS H. EWING, *Vice-President*

---

RCA REVIEW

C. C. FOSTER, *Manager*

C. H. VOSE, *Business Manager*

PRINTED IN U.S.A.

RCA REVIEW, published quarterly in March, June, September, and December by RCA Laboratories, Radio Corporation of America, Princeton, New Jersey. Entered as second class matter July 3, 1950 at the Post Office at Princeton, New Jersey, under the act of March 3, 1879. Subscription price in the United States and Canada; one year \$2.00, two years \$3.50 three years \$4.50; in other countries: one year \$2.40, two years \$4.30, three years \$5.70. Single copies in the United States, \$.75; in other countries, \$.85.

# RCA REVIEW

*a technical journal*

RADIO AND ELECTRONICS  
RESEARCH • ENGINEERING

*Published quarterly by*

RCA LABORATORIES

*in cooperation with all subsidiaries and divisions of*

RADIO CORPORATION OF AMERICA

---

---

VOLUME XVII

DECEMBER, 1956

NUMBER 4

---

## CONTENTS

|   | PAGE |
|---|------|
| Reduction of Co-Channel Television Interference by Precise Frequency Control of Television Picture Carriers ..... | 443  |
| W. L. BEHREND   |      |
| A Miniature Vidicon of High Sensitivity .....   | 460  |
| A. D. COPE  |      |
| Transistorized Television Cameras Using the Miniature Vidicon ....  | 469  |
| L. E. FLORY, G. W. GRAY, J. M. MORGAN, AND W. S. PIKE   |      |
| Viewing Storage Tubes for Large Displays .....  | 503  |
| H. O. HOOK, M. KNOLL, AND R. P. STONE   |      |
| The Apparent Contact Potential of a Pseudo-Abrupt P-N Junction ..   | 515  |
| H. KROEMER  |      |
| Bigradient Uniaxial Microphone .....  | 522  |
| H. F. OLSON, J. PRESTON, AND J. C. BLEAZEY  |      |
| Analytical Approaches to Local Oscillator Stabilization .....   | 534  |
| W. Y. PAN AND D. J. CARLSON   |      |
| Test Signal for Measuring "On-The-Air" Color-Television System Performance .....                                  | 553  |
| R. C. KENNEDY   |      |
| A Video Automatic-Gain-Control Amplifier .....  | 558  |
| J. O. SCHROEDER   |      |
| A method of Predicting the Coverage of a Television Station .....   | 571  |
| D. W. PETERSON AND J. EPSTEIN   |      |
| RCA TECHNICAL PAPERS .....  | 583  |
| AUTHORS .....   | 585  |
| INDEX, VOLUME XVII (1956) .....   | 589  |

---

© 1956 by Radio Corporation of America  
All rights reserved

---

RCA REVIEW is regularly abstracted and indexed by *Industrial Arts Index Science Abstracts* (I.E.E.-Brit.), *Electronic Engineering Master Index*, *Chemical Abstracts*, *Proc. I.R.E.*, and *Wireless Engineer*.

# RCA REVIEW

## BOARD OF EDITORS

*Chairman*

R. S. HOLMES  
*RCA Laboratories*

M. C. BATSEL  
*Defense Electronic Products*

G. L. BEERS  
*Radio Corporation of America*

H. H. BEVERAGE  
*RCA Laboratories*

G. H. BROWN  
*RCA Laboratories*

I. F. BYRNES  
*Commercial Electronic Products*

D. D. COLE  
*RCA Victor Television Division*

O. E. DUNLAP, JR.  
*Radio Corporation of America*

E. W. ENGSTROM  
*Radio Corporation of America*

D. H. EWING  
*RCA Laboratories*

A. N. GOLDSMITH  
*Consulting Engineer, RCA*

A. L. HAMMERSCHMIDT  
*National Broadcasting Company, Inc.*

O. B. HANSON  
*Radio Corporation of America*

E. W. HEROLD  
*RCA Laboratories*

J. HILLIER  
*Commercial Electronic Products*

C. B. JOLLIFFE  
*Radio Corporation of America*

E. A. LAPORT  
*Radio Corporation of America*

C. W. LATIMER  
*RCA Communications, Inc.*

H. W. LEVERENZ  
*RCA Laboratories*

G. F. MAEDEL  
*RCA Institutes, Inc.*

L. MALTER  
*Semiconductor Division*

H. F. OLSON  
*RCA Laboratories*

D. S. RAU  
*RCA Communications, Inc.*

D. F. SCHMIT  
*Radio Corporation of America*

S. W. SEELEY  
*RCA Laboratories*

G. R. SHAW  
*Tube Division*

L. A. SHOTLIFF  
*RCA International Division*

A. W. VANCE  
*RCA Laboratories*

I. WOLFF  
*RCA Laboratories*

*Secretary*

C. C. FOSTER  
*RCA Laboratories*

---

### REPUBLICATION AND TRANSLATION

Original papers published herein may be referenced or abstracted without further authorization provided proper notation concerning authors and source is included. All rights of republication, including translation into foreign languages, are reserved by RCA Review. Requests for republication and translation privileges should be addressed to *The Manager*.

# REDUCTION OF CO-CHANNEL TELEVISION INTERFERENCE BY PRECISE FREQUENCY CONTROL OF TELEVISION PICTURE CARRIERS

BY

W. L. BEHREND

RCA Laboratories,  
Princeton, N. J.

*Summary*—The visibility of co-channel interference has maxima and minima at carrier offset frequencies which are multiples of frame frequency. Subjective tests at RCA Laboratories determined the reduction in visibility of co-channel interference which might be achieved by precise carrier frequency control and established the stability requirements on the carrier frequency.

Precise-frequency sources have been developed which are believed adequate for the requirements. Experimental equipment was installed at WRCA-TV (New York) and WRC-TV (Washington, D. C.). Field tests were conducted to verify the laboratory relationships previously obtained.

\* \* \* \* \*

OFFSET-CARRIER operation of television stations to reduce co-channel interference has been in use for a number of years. An observer of co-channel interference views the desired picture through a superimposed pattern of regularly spaced horizontal bars of light and shade. The spacing of the bars corresponds to the difference frequency of the two picture carriers. The visibility of the bars as a function of the difference frequency varies in a cyclical manner with alternating minima and maxima having a separation of 30 cycles. This is illustrated in Figure 1, which is taken from a paper by Fredendall;<sup>1</sup> the curve is only an illustrative sketch. One can see that in addition to the rapid variations of visibility, the minima are a function of the horizontal line frequency, with the least minima occurring at approximately odd multiples of half horizontal line frequency.

An allocation plan for television stations cannot utilize the optimum offsets corresponding to the least minima since two stations in a group of three stations would be offset by an even multiple of half line frequency; this results in maximum interference. However, stations may be offset by approximately 10 kilocycles with approximately equal, though somewhat reduced, benefit to each. The offset of 10

<sup>1</sup> G. L. Fredendall, "A Comparison of Monochrome and Color Television with Reference to Susceptibility to Various Types of Interference," *RCA Review*, Vol. XIV, p. 346, September, 1953.

kilocycles adopted by the Federal Communications Commission was not specified with a view of taking advantage of one of the minima near 10 kilocycles. In fact, the data<sup>2</sup> taken at that time to determine the offset frequency and tolerable ratios for an allocation plan was intentionally taken at one of the points of maximum visibility near 10.5 kilocycles. This was considered desirable because broadcast crystals used at that time did not have the required stability for holding the frequency offset within a few cycles of the optimum. At present, the FCC rules specify a carrier frequency accuracy of  $\pm 1,000$  cycles.

Recent developments in crystal techniques and oscillator circuits have been such that it appeared desirable to investigate the reduction

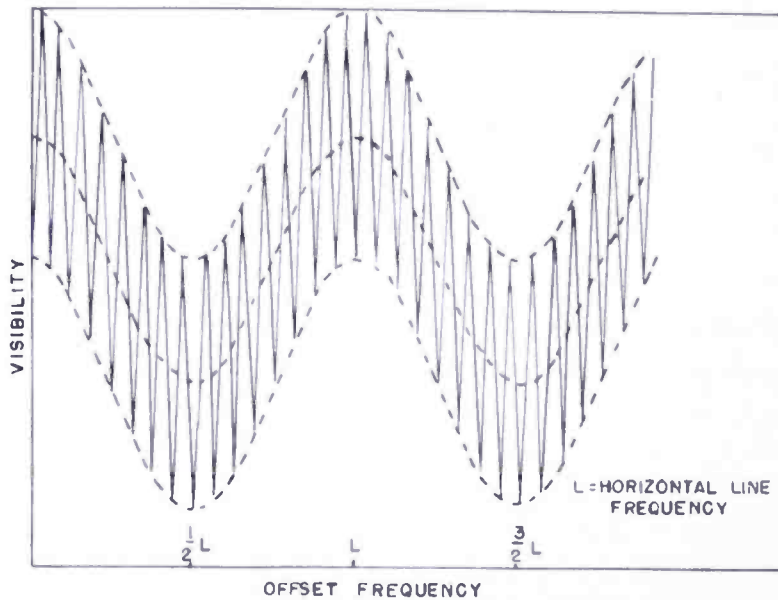


Fig. 1—Visibility of co-channel interference as a function of the offset frequency.

in the visibility of co-channel interference which would be possible by the use of precise picture carrier frequency control; that is, to take advantage of one of the minima near 10 kilocycles.

It was known that the minima of visibility occurred when the frequency difference between the carriers was an even multiple of the frame frequency. Since the frame frequency of color television is 29.97 cycles, a multiplier of 334 yields 10,010 cycles as an appropriate offset frequency. The solid curve of Figure 2 shows the results of subjective tests made for offset frequencies around 10,010 cycles.

<sup>2</sup> RCA Laboratories Division, "A Study of Co-Channel and Adjacent-Channel Interference of Television Signals, Part I," *RCA Review*, Vol. XI, p. 99, March, 1950.

The data shown is what an average observer considered a tolerable ratio of the desired carrier to the undesired carrier, in decibels, as a function of the offset frequency. A minimum tolerable ratio of 21 decibels is obtained at 10,010 cycles, and a maximum of 33 decibels at 10,035 cycles; thus there is an improvement of 12 decibels. An inspection of the minimum shows that a  $\pm 5$ -cycle variation in the offset frequency would have little effect on the tolerable ratio.

If three stations were operating on the same channel, station A would be assigned a carrier frequency  $F_0$ , station B might be assigned a frequency  $F_0 - 10,010$ , while station C might be assigned a frequency  $F_0 + 10,010$ . Then stations B and C would differ in frequency by 20,020 cycles. This frequency difference is also an even multiple of frame frequency. The solid curve of Figure 3 shows the results of

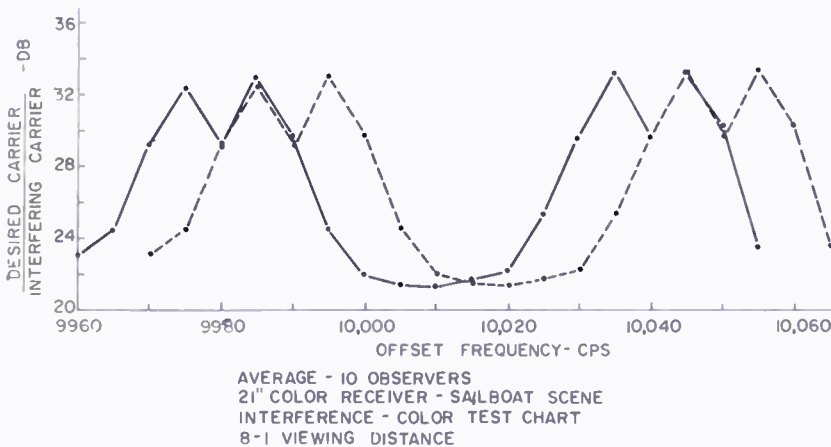


Fig. 2—Carrier ratio for tolerable interference for offset frequencies centered about 10,010 cycles (solid curve) and 10,020 cycles (dashed curve).

subjective tests made for frequency differences around 20,020 cycles. Note that this offset is no more desirable than the previous offset of 10,010 cycles, as they both have the same tolerable ratio of 21 decibels for the minimum. However, the maximum is 39 decibels and there is an improvement of 18 decibels. Inspection of the minimum again indicates that a stability of  $\pm 5$  cycles in the offset frequency has little effect on the tolerable ratio.

With respect to the improvements of 12 decibels for 10,010 cycles and 18 decibels for 20,020 cycles, it should be noted that these improvements are from the extreme maximum peak of the tolerable ratio curve to the minimum of the curve. The precise carrier control system does not give these magnitudes of improvement over the presently used system in the sense that the present system is not at all times at the offset frequency which produces maximum visibility. The present fre-

quency difference of two picture carriers changes with time. Thus, at times the difference frequency may be at the value for minimum visibility and at other times at the value for maximum visibility, and covers all points in between these two.

It is of interest to consider the effects on the visibility of co-channel interference between black-and-white transmissions when the offset frequency is chosen so as to produce the maximum improvement for color transmissions. At the present time, the standards for color television prescribe a frame frequency of 29.97 cycles, with an accuracy of approximately three parts per million. However, for black-and-white television, there is only a nominal value of 30 cycles specified, with no tight control on stability. If a value of 30 cycles is assumed, multiplication by 334 gives an offset frequency of 10,020

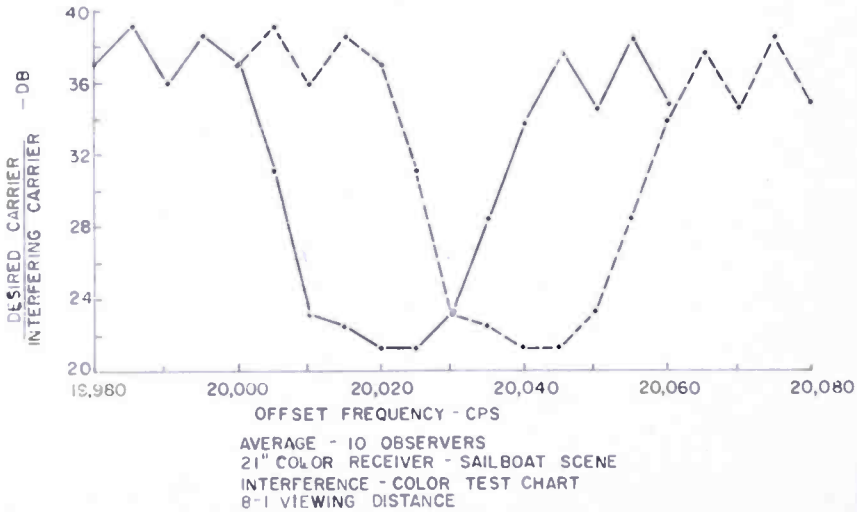


Fig. 3—Carrier ratio for tolerable interference for offset frequencies centered about 20,020 cycles (solid curve) and 20,040 cycles (dashed curve).

cycles, resulting in a difference of 20,040 cycles between stations B and C in a three-station arrangement. The dashed curve in Figure 3 is for the 20,040-cycle offset. Inspection of this curve shows that when the transmissions have a frame frequency of 30 cycles and the offset frequency is 20,020 cycles, co-channel interference has almost maximum visibility. Referring to the dashed curve in Figure 2, which is for the 10,020-cycle offset, one sees that an offset of 10,010 cycles is a condition for almost minimum visibility of the interference whether the transmissions have a frame frequency of 30 cycles or 29.97 cycles.

Thus, for the plan of precise control to be completely and properly used, it is necessary to use the same frame rate, controlled with the

same accuracy, for all television transmissions, color or black-and-white. Each television station would then require, in addition to the stable carrier frequency, an accurate control for all sync generators.

The arbitrary stability requirement of  $\pm 5$  cycles on the offset frequency imposes a relative stability on the picture carriers for the low VHF channels of plus or minus three parts per hundred million. The high VHF channels require a relative stability of plus or minus one part per hundred million. Two oscillators having this stability were constructed for NBC's Channel 4 (66.72 megacycles) stations, WRCA-TV in New York and WRC-TV in Washington, D. C.

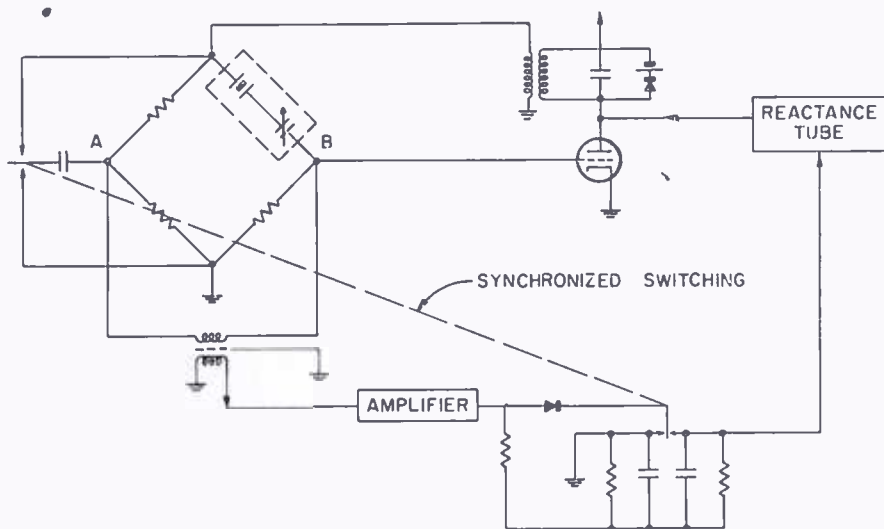


Fig. 4—Crystal oscillator.

The oscillators are similar to those described by P. G. Sulzer.<sup>3</sup> Figure 4 shows a simplified diagram of the oscillator. The oscillator is extremely stable; its stability is essentially independent of circuit changes and depends almost entirely on how well the natural resonant frequency of the crystal can be maintained. Extreme stability is produced by using the crystal in an oscillator circuit and also in a bridge circuit.<sup>4</sup> The crystal is used in the bridge circuit as a means of indicating when a phase shift has occurred in the oscillator circuit due to changes in components.

The plate circuit has an amplitude limiter to maintain constant current through the crystal. Feedback for the oscillator is obtained

<sup>3</sup> P. G. Sulzer, "High-Stability Bridge-Balancing Oscillator," *Proc. I.R.E.*, Vol. 43, p. 701, June, 1955.

<sup>4</sup> Norman Lea, "Quartz Resonator Servo—A New Frequency Standard," *The Marconi Review*, Vol. 17, p. 65, 3rd Quarter, 1954.

between grid and ground across one of the resistors in the bridge circuit. When the crystal is at its natural series resonant frequency, the bridge is balanced. If, because of changes in phase shift around the oscillating loop, the crystal is operating at a frequency slightly different from its resonant frequency, an output is obtained from the bridge. Information as to whether the crystal is operating above or below its natural resonant frequency is obtained by switching the small capacitor across one arm of the bridge and then the other arm. When the bridge is balanced it has equal outputs for each position of the capacitor. If the crystal is operating on the high side of its natural resonant frequency the bridge output will be higher when the capacitor is across the upper arm than when it is across the lower arm. The output of the bridge is maximum for the capacitor across the lower arm if the crystal is operating below its series resonant

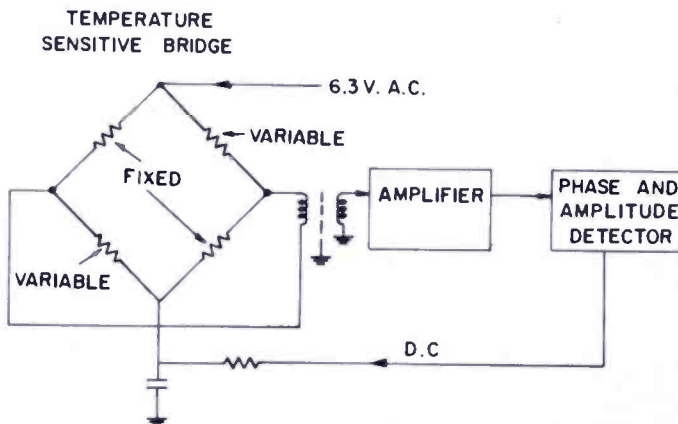


Fig. 5—Method of controlling the temperature of the crystal oven.

frequency. The circuit for detecting the amplified output signal of the bridge circuit has a switch which is synchronized with the switching of the capacitor across the arms of the bridge. This switch connects a different R-C circuit into the detection circuit for each position of the bridge capacitor. The voltages across the R-C circuits add with respect to ground and are applied to a reactance tube which corrects the oscillator circuit.

The method of maintaining the crystal at a constant temperature is shown in Figure 5. A temperature-sensitive bridge is used to supply the necessary heat to the oven, and to detect temperature changes within the oven. Two arms of the bridge (labeled FIXED) have resistances which do not change with temperature. The other two arms (labeled VARIABLE) change resistance with temperature. At the operating temperature of the crystal, the resistances are made equal. An a-c voltage is applied across the bridge. If the ambient

temperature decreases, causing the winding temperature to decrease, a 60-cycle output is obtained from the bridge. The output is amplified and detected; the detector provides a direct current to the bridge and increases the heat into the oven. The detector is also phase sensitive to prevent the bridge from operating at a temperature above the balance temperature; its output is zero if the bridge output signal changes phase by  $180^\circ$ .

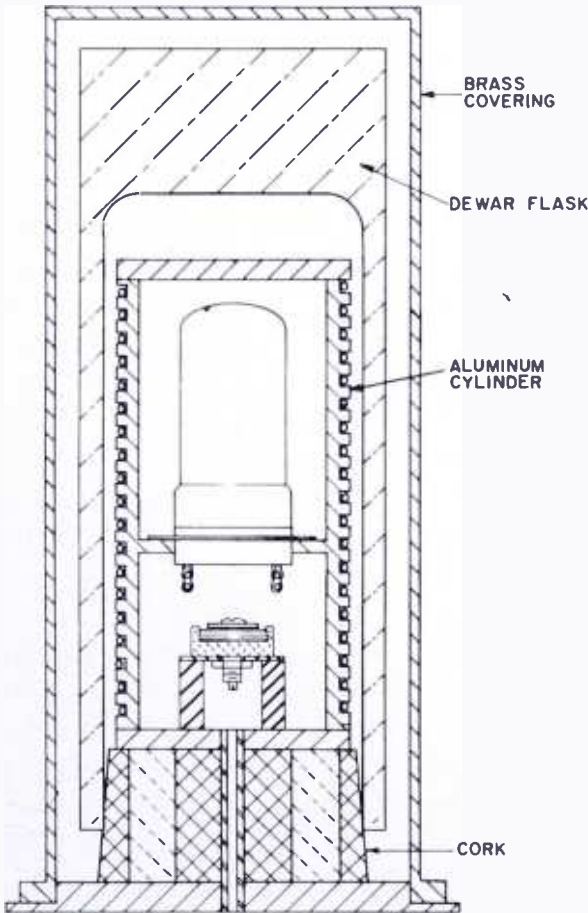


Fig. 6—Crystal oven.

A cross section of the crystal oven is shown in Figure 6. The crystal and the capacitor in series with it are mounted inside an aluminum cylinder. The ends of the cylinder are closed by aluminum caps. The temperature-sensitive bridge wire is wound in the slots on the outer wall of the aluminum cylinder. This aluminum unit is mounted on a cork and enclosed by a Dewar flask. A brass covering encloses the entire unit.

The relative stability of the two frequency units was measured in the laboratory for a 70-hour period; the results are given in

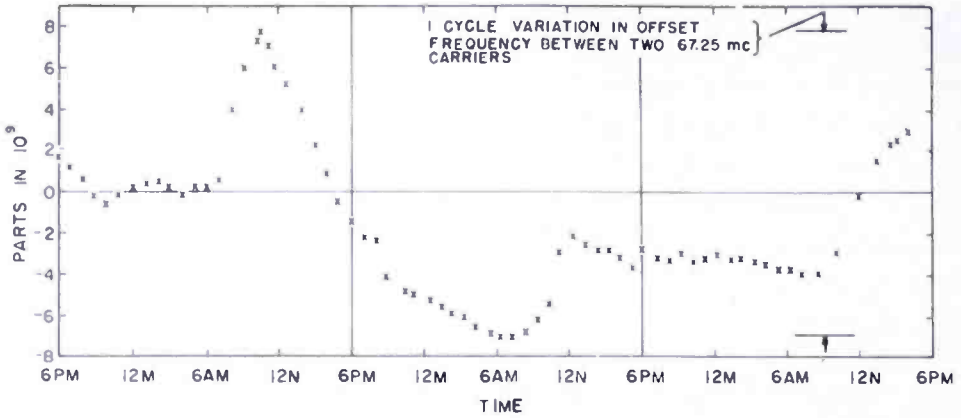


Fig. 7—Relative stability of the two frequency units.

Figure 7. Frequency variations over this period were  $\pm 7$  parts in  $10^9$  and were due to an ambient temperature change of  $10^\circ\text{C}$ . It is known that the units change frequency in the opposite direction with increasing temperature; thus the frequency difference between them increases with increasing temperature. The stability is better than required; the marks on the right of the drawing indicate a one-cycle variation in the offset frequency between two channel 4 carriers.

Unit #1 was installed at the WRCA-TV transmitter in New York. The WRCA-TV picture carrier, as received at RCA Laboratories, Princeton, was compared with the signal from unit #2, and the stability of the difference signal was measured over a 48-hour period. Figure 8 gives the measurements made every hour that WRCA-TV's carrier was on the air. There was a change of  $\pm 0.2$  of a cycle in the offset frequency; this is a relative stability of  $\pm 3$  parts in  $10^9$ .

With the equipment being tested, it was convenient to use an offset frequency of 9,950 cycles. This is the first even multiple of frame frequency (29.97 cycles) below 10,010 cycles. Subjective tests in the laboratory showed that this offset frequency would reduce the visibility of the co-channel interference by the same amount as 10,010 cycles.

Unit #2 was then installed at the WRC-TV transmitter in Washington, and the offset frequency checked by the method shown in Figure 9. The procedure is to take the Washington transmitter off the air, and receive the New York signal on the Washington trans-

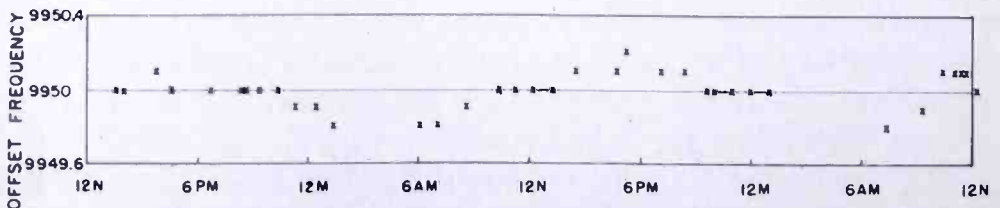


Fig. 8—48-hour stability test.



such a frequency that the carrier produced by it was 90 cycles higher in frequency than the carrier produced by the precise source. Thus the carrier which was higher by 90 cycles produced an offset frequency equal to an odd multiple (329) of the frame frequency or 9,860 cycles. During color programs the transmitter operator at Washington switched the transmitter to each of these frequency sources at pre-determined time intervals. The results of the previous laboratory subjective tests indicated the offset of 9,950 cycles should produce the minimum visibility of co-channel interference, and the offset of 9,860 cycles would produce nearly maximum visibility of the interference.

Since installation of the units field tests have been made, and over a period of six weeks, sixteen color programs were observed at several

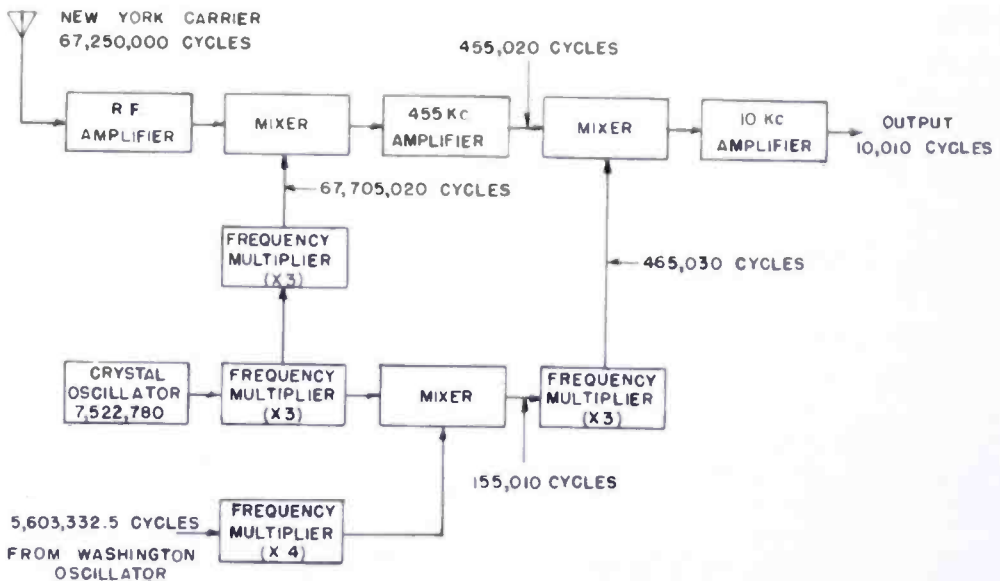


Fig. 10—Washington receiver.

homes and at RCA Laboratories in Princeton and at one home in Seaside Park, N. J. Princeton is approximately 40 miles from New York and 150 miles from Washington. Seaside Park is 55 miles from New York and 165 miles from Washington. All of the shows were not observed at all of the viewing locations, but when observed and co-channel interference was noticeable, a definite improvement was reported by all observers for the offset frequency equal to an even multiple of frame frequency.

Also, for purposes of field testing, a truck was equipped as shown in Figure 11. The field intensity meter was tuned to the Channel 4 picture carrier from New York, and its field strength recorded on recorder No. 1. At the audio output of the field intensity meter the output signal contained the 9,950-cycle beat between the Washington

and New York picture carriers. A filter selected the 9,950-cycle component and applied it to the vertical plates of the oscilloscope. The output signal of the filter was also rectified and the direct current applied to recorder No. 2, to produce a record of the beat amplitude. The output of the audio oscillator was used to trigger the sweep circuits of the oscilloscope. A counter measured the frequency of the audio oscillator. An operator adjusted the audio oscillator to maintain a stationary sine wave pattern on the oscilloscope for the 10 seconds required by the counter to measure the frequency of the audio oscillator. It was possible to repeat the frequency measurements to  $\pm 1/10$  cycle. With this arrangement the effects of propagation on the frequency stability of the offset frequency could be observed. Spot checks were made at various times at different locations and at no time were

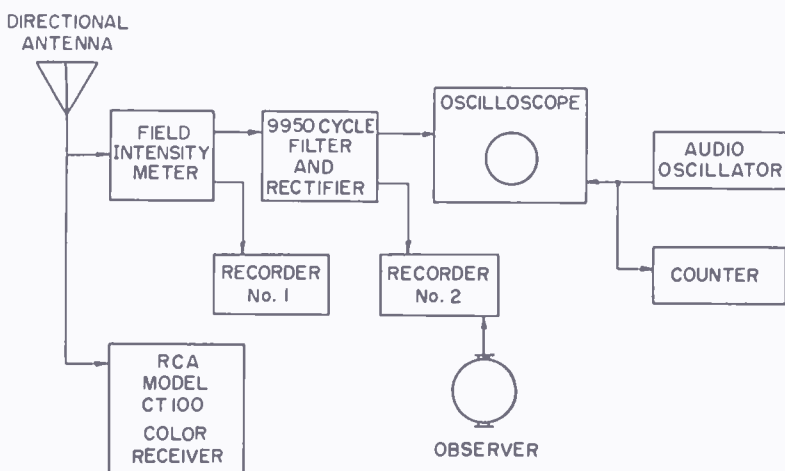


Fig. 11—Field truck equipment.

frequency changes observed which would cause a reduction in the improvement obtainable by precise picture carrier frequency control.

The offset frequency was measured by the previously described technique over a period of 60 days. A frequency change of 5 cycles was measured; the results are given in Figure 12. No adjustments of any kind were made on either of the frequency control units during this period. At the end of the sixty-day period the crystal bridge in each unit was balanced and the offset frequency reset to 9,948 cycles. Since this adjustment the frequency has changed 0.5 cycle in two weeks.

The field truck was also equipped with a color receiver which was used for observations at various locations and also for subjective tests. Tests were made on six observers to obtain an improvement factor comparing transmissions using an offset frequency at an even multiple of color frame frequency (9,950 cycles) with transmissions using an offset frequency at an odd multiple of color frame frequency (9,860

cycles). Black-and-white transmissions were used for the tests as they were available when desired, and if the frame frequency was adequate to give an improvement, a greater improvement would be expected at a frame frequency of 29.97 cycles. Also, for a limited number of transmissions it would be known whether the 30-cycle frame frequency was such as to produce an improvement. The tests covered only two afternoons of transmissions. However, the program material included studio programs, film, and remote pickups. The entire test period for one observer and part of the test period for another observer were made on the Republican Convention program originating in San Francisco.

The persons tested observed 15 minutes of program for each offset frequency. Some observers were tested for more than one period of

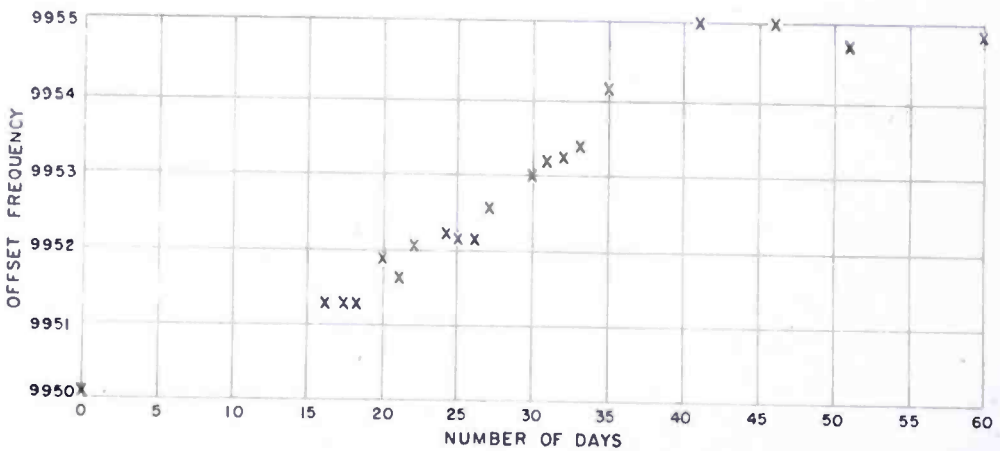


Fig. 12—Change in offset frequency after units were installed in television stations.

each condition. The observer was seated at a viewing distance equal to eight times picture height, and instructed to push a button supplied to him, if he saw the bars due to the interference. This produced a record, on the recording of the beat amplitude, as to the time when each observer could see the co-channel interference. This test did not measure the tolerable ratio, but simply indicates if an improvement is obtained for the 9,950 cycle offset. It is a visual acuity and perception test and depends upon the conditions of the experiment.

From this data, the per cent of time the observer saw the interference for each of the offset frequencies was determined. The results are given in Figure 13. Each observer saw a definite improvement for 9,950 cycles, compared to 9,860 cycles. The average observer saw the interference in the picture 61 per cent of the time for the offset of 9,860 cycles, compared to only 9 per cent for 9,950 cycles.

As long as synchronizing signal generators for monochrome transmissions are locked to the power line, the improvement obtained with black-and-white pictures will be a function of the stability of the power-line frequency in the areas involved. As previously indicated, in a three-station arrangement no improvement can be expected between the two stations that are nominally 20,000 cycles apart as long as the power line is the sync generator reference.

Several black-and-white broadcasts were observed for an hour at different locations. For all locations and broadcasts an improvement was observed.

If this plan of precise picture carrier frequency control were to be universally used, and if optimum improvements were to be obtained, it would be necessary, on black-and-white transmissions, to lock the sync generator to the color subcarrier generator, or some equivalent source, to produce a frame frequency of 29.97 cycles with adequate stability.

| OBSERVER | % OF TIME<br>9860 CYCLES | % OF TIME<br>9950 CYCLES |
|----------|--------------------------|--------------------------|
| A        | 44.4                     | 14.8                     |
| B        | 89.5                     | 24.2                     |
| C        | 52                       | 2.4                      |
| D        | 43.5                     | 0                        |
| E        | 45.5                     | 3.2                      |
| F        | 89                       | 11.4                     |
| AVERAGE  | 61                       | 9                        |

Fig. 13—Percentage of time co-channel interference was observed for 9,860 and 9,950 cycle offsets.

#### ACKNOWLEDGMENTS

The author wishes to acknowledge the material contributions made by many individuals to this project. These include G. L. Fredendall, E. M. Leyton, W. C. Morrison, and Juri Tufts, all of RCA Laboratories. In addition, the transmitter engineers at WRCA-TV and WRC-TV were very helpful in conducting the field tests.

#### APPENDIX

It was considered desirable to make additional subjective tests to verify the expected improvement resulting from the use of precise carrier frequency control. Therefore a new series of tests was made using a different method of subjective evaluation.

A set-up was arranged to measure the improvement by the "method of equality." This means that the observer could change the viewed

scene back-and-forth between a reference picture (with a fixed interference level) and the same scene with the interference at a different offset frequency and an adjustable interference level. Measurements were made by varying the amount of interference in the test picture until the viewer indicated no preference for either picture. The improvement is then expressed as the difference, in decibels, between the signal levels of the two interfering signals.

The tests were made using four different receivers from several manufacturers—a 21-inch color receiver, a 21-inch black-and-white receiver, and two 17-inch black-and-white receivers. Tests were made with offset frequencies of 10,010 cycles and 20,020 cycles using slides (the "sailboat scene," as used for previous tests, as the desired picture and color bars as the interfering picture) and with off-the-air moving pictures. Several reference ratios were employed. The results are summarized in Figures 14, 15, 16, and 17. The original test results

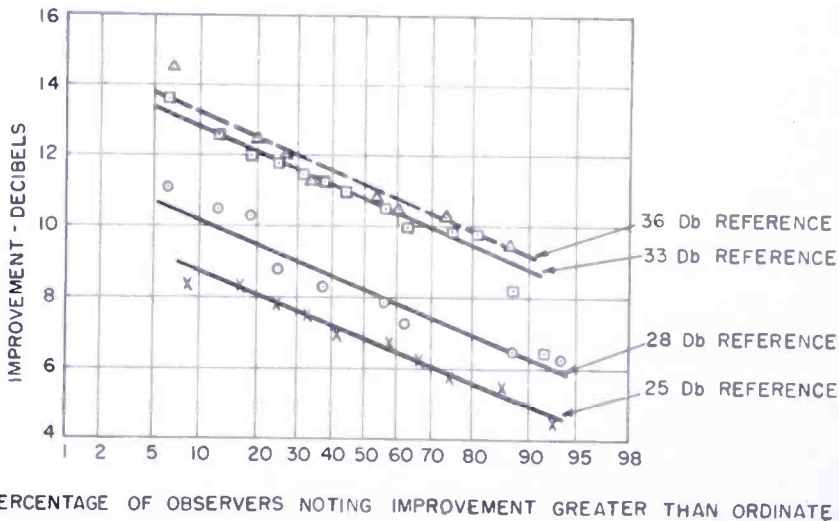


Fig. 14—Reduction in visibility of co-channel interference for a 10,010-cycle offset frequency compared with a 9,985-cycle offset. The desired picture was the sailboat scene. The interfering picture was color bars.

given by the solid curve of Figure 2 show a maximum ratio of 33 decibels required at 9,985 cycles and a minimum ratio of 21.5 decibels at 10,010 cycles to give an improvement of 11.5 decibels. This checks remarkably well with the 10.8-decibel improvement measured for 50 per cent of the observers when a 33-decibel reference was used with this new test method. The 20-kilocycle data shows a similarly close check between the two methods. It is quite evident from the data given that the improvement measured will be a function of the quality of the reference picture.

As an example, to show how the tests were conducted, tests using a 28-decibel reference level at an offset of 9,985 cycles will be described. The observer was seated at a viewing distance of eight times picture height from four different television receivers. Tests were made on each receiver and the order in which the receivers were viewed by the observers was random. The observer was given a switch. For one position of the switch the observer viewed a picture which had a ratio of desired signal to undesired signal of 28 decibels with the undesired carrier offset by 9,985 cycles. The other position of the switch produced a picture with the interference at a 10,010-cycle offset and a ratio of

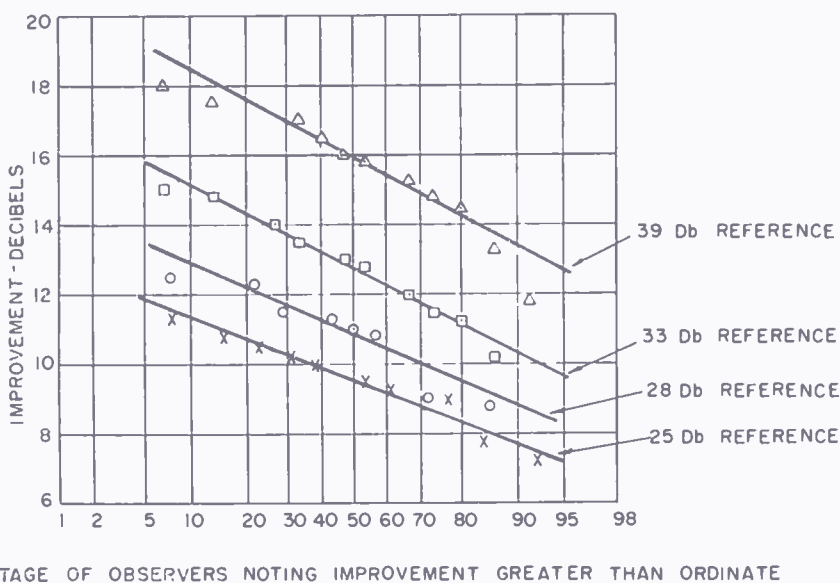


Fig. 15—Reduction in visibility of co-channel interference for a 20,020-cycle offset frequency compared with a 19,995-cycle offset. The desired picture was the sailboat scene. The interfering picture was color bars.

desired signal to undesired signal that could be varied by the person conducting the test. The observer viewed each picture as often as desired and the level of the interference at the 10,010-cycle offset was changed until the observer stated that the two pictures were equal. This procedure was repeated for each of the four television receivers. The improvement was then taken as the difference between 28 decibels and the signal ratio obtained at the 10,010-cycle offset.

Figures 14 and 15 show the results obtained using slides; twelve to fifteen observers were tested for each condition shown. Figures 16 and 17 show the results obtained using off-the-air motion pictures; eight to ten observers were tested for each condition shown.

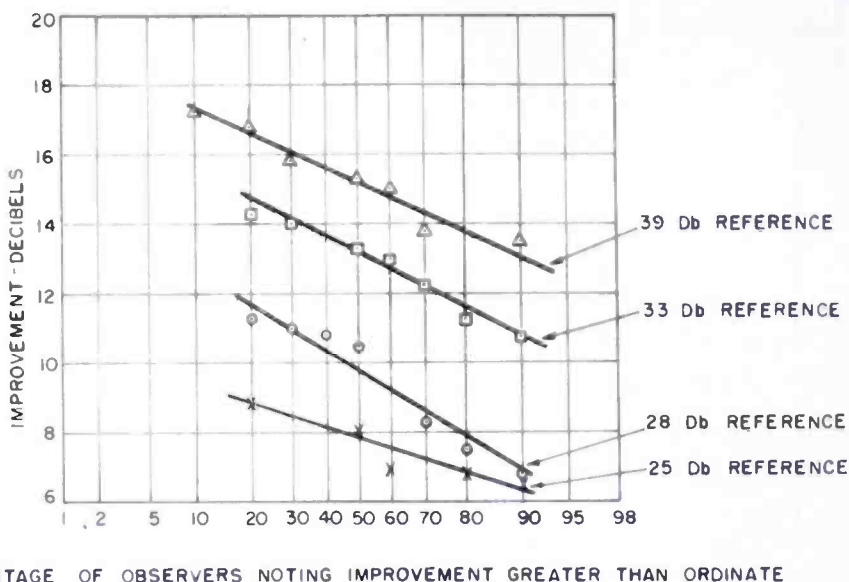


Fig. 16—Reduction in visibility of co-channel interference for a 20,020-cycle offset frequency compared with a 19,995-cycle offset. Desired picture was color program material from a commercial television station. The interfering picture was program material from a commercial television station.

It is interesting to examine the results obtained with the different sets. Although individual observers sometimes found differences between sets, when all observers were averaged, the differences were small. For the 10-kilocycle tests, each set gave an improvement that was within 1 decibel of the others. At the 20-kilocycle offset, the

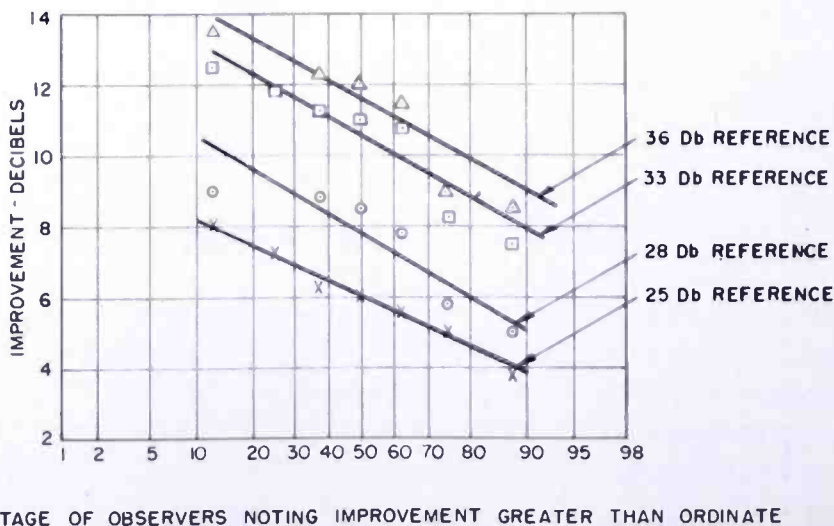


Fig. 17—Reduction in visibility of co-channel interference for a 10,010-cycle offset frequency compared with a 9,985-cycle offset. Desired picture was color program material from a commercial television station. The interfering picture was program material from a commercial television station,

difference between sets varied from less than 1 decibel to just over 3 decibels. For these 20-kilocycle tests the color receiver tended to give about 1 decibel less improvement than the black-and-white sets.

From the data presented it is evident that the *anticipated improvement* due to the use of precise frequency control will be a function of the interference level considered tolerable with the present system. We now have made two relatively independent tests of improvement and the two methods have been found to check. An examination of Figures 14, 15, 16, and 17 shows that the improvement decreases as the ratio of the desired signal to the undesired signal decreases. The reduction in improvement is probably due to the observer's becoming aware of the interfering picture in the background. A consideration of the data presented in this paper, and past experience, indicates that a tolerable ratio of 20 decibels is satisfactory when precise carrier frequency control is used.

# A MINIATURE VIDICON OF HIGH SENSITIVITY

BY

A. D. COPE

RCA Laboratories,  
Princeton, N. J.

*Summary*—Experimental models of a sensitive miniature Vidicon pickup tube  $\frac{1}{2}$  inch in diameter and 3 inches long have been built and operated in prototype equipment. With such a small photolayer area, the use of a photoconductor having the sensitivity of conventional one-inch by six-inch Vidicons would require an excessively fast lens or an increase in scene illumination. A new photoconductor has been developed which has sufficient operating sensitivity to more than offset the reduction in light collecting area.

The spectral response of the new tube covers the approximate range from 400 to 800 millimicrons with its maximum in the neighborhood of 600 millimicrons. Resolution and picture lag are adequate for many applications where the small size is particularly attractive. The  $\frac{1}{2}$ -inch tube requires only one-fourth the heater power and one-third the deflection power of the conventional one-inch Vidicon.

## INTRODUCTION

IN 1950 a new class of television pickup tubes was described for which the name Vidicon was adopted.<sup>1</sup> The Vidicon type tube, first produced commercially as the 6198 and 6326, differs from earlier camera tubes in that the light sensitive surface is photoconductive rather than photoemissive. Such photoconductive materials have the inherent promise, now only partially realized, of more efficient use of the incident light energy to generate a video signal.

The present commercially available Vidicons produce pictures of 600 television lines at light levels of from 3 to 10 foot-candles incident upon the tube. They have proved to be useful in a variety of closed-circuit applications where the simplicity and compactness of the associated equipment has been of value.<sup>2</sup> In the broadcast field the major use so far has been in film pickup apparatus.<sup>3</sup> Indicative of the current trend, this past summer at the political conventions considerable use was made of portable Vidicon equipment for live pickup.

---

<sup>1</sup> P. K. Weimer, S. V. Forgue, and R. R. Goodrich, "The Vidicon — Photoconductive Camera Tube," *Electronics*, Vol. 23, p. 70, May, 1950.

<sup>2</sup> V. K. Zworykin and G. A. Morton, *Television*, Chapter 20, John Wiley & Son, 1954.

<sup>3</sup> W. L. Hurford and R. J. Marian, "Monochrome Vidicon Film Camera," *RCA Review*, Vol. XV, p. 372, September, 1954.

The trend toward miniaturization of television pickup equipment has been given added impetus by the rapid progress in transistorized video circuits.<sup>4</sup> Further size and weight reduction of Vidicon cameras was severely limited both by the size of the one inch by six inch commercial tube with its associated deflection and focus field assemblies, and by the operating power requirements of the gun heater and the deflection yoke.

Because the scene to be transmitted must be focussed on the light-sensitive element of the pickup tube, the area of the photolayer is chosen to be suitable for use with readily available camera optics. The one-inch tube was designed to make use of the variety of lenses available for 16-millimeter motion picture cameras. When considering a reduction in the size of the pickup tube, a photolayer area matched to 8-millimeter motion picture lenses is a natural choice. Recently, a small Vidicon tube has been available from Germany\* which employs a target of this size.

There are a number of effects associated with the reduction by a factor of four in the area of the photolayer of the pickup tube. An 8-millimeter lens operating at the same  $f$ : number as its 16-millimeter equivalent has one-fourth the light-gathering power and twice the depth of field. If a photoconductor of the same sensitivity is used in both the large and small tubes, and the associated lenses are set at the same  $f$ : number, the scene illumination for the small tube would have to be four times that for the large tube in order to produce equal output signals. This is strictly true only if the signal generated is proportional to the amount of incident light. If the gamma of the surface, that is the slope of the log signal versus log illumination plot, is less than unity, then an even greater increase in scene brightness is required. A gamma of less than unity is a desirable characteristic in the pickup tube since it increases the dynamic range of the device. The photoconductor used in the present Vidicon has a gamma of about 0.7.

An increase of scene illumination can be avoided by using a faster lens for the small camera and sacrificing depth of field. Consider the case where the depth of field of the two lenses is made equal. This is done by making the actual aperture diameters identical, that is by employing a smaller  $f$ : number with the 8-millimeter lens. This brings the total light flux back to the same level for each tube, although once again the signal of the small tube is reduced by the gamma factor.

---

<sup>4</sup> L. E. Flory, W. S. Pike, G. W. Gray, and J. M. Morgan, "Transistorized Television Cameras Using the Miniature Vidicon," *RCA Review*, Vol. XVII, p. 469, December, 1956.

\* Physicalish-Technische Werkstätten, Wiesbaden, Germany.

The practical limits to this approach are the availability and cost of 8-millimeter lenses of speeds greater than  $f:1.9$ . It is apparent, therefore, that a small Vidicon should have a photoconductor of greater sensitivity to compete successfully with the one-inch tube.

It is the purpose of this paper to describe the characteristics of an experimental miniature Vidicon tube which employs a new photoconductor layer of higher operating sensitivity than has previously been available. Adequate signal is generated with a scene illumination of 10 foot-candles and an  $f:1.9$  lens to give a noise-free display.

### DESCRIPTION OF THE NEW TUBE

#### *General*

Figure 1 shows the experimental small Vidicon, the standard one-inch Vidicon, and the image orthicon pickup tubes. The diameter of

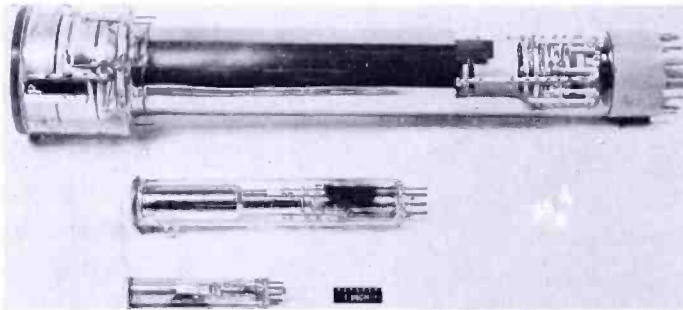


Fig. 1—Image orthicon, typical one-inch Vidicon, and experimental miniature Vidicon.

this new tube is  $\frac{1}{2}$  inch, the length 3 inches. As with the standard Vidicon, the  $\frac{1}{2}$ -inch tube operates in an axial magnetic field of 80 gauss (Figure 2). This can be either an electromagnetic or a permanent magnet field. The power required to deflect the tube electromagnetically is about 20 ampere-turns or approximately  $\frac{1}{3}$  that of the larger Vidicon. This modest power requirement falls within the capabilities of low-power transistors of the audio-amplifier variety.

The small heater-cathode assembly has been designed to minimize the heat conducted away through its support structure. The gun dissipates approximately 0.8 watt,  $\frac{1}{4}$  that of the larger tube. The beam spot has been made smaller by reduction of the limiting gun aperture, so that the resolution is not greatly reduced as compared with larger tubes, even though the scanning raster is only  $0.24 \times 0.18$  inch.

In order that the optical scene can be imaged on the light-sensitive material, the uniform layer of photoconductor, which is only a few

microns thick, is deposited on a transparent, conducting signal plate. Contact to the other surface of the layer is made by the electron beam which scans over the entire raster once each  $1/30$  second if the normal television scanning rate is used.

With an electric field applied across the photoconductor layer, the effect of exposure to an optical image is to produce a point-by-point variation in conductivity. This causes a charge pattern which is related to the light image to be built up on the scanned surface. As each point of the raster is contacted cyclically by the low-velocity beam, sufficient charge is deposited to restore the surface to cathode potential, at the same time causing a video signal current to flow in the lead connected to the signal plate. In order that full use will be

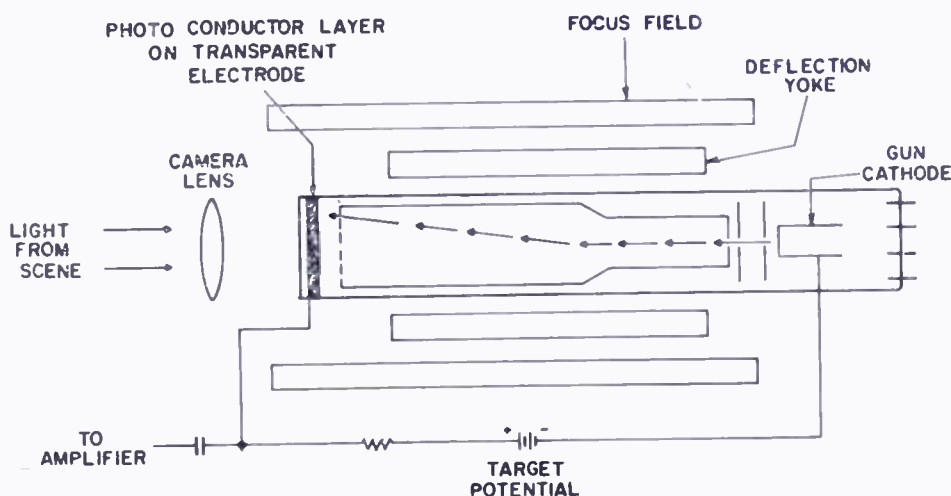


Fig. 2—Schematic diagram of Vidicon tube and its associated components.

made of the charge generated by the absorbed light, the photoconductor must be sufficiently resistive in the dark for its dielectric time constant to be greater than the  $1/30$  second frame time. This requirement places the photoconductor in the insulator class, the dark resistivity being of the order of  $10^{11}$  ohm-centimeters or greater.

### Photolayer

The new photoconductive layer used in the miniature Vidicon has a sensitivity in the range from 1,000 to more than 2,000 microamperes per lumen when operating at signal levels of the order of .02 to .05 microampere. The spectral response for the higher-sensitivity layers peaks at 650 millimicrons, as shown by curve A of Figure 3. A more panchromatic layer with a peak response at 550 millimicrons, as shown by curve B, can also be made. The gamma of the surface is

dependent upon the current density. At low illumination levels the signal varies linearly with light. At higher illumination levels such as will produce an output signal of the order of 0.05 microampere or greater, the gamma drops to 0.5. The abruptness of the change in gamma has varied from one sample to another. In some cases the break has been sharp, and in others there has been a gradual shift. The reduced gamma at high light levels permits the tube to operate with a broad range of light levels in a given scene.

The operating potential of the signal plate varies from 10 to 30

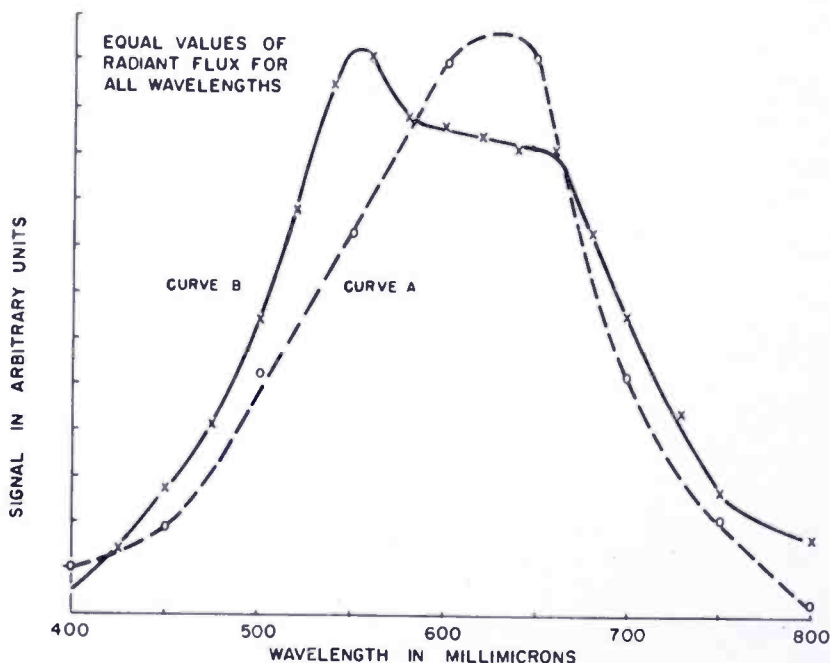


Fig. 3—Spectral response of new photoconductor surface being used in miniature Vidicon. Relative output signal of the tube is shown as a function of wavelength for equal energy illumination.

volts. The value chosen for the sensitivity data quoted above is that which will limit the dark current to the order of 0.01 to 0.02 microampere.

The photoconductor material is deposited on the signal plate of the bulb face by high-vacuum evaporation. The layer appears as a dark, glassy deposit about 2.5 microns thick. X-ray diffraction studies indicate that this type of layer is amorphous. Since the deposit is not affected by exposure to the atmosphere at reasonably low temperatures, it is possible to fabricate the film before the bulb is sealed to the gun assembly.

For the beam to discharge the pickup tube target in one sweep, the capacitive time constant, determined by the product of the target capacitance and the beam resistance, should be less than 1/30 second. The smaller target capacitance resulting from a reduction in the area of the target makes it possible to use layers which are thinner or have a higher dielectric constant.

Variations in the technique of evaporation of the same material can produce a wide variation in physical properties. A case in point is antimony tri-sulfide ( $\text{Sb}_2\text{S}_3$ ) in which a variation of the effective dielectric constant of 5 times can be achieved.<sup>5,6</sup> Table I shows the associated properties of the dense high-capacitance form and the

Table I—Antimony Tri-Sulfide Evaporated Layers

|  | Porous Layer                   | Glassy Layer                     |
|--|--------------------------------|----------------------------------|
| Capacitance/cm <sup>2</sup>  | 1,500 $\mu\mu\text{f}$         | 12,000 $\mu\mu\text{f}$          |
| Operating potential<br>(dark current = 0.02 $\mu\text{a}/\text{cm}^2$ )  | 30-70 volts                    | 3-5 volts                        |
| Sensitivity  | 100 $\mu\text{a}/\text{lumen}$ | 1,000 $\mu\text{a}/\text{lumen}$ |
| Peak of spectral response  | 450 $\text{m}\mu$              | 700 $\text{m}\mu$                |
| Picture lag<br>(residual signal 1/20 second after<br>removal of illumination level of<br>3 foot-candles on the photolayer) | < 20%                          | 50%                              |

porous low-capacitance forms of  $\text{Sb}_2\text{S}_3$ . The operating potential of this latter form indicates that there has been a highly desirable increase in dark resistivity, but a reduced sensitivity. The slow decay of the photocurrent for the glassy form restricts its usefulness to special applications.

If the lag, that is the residual signal remaining after the illumination is removed, was due solely to the capacitive time constant, a reduced area target of the dense  $\text{Sb}_2\text{S}_3$  would have several attractive characteristics. Unfortunately the major portion of the lag signal from this layer is of the type associated with the photoconductive process itself.

Photoconductive lag can generally be reduced by increasing the

<sup>5</sup> S. V. Forgue, R. R. Goodrich, and A. D. Cope, "Properties of Some Photoconductors, Principally Antimony Tri-Sulfide," *RCA Review*, Vol. XII, p. 335, September, 1951.

<sup>6</sup> B. H. Vine, R. B. Janes, and F. S. Veith, "Performance of the Vidicon, a Small Developmental Television Camera Tube," *RCA Review*, Vol. XIII, p. 3, March, 1952.

current density in the material. It follows that the same amount of light concentrated on a smaller area of photoconductor will give reduced lag while preserving the same depth of field in the scene. However, the factor is not sufficient to cause the normal solid form of  $\text{Sb}_2\text{S}_3$  to have sufficiently low lag to be suitable for a  $\frac{1}{2}$ -inch tube of general utility. It was therefore necessary to develop the new photoconductive layer with better lag characteristics.

Figure 4 shows the per cent of signal remaining after each of the first six sweeps of the beam following the removal of illumination. This is shown for a number of levels of illumination on the tube face. At three of these light levels the signal current was made the same by adjusting the target potential to yield a signal of 0.2 microampere.

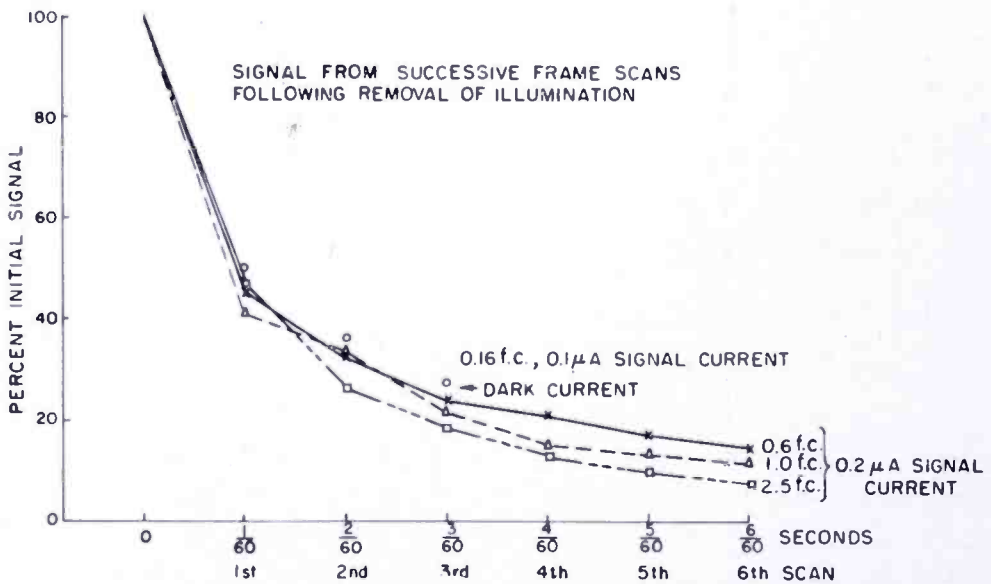


Fig. 4—Decay of photocurrent in the miniature Vidicon after the removal of illumination. This is shown as the per cent of the initial signal remaining after each successive sweep of the beam for six frames spaced  $1/60$  second apart. This data is given for four different levels of illumination on the target.

Thus, the lower the illumination level the higher the dark current because of the higher operating potential. This accounts for the signal being rapidly buried in dark current for the 0.16-foot-candle case, which is why the curve is not extended beyond  $3/60$  second.

The shape of the signal decay versus time plot of the new photosurface when compared with the photosurface used in earlier Vidicons is somewhat different. The initial decay is not as rapid, but there

is a smaller long-term component of lag. This makes exact comparison somewhat difficult by subjective tests.

#### COMPARATIVE PERFORMANCE

Tests were conducted with an experimental  $\frac{1}{2}$ -inch Vidicon and a typical 1-inch tube operating in the same type of equipment and producing comparable images of the same scene. With 10 to 20 foot-candles falling on the scene, equivalent output signals with comparable lag were observed in each picture when the small camera was operating with the lens at  $f:4$  and the lens of the large camera at  $f:2$ . The combined difference of two lens stops and the four-to-one area difference indicates an operating sensitivity for the small tube 16 times greater than for the larger tube. Using the same  $f$ : number with the

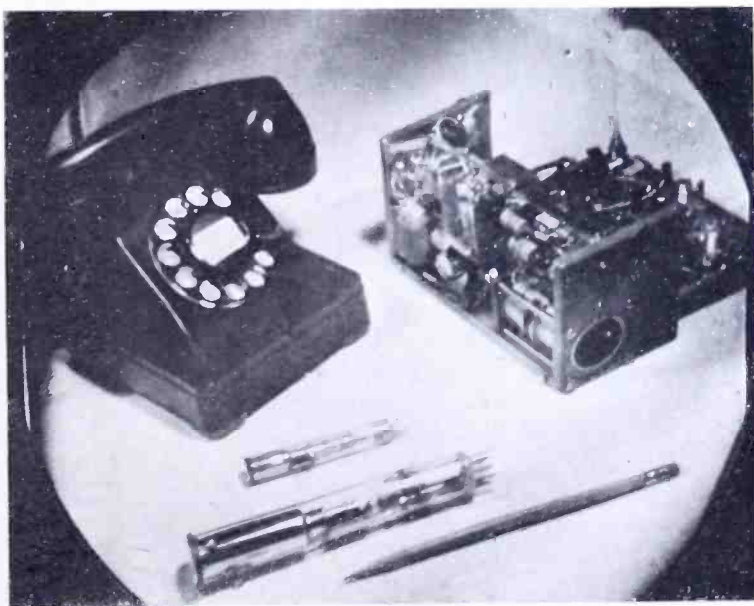


Fig. 5—Kinescope display of scene picked up by the miniature Vidicon operating in a standard industrial television equipment. In the upper right hand corner is a developmental all-transistor camera for use with the new tube.

small camera as with the large, the scene illumination could be reduced to one-fourth its previous value, at the same time preserving an increased depth of field.

Figure 5 is a photograph of the kinescope display of a standard industrial television equipment using a miniature Vidicon in the camera. The bandwidth of the amplifier was 6.5 megacycles and there was no aperture correction.

## ACKNOWLEDGMENTS

The helpful guidance of P. K. Weimer, who directed the tube development, and the inspiration of V. K. Zworykin are gratefully acknowledged. The camera developments of the group under the direction of L. E. Flory were closely coordinated with the tube development. Without the detailed evaluation of tube performance in their equipment, this program could not have been completed.

# TRANSISTORIZED TELEVISION CAMERAS USING THE MINIATURE VIDICON

BY

L. E. FLORY, G. W. GRAY, J. M. MORGAN, AND W. S. PIKE

RCA Laboratories,  
Princeton, N. J.

*Summary*—The development of a highly sensitive half-inch-diameter Vidicon together with recent transistor developments has made it possible to design television cameras of extremely small size and low power consumption. Transistor video amplifiers with a bandwidth of 8 megacycles or more and with satisfactory input noise characteristics have been designed. The low power required for deflection of the beam in the half-inch Vidicon makes deflection with small standard transistors quite easy.

An experimental closed-circuit camera has been built which weighs only three pounds and consumes about three watts of power. The output is a modulated 60-megacycle signal which can be connected to the antenna terminals of any standard receiver.

The camera may be powered by an internal a-c supply or by batteries. A one-pound silver-alkali storage battery will operate the camera for five hours. Sensitivity is greater than standard 1-inch closed-circuit cameras and resolution is limited by the bandwidth of the receiver.

In another version, a completely portable pickup station capable of picking up a scene and relaying it on a 2,000-megacycle carrier to a base station up to half a mile away has been built. This unit consisting of camera, synchronizing generator, transmitter and monitor, completely transistorized except for the transmitter itself, weighs 20 pounds including batteries for 5 hours operation. It was used by the National Broadcasting Company in covering the 1956 political conventions.

## INTRODUCTION

THE development of the half-inch-diameter vidicon has made it possible to design transistorized television cameras of small size, low weight, low power consumption, and high sensitivity. Two experimental camera equipments are described. The first, which is shown in Figure 1, is a relatively simple unit which, in connection with any standard television receiver, will form a complete closed-circuit television system. This camera, hereafter designated as the "Transistorized TV Eye" (abbreviated TTV) employs 19 transistors and has rather flexible power supply arrangements. The second equipment, shown in Figure 2, is a much more elaborate device. It is in reality a complete portable television transmitting station including a synchronizing generator, a picture monitor and a 2,000-megacycle transmitter. The unit employs 72 transistors and weighs 19 pounds including a rechargeable battery providing about five hours of opera-

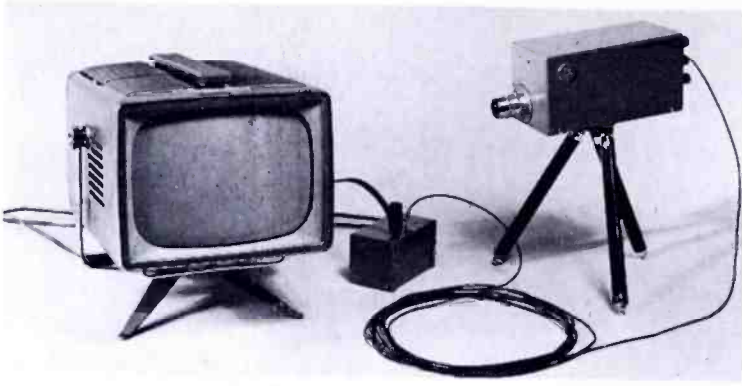


Fig. 1—Transistorized "TV Eye" camera (TTV).

tion. The term "Creepie Peepie" seems to have received considerable popular acceptance for this type of equipment. Consequently it will hereafter be referred to as "Transistorized Creepie Peepie" (abbreviated TCP).



Fig. 2—Transistorized "Creepie Peepie" (TCP).

## THE HALF-INCH VIDICON

The experimental  $\frac{1}{2}$ -inch Vidicon<sup>1</sup> is shown in Figure 3. Its dimensions may be deduced from the photograph. For use with transistor circuits the tube has the advantage of requiring only about 20 ampere-turns of deflection field. This is about one-third of the amount required by the conventional one-inch Vidicon (6198). The tube is also somewhat more sensitive than the 6198.

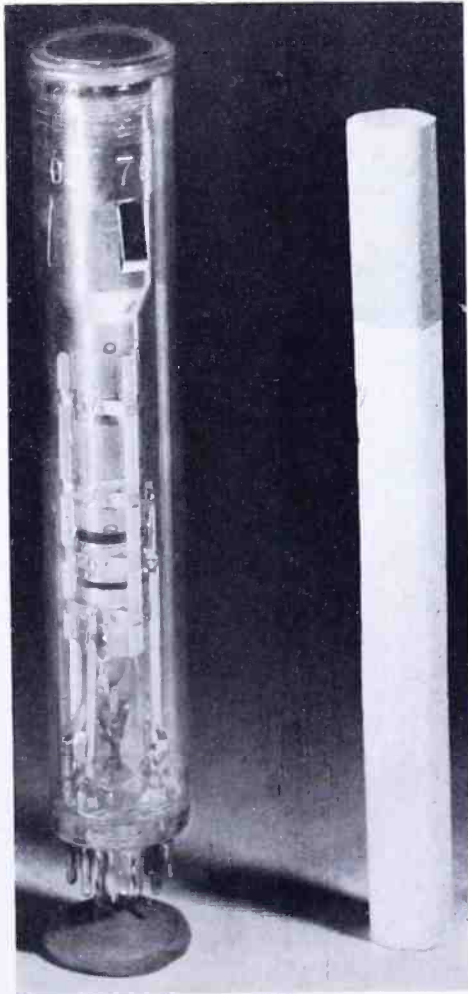


Fig. 3—Half-inch Vidicon shown in comparison with a cigarette.

## TRANSISTOR CIRCUIT CONSIDERATIONS

Operation of the Vidicon requires video amplifiers, deflection circuits, and a high-voltage supply. The requirements of these circuits depend on the particular application. For example, the video ampli-

<sup>1</sup> A. D. Cope, "A Miniature Vidicon of High Sensitivity," *RCA Review*, Vol. XVII, p. —, December, 1956.

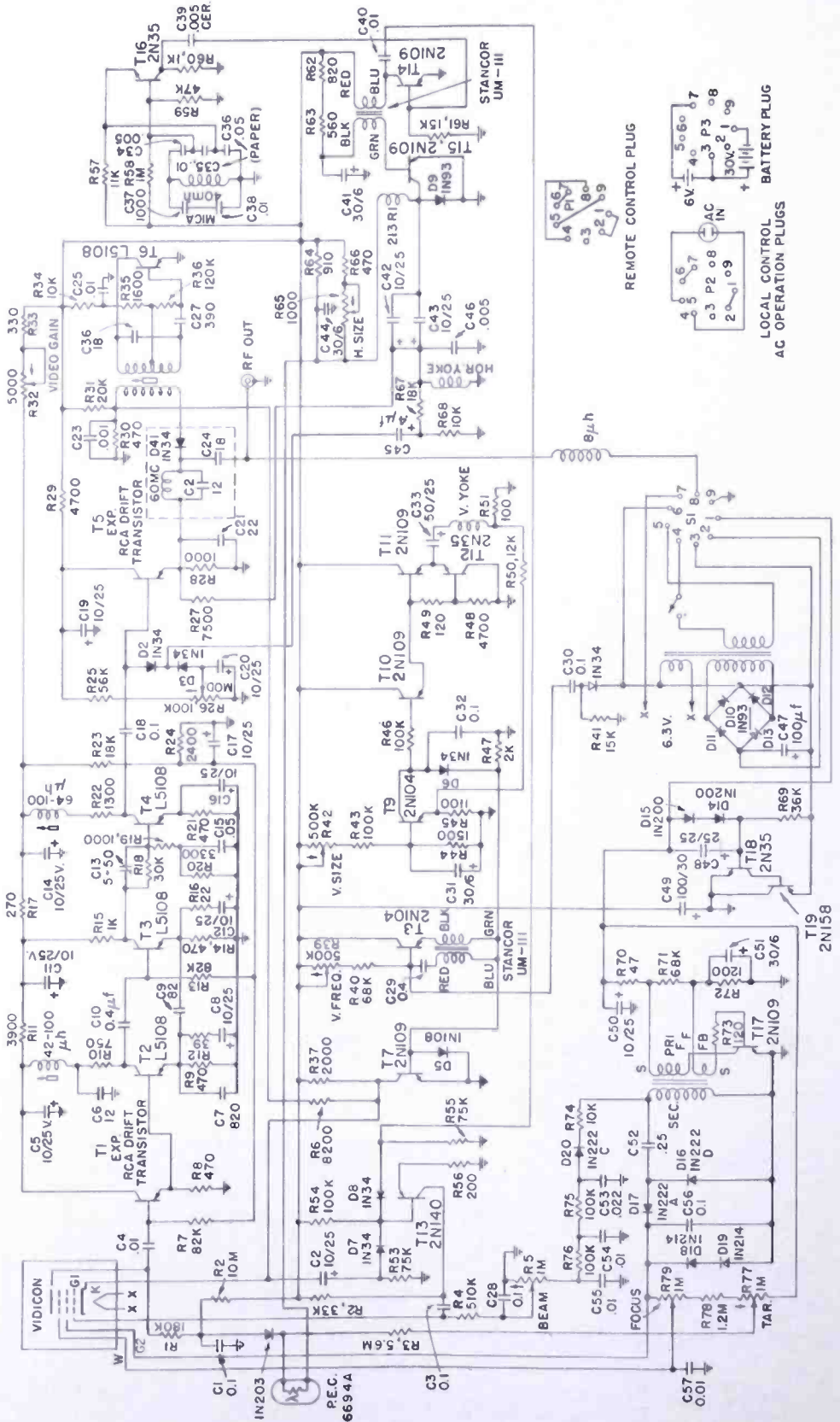


Fig. 4—Circuit of TTV camera.

fiers may include driven clamps and modulators, and the deflection circuit may require a sync generator.

Video amplifiers of adequate bandwidth and satisfactory input noise characteristics have been constructed with high-frequency junction transistors. The low deflection field requirements of the  $\frac{1}{2}$ -inch Vidicon are such that small low-power transistors of the audio amplifier variety are suitable. A satisfactory transistor sync generator was developed for use in the TCP equipment. Transistors offer some unique advantages for use in the high-voltage power supply for the Vidicon.

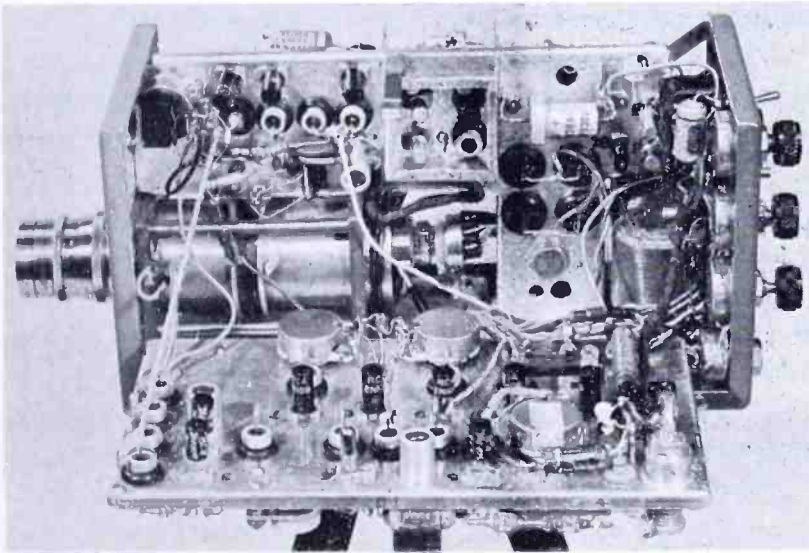


Fig. 5—TTV camera opened.

#### THE "TRANSISTORIZED TV EYE" CAMERA

The complete circuit of the TTV unit is shown in Figure 4. The video amplifier appears across the top, the center section includes the deflection and blanking circuits, and the power supplies are at the bottom. Figure 5 is a photograph of the camera with the cover removed.

##### *Video Amplifier*

The video amplifier must accept a signal current from the  $\frac{1}{2}$ -inch Vidicon of about  $10^{-7}$  ampere and amplify it to a level sufficient to drive the modulator in which the video information is used to modulate a carrier frequency which may be adjusted to either of the two lowest VHF television channels. The camera output may thus be connected directly to the antenna terminals of the associated receiver. The video bandwidth is about 4 megacycles.

For best signal-to-noise ratio, the input impedance of the amplifier

is made high even though this results in a nonuniform frequency response, i.e., a considerable high-frequency roll-off. The characteristics of a later stage in the amplifier are altered in an inverse manner to produce an over-all flat response. This well known technique, called high peaking, results in about 14 decibels improvement in the apparent low-frequency signal-to-noise ratio. In practice, the input impedance of the amplifier is made about 50,000 ohms. The vidicon signal current thus develops about 5 millivolts across this load at low frequencies. The modulator requires about 200 millivolts at about 200 ohms impedance. Therefore, a power gain of approximately 57 decibels is required. The "high peaker" requires about 26 decibels more gain to adequately equalize the falling high-frequency response of the input network, and it is advantageous to provide an additional 22 decibels of high-frequency gain to compensate for the apparent spot size of the camera tube (aperture correction). The total required high-frequency gain is 105 decibels.

The first video stage, transistor T1, is connected as an emitter follower. It provides the required high input impedance. The output of this stage is direct-coupled to the base of a second transistor, T2. As might be expected, the first transistor presents the greatest problem in transistor selection. Although other transistors may be used, a pre-production "drift" transistor, has proven the most suitable in this application due to its high input impedance, good frequency response, and low noise.

The second and third stages of the amplifier must be considered together. Neglecting their emitter circuits, they will be seen to be conventional a-c coupled common-emitter amplifiers. A shunt peaking inductance in the collector circuit of T2 maintains the high-frequency response out to 4 megacycles. The emitter circuits are complex. In each emitter circuit a 470-ohm resistor (R9, R14) provides a d-c path of sufficient resistance to obtain adequate d-c stability. Since such a high resistance would reduce the stage gain to a very low value, RC networks comprising R12 and C8 and R16 and C12 are shunted across these emitters. It will be noted that this does not remove all the a-c degeneration. Positive feedback at high frequencies is now applied from the emitter of T3 to the emitter of T2 via a capacitive divider comprising C9 and C7. This artifice increases the high-frequency gain of the circuit sufficiently to provide the necessary aperture correction. Transistors T1 and T3 are biased by means of a common bleeder network (R23, R24) while T2 is biased by its direct connection to T1.

The adjustable "high peaker" is located between the collector of

T3 and the base of T4. It is a high-frequency equalizer in which the amount of high-frequency equalization is fixed by the circuit resistances; the turn-over frequency is adjusted by means of C13. The latter is adjusted to match the loss characteristic of the input network. In practice this adjustment is most readily carried out by observing a test pattern and visually adjusting the high peaker to minimize "trailing."

T4 is a conventional common-emitter stage. Its emitter is bypassed and a peaking inductance in its collector maintains its high-frequency gain. Bias is applied via the high-peaker resistors to its base.

The transmission of a good television picture imposes special requirements on the low-frequency response of the system amplifiers. There are several possible solutions to this general problem. The response may be extended to d-c, for example. This is usually impractical. A more usual technique is to adjust the amplifier low-frequency gain and phase response in such a fashion that it will adequately reproduce a square wave at the horizontal scanning frequency and then to employ clamping or d-c restoration to re-insert the d-c component. Where space is at a premium, as in this camera, the latter technique results in much smaller coupling and bypass capacitors. In this equipment an over-all low-frequency correction can conveniently be made by placing a capacitor, C15, across R20, the latter resistor being required to bias T4 properly. This one capacitor will adequately compensate the low-frequency response of the amplifier through T4 in the desired fashion.

The signal from the collector of T4 is coupled to the base of T5 via a relatively small capacitor, C18, while a driven clamp, comprising diodes D2 and D3, sets the base potential of T5 at the start of each horizontal line. Negative drive pulses for the clamp are derived from the horizontal-deflection circuit via R67, R68 and C45. On each pulse the diodes conduct, thereby clamping the base of T5 to a potential which is adjusted for optimum operation of the modulator by means of R26. D-C information is thus reinserted at this point in the amplifier.

The modulator, D4, operates as a variable impedance in series with the carrier oscillator output. This impedance is caused to vary in accordance with the video information. T6 is a transistor oscillator which is tunable from 54 to 66 megacycles. Oscillation is maintained by feedback from collector to base via the tuned transformer shown. Energy from the oscillator is applied to the anode of the modulator diode, D4, via a two-turn coupling coil on the oscillator transformer. D-C bias is also applied at the same point from a divider comprising

R30 and R31. The cathode of the modulator diode is connected through a trap broadly tuned to the carrier frequency to the emitter of T5. By means of R26 the modulator diode is adjusted to be conducting. R-F from the oscillator, T6, now can pass through the modulator diode to the output terminal of the camera via a small capacitor, C18. Video signals at the emitter of T5 will vary the diode impedance thus modulating the video signal on the carrier.

Synchronizing pulses are also added to the outgoing signal in the modulator. Negative horizontal synchronizing pulses from the deflection circuit are applied via R27, which imposes a negligible load on the video signal. Positive vertical synchronizing pulses from the vertical blanking amplifier, T7, are applied to the other electrode of the modulator diode by means of R6. These circuit arrangements produce a composite output signal in which both horizontal and vertical synchronizing components are of the correct polarity with respect to the video information.

#### *Vertical-Deflection System*

A blocking oscillator, T8, generates negative pulses across R47 at vertical frequency. During a-c operation this oscillator is locked to the power line by means of a circuit comprising D22, R41, and C30. This circuit injects the requisite amount of suitably shaped line-frequency signal into the base circuit of the oscillator to accomplish this function. During battery operation the blocking oscillator runs free.

The negative pulses across R47 are amplified and inverted in T7, the vertical blanking amplifier, and applied to the cathode of the Vidicon. Landing of the electron beam is thus prevented during the vertical flyback. A portion of the output of T7 is also used as vertical sync, as previously explained.

Each negative pulse across R47 charges C32 via diode D6. A linear sawtooth voltage is generated across this capacitor by allowing it to discharge between pulses through constant-current transistor T9. The magnitude of the discharge current is adjustable by means of R42, the vertical-size control. The generated sawtooth voltage waveform has a maximum amplitude of about ten volts, this limitation being set by the magnitude of the pulse available across R47.

The vertical-deflection-yoke windings have a resistance of about 200 ohms and an inductance of about 57 millihenries. This inductance is negligible. The sawtooth voltage appearing across C32 must be coupled into these windings and must cause an accurately linear sawtooth current to flow in them. Impedance conversion is performed in the following stages as a first step in accomplishing this. T10 is

an emitter follower direct-coupled to a class-B complementary symmetry output amplifier comprising T11 and T12. R46 limits the voltage which can be applied to this system and swamps out the somewhat nonlinear input impedance characteristics of T10 as well as raising the load impedance seen by the sawtooth generating circuit. As a d-c connection to the yoke would cause prohibitive de-centering of the Vidicon beam, capacitive coupling to the yoke is used. The coupling capacitor, C32, is too small to adequately reproduce the sawtooth, but space did not permit a larger unit. The application of negative feedback via R51, R50, and R45 corrects the resulting non-linearity in acceptable fashion. The available maximum peak-to-peak deflection current is about 25 milliamperes.

### *Horizontal-Deflection Circuit*

The horizontal-deflection circuit operates in much the same fashion as its counterpart in home television receivers; that is to say, it generates a sawtooth current waveform by periodic interruption of the current flowing in an inductance. Fortunately, transistors make better switches than vacuum tubes in that the impedance of a transistor when conducting is materially lower than that of a vacuum tube.

Transistor T16 is an oscillator operating at the horizontal-scanning frequency. It is similar to a vacuum-tube Colpitts oscillator. Some temperature compensation is applied, in the interest of stability, by means of temperature-sensitive capacitor, C38. Although the waveform across the oscillator tuned circuit is sinusoidal, the collector-circuit waveform is a negative pulse. This keys on transistor T14. The large positive pulse on the collector of T14 is coupled into the base of horizontal-output transistor T15, without inversion, by the stepdown transformer shown. This cuts off T15, causing a large pulse to appear across the yoke windings. This occurs during the horizontal-retrace period. D9 is the usual damper diode, as in a conventional receiver. C46 adjusts the resonant frequency of the yoke system. It is chosen to lengthen the retrace period to the maximum permissible amount, as this reduces the peak pulse voltage occurring during the flyback and materially improves the efficiency of the circuit. Again d-c must be blocked from the yoke windings, hence a choke provides a d-c path for the collector current of T15, and capacitors C42 and C43 couple the collector to the yoke. The horizontal-yoke windings have an inductance of about 1 millihenry and a resistance of about 3 ohms. For good linearity the L/R ratio of the yoke must be as high as possible, the figures given representing about the lowest value of this ratio permissible.

In principle, as a transistor such as T15 really contains a built-in diode in its collector circuit, diode D9, could be omitted. In practice, due to the relatively high forward impedance of the collector-to-base junction of small transistors, better results can be obtained by adding an additional low impedance diode as shown. In higher power deflection circuits using power transistors, the improvement due to the added diode is not as marked.

Associated with the horizontal deflection system is an additional blanking amplifier, T13. The Vidicon requires about 15 to 20 volts of positive blanking signal on its cathode to positively prevent beam landing during the retrace periods under all conditions of beam current and illumination. It is obviously difficult to provide this in a camera in which the maximum supply voltage is 15 volts. For this reason additional blanking is applied to the Vidicon grid to reduce the beam current during the retrace intervals. Diodes D7 and D8 mix positive horizontal pulses from T14 and positive vertical pulses from T7 nonlinearly. (They form an "or gate.") The resultant is applied to the base of T13. Amplified negative blanking pulses at the collector of T13 are applied to the Vidicon grid.

It will be noted that this arrangement, in conjunction with T7, results in the application of positive vertical blanking pulses to the Vidicon cathode and negative mixed blanking pulses to the Vidicon grid. Thus double blanking is supplied during the more critical vertical blanking interval. The vertical blanking interval is the more critical as it encompasses a number of complete horizontal scans during the forward scanning portions of which the beam is moving relatively slowly. On the other hand during the horizontal retrace the beam is always in rapid motion and the resulting current density at the Vidicon target is proportionately lower.

#### *High-Voltage Power Supply*

The Vidicon requires a positive accelerating potential of about 300 volts, a positive focussing voltage adjustable from 250 to 300 and a negative source of bias adjustable from zero to about minus 100 volts for beam current control. All voltages are referred to the Vidicon cathode, which is near ground potential, being returned to the collector of T7. These voltages are supplied by a transistor converter, T17, operating from the minus 15-volt bus which powers all the transistor circuits of the camera. Since battery operation was one of the design objectives, this scheme greatly simplifies the power and switching arrangements. Further, as the converter operates at a high-frequency (15 kilocycles) the size and weight of the required filter components is greatly reduced.

T17 is a transistor square-wave oscillator. Its operating frequency is controlled by the associated transformer. A convenient design procedure is given by Light and Hooker.<sup>2</sup> As a d-c to d-c power converter, the efficiency is high because the transistor is operated as a switch. The waveform at the collector of T17 is nearly square, and its amplitude approaches the supply voltage. The transistor in this circuit thus is switched rapidly between its fully conducting state in which its current is high but the voltage across it nearly zero, and its off state in which its current is zero and the voltage across it is considerable. Under these conditions the power dissipated in the transistor is very low, and over-all efficiencies of the order of 70 to 90 per cent may be achieved.

The voltage at the transistor collector is stepped up in the transformer and applied to two separate rectifier systems. The first, comprising D16 and D17 is a doubler. Its output is regulated by a pair of silicon "zener" diodes, D18 and D19. Two diodes in series are used to reduce the power dissipated in each. The output voltage is adjusted to 280 to 300 volts by selection of the regulator diodes which have fairly wide tolerances as received from the manufacturer. A bleeder comprising R77, R78, and R79 then provides the necessary wall, focus, and target potentials for the Vidicon. The maximum current available from this rectifier system is about 800 microamperes.

Another rectifier, D20, supplies about 100 volts negative to the beam current control, R5. Resistance-capacitance filters are used throughout. It will be noted that some decoupling is provided between the converter and the minus 15-volt bus (R70 and C50); this was necessary to prevent interference from the free-running converter from getting into the video circuits.

#### *Low-Voltage Power Supply*

The camera may be operated either from the a-c line or from batteries. The user has a further option during a-c operation; power for the camera may either be taken from the nearest a-c outlet or it may be sent to the camera from the remote viewing point over the same coaxial cable which carries the r-f output of the camera. During either the local or remote a-c mode of operation the 15-volt bus which operates all the transistor circuits in the camera is energized by a low-voltage regulated supply comprising power transformer XF-1, rectifiers D10-D13, and transistor voltage regulators T18 and T19.

For the remote method of supplying power, plug P1, is inserted

---

<sup>2</sup>L. H. Light and P. M. Hooker, "Transistor DC Converter," *Proc. Inst. Elec. Eng. (Brit.)*, Part B, Vol. 102, p. 775, April, 1955.

into socket S1. This connects the primary of the power transformer across the r-f output connector through a small (8 microhenry) r-f choke. Power is applied to the end of the output coaxial cable remote from the camera by means of an adapter box shown in Figure 6 which interconnects the cable and the remote receiver. Because of the great frequency separation between the camera output radio frequency and the power-line frequency, the simple chokes and capacitors shown effect entirely adequate isolation of the two signals. As the primary current of the power transformer in the camera is only about 45 milliamperes, a considerable length of coaxial cable may be used to interconnect the camera and the remote receiver.

To change over to local a-c operation, plug P2, to which is connected an ordinary line cord, is inserted in socket S1.

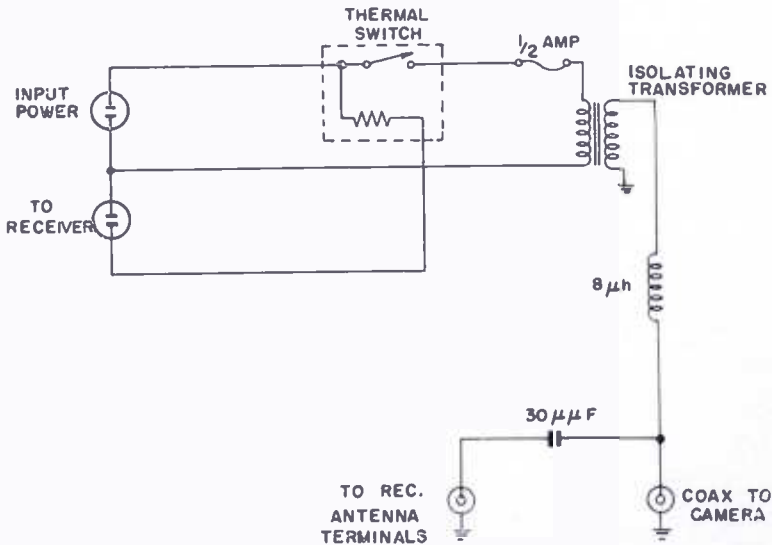


Fig. 6—Circuit of remote adaptor for TTV camera.

In either of the above modes of operation transformer, XF-1, steps down the incoming line voltage to about 24 to 26 volts. This is rectified by the bridge rectifier, D10-D13, and applied to the transistor regulator. Although this circuit looks unconventional, its action is identical to the usual vacuum-tube series regulator. In this case transistor T19 is the series element and T18 is the amplifier. A pair of "zener" diodes provide the necessary voltage reference. The regulator delivers about 150 milliamperes to the 15-volt bus and will hold the output voltage within 0.1 volt of the specified value for any input voltage between 100 and 130. It also reduces the ripple content at the output of the bridge rectifier (about 2 volts) by a factor of about 100. It is apparent that a choke to perform this function would be prohibitively bulky.

The camera may be operated on batteries by inserting plug P3 into S1 and connecting the appropriate batteries to the leads terminating in P3. The power-supply regulator remains in the circuit to hold the voltage of the 15-volt bus constant. Although this wastes some power it greatly increases operating stability.

The total power consumed by the camera is about 5.2 watts during a-c operation. Of this input power about 1.5 watts is dissipated in the power-supply regulator, this dissipation decreasing at lower line voltages. Another watt is used in the heater of the 1/2-inch Vidicon. About 0.5 watt is lost in the power transformer and rectifier system. The remaining 2.2 watts powers all the transistor circuits in the camera. This is less than the heater power alone of many receiving-type vacuum tubes.

### *Miscellaneous*

A few details remain for discussion. The 1/2-inch Vidicon is focussed by means of a permanent-magnet assembly which is simply a scaled down version of a similar assembly used with the 1-inch Vidicon. It is easily fabricated of low precision parts and gives excellent results. It requires no power and also eliminates the coil current regulator circuit which would be required with electromagnetic focus.

A novel feature of the TTV camera is an experimental arrangement for automatically varying the camera sensitivity as a function of the ambient illumination of the scene being viewed. D21 is a photodiode which is arranged at the proper distance behind a hole of suitable diameter in the front surface of the camera so that it "sees" a solid angle identical to that of the camera lens. Increasing light increases the current through the photodiode. This is arranged to reduce the target voltage of the Vidicon, thus reducing its sensitivity. A "zener" diode, D1, provides a d-c level shift in this circuit merely for convenience in selecting appropriate operating points for the Vidicon and the photo-diode. Compensation for ambient illumination changes of the order of 50 to 1 may be provided by this method. The usefulness of such compensation where the camera operator is unskilled or the camera itself inaccessible is obvious.

### THE TRANSISTORIZED "CREEPIE PEEPIE"

The TCP comprises three distinct units, the camera, the monitor (electronic viewfinder), and the backpack. The camera and monitor may be fastened together by means of captive screws during operation, or the viewfinder may be slung around the user's neck on a suitable

lanyard and viewed in a manner similar to a reflex camera. For most shots the viewfinder is left fastened to the camera, but it may occasionally be advantageous to employ the other mode of operation to obtain a picture over the heads of persons in a crowd, as shown in Figure 7.

A block diagram of the equipment is shown in Figure 8. The camera contains a video pre-amplifier, horizontal- and vertical-deflection circuits, and a blanking amplifier in addition to the  $\frac{1}{2}$ -inch



Fig. 7—Operation of the TCP with the monitor detached from the camera.

Vidicon with its yoke and focus magnet. Horizontal-drive pulses, vertical-drive pulses, and mixed blanking pulses, as well as all necessary d-c voltages, are supplied to the camera over a four-foot cable from the backpack. The video signal from the camera video pre-amplifier is sent back to the backpack on a coaxial conductor braided into the same cable.

The monitor contains horizontal- and vertical-deflection circuits and a video amplifier. Most of the space within the monitor case,

which is identical in size to the camera, is taken up by the 1½-inch-diameter monitor tube and its deflection yoke. Appropriate cables carry horizontal drive pulses, vertical drive pulses, and video information to the monitor as well as all necessary d-c voltages.

A switch on the backpack permits the operator to view on the monitor either the video signal at a suitable point in the modulator

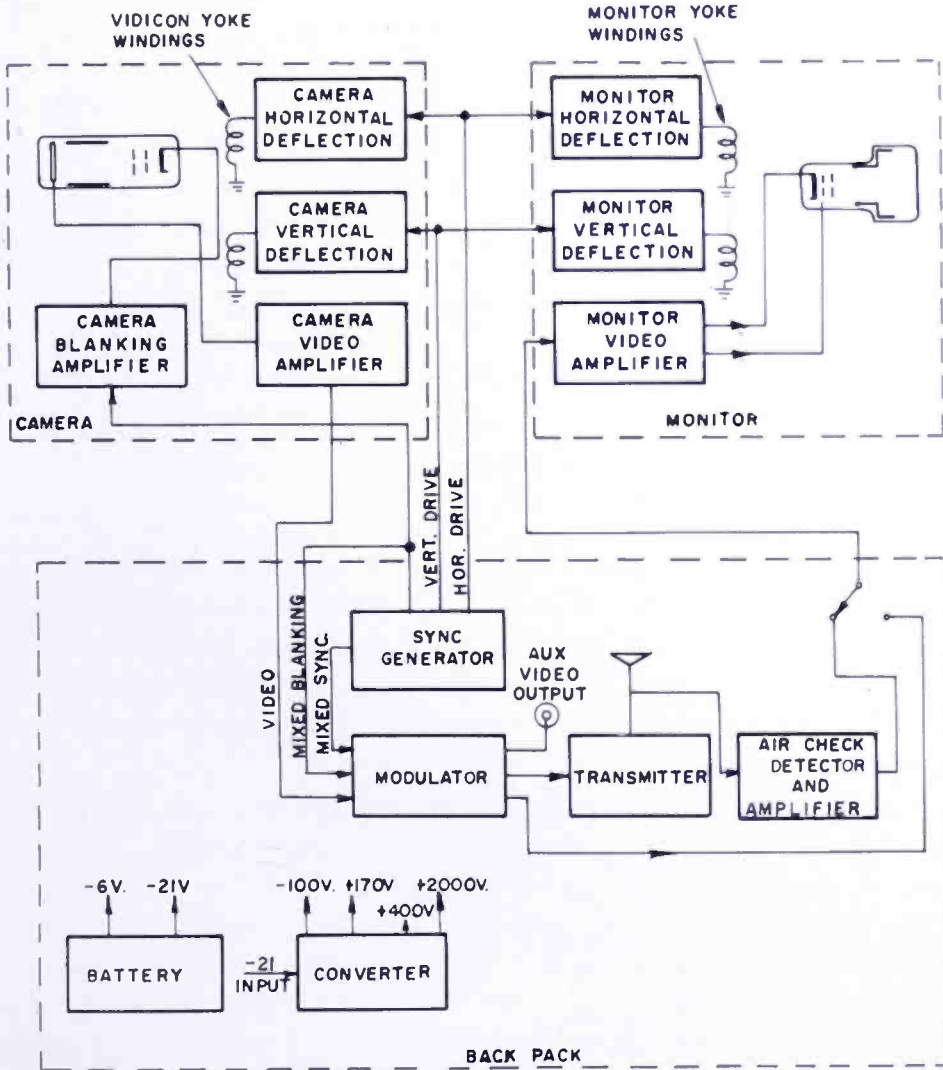


Fig. 8—Block diagram of TCP.

or a rectified and amplified sample of the transmitter output. The latter mode of operation has proven more desirable as it gives the operator an instantaneous indication of transmitter overmodulation. The electronic viewfinder also permits the cameraman to check the vidicon electrical focus. This would be impossible with an ordinary optical viewfinder.

The backpack contains a rechargeable battery which will run the equipment for about five hours; a transistor power converter to supply high-voltage for the camera, monitor and transmitter tubes; a crystal-controlled synchronizing generator; a 2,000-megacycle transmitter; a modulator amplifier in which d-c level setting, sync addition, setup addition, etc. are performed; and a small auxiliary video amplifier and rectifier which samples the transmitter output. The transmitting antenna projects from the top of the backpack.

It is instructive to compare the weight, size, and power data for the TCP with that for a similar vacuum-tube equipment built by the authors several years ago.<sup>3</sup> The TCP camera with its viewfinder weighs 4 pounds. The earlier unit, which used a 1-inch Vidicon and a similar monitor tube, weighed 8 pounds. The backpack unit of the TCP weighs 15 pounds and is 3 by 12 by 13 inches in size. The corresponding part of the earlier equipment weighed 50 pounds and occupied four times the volume. The same equipment consumed nearly 200 watts of power from its batteries which would operate it for about two hours. The TCP consumes 30 watts and operates for nearly five hours from a smaller battery.

### *The TCP Camera*

The camera and monitor are shown with covers removed in Figures 10 and 14. As the heat dissipated in the transistors themselves is negligible, their accessibility has been sacrificed in order to make their socket connections more readily accessible. The deflection circuits occupy the small fixed chassis directly behind the Vidicon assembly.

The circuit of the camera video pre-amplifier is shown in Figure 9. The blanking amplifier is also included in this drawing, as well as the Vidicon beam, focus, and target-voltage controls. As a higher supply voltage, 21 volts, is available in this unit, the Vidicon blanking amplifier presents no problem. T4 is a common emitter amplifier which is connected directly to the Vidicon cathode. Negative mixed blanking signals from the sync generator in the backpack are applied to its base. Twenty volts peak-to-peak of positive mixed blanking are available at its collector, and this is adequate to prevent landing of the Vidicon beam under any conditions during the horizontal and vertical retrace periods.

A somewhat different design philosophy has been adopted in this

---

<sup>3</sup> L. E. Flory, J. E. Dilley, J. M. Morgan, and W. S. Pike, "A Developmental Portable Television Pickup Station," *RCA Review*, Vol. XIII, p. 58, March, 1952.

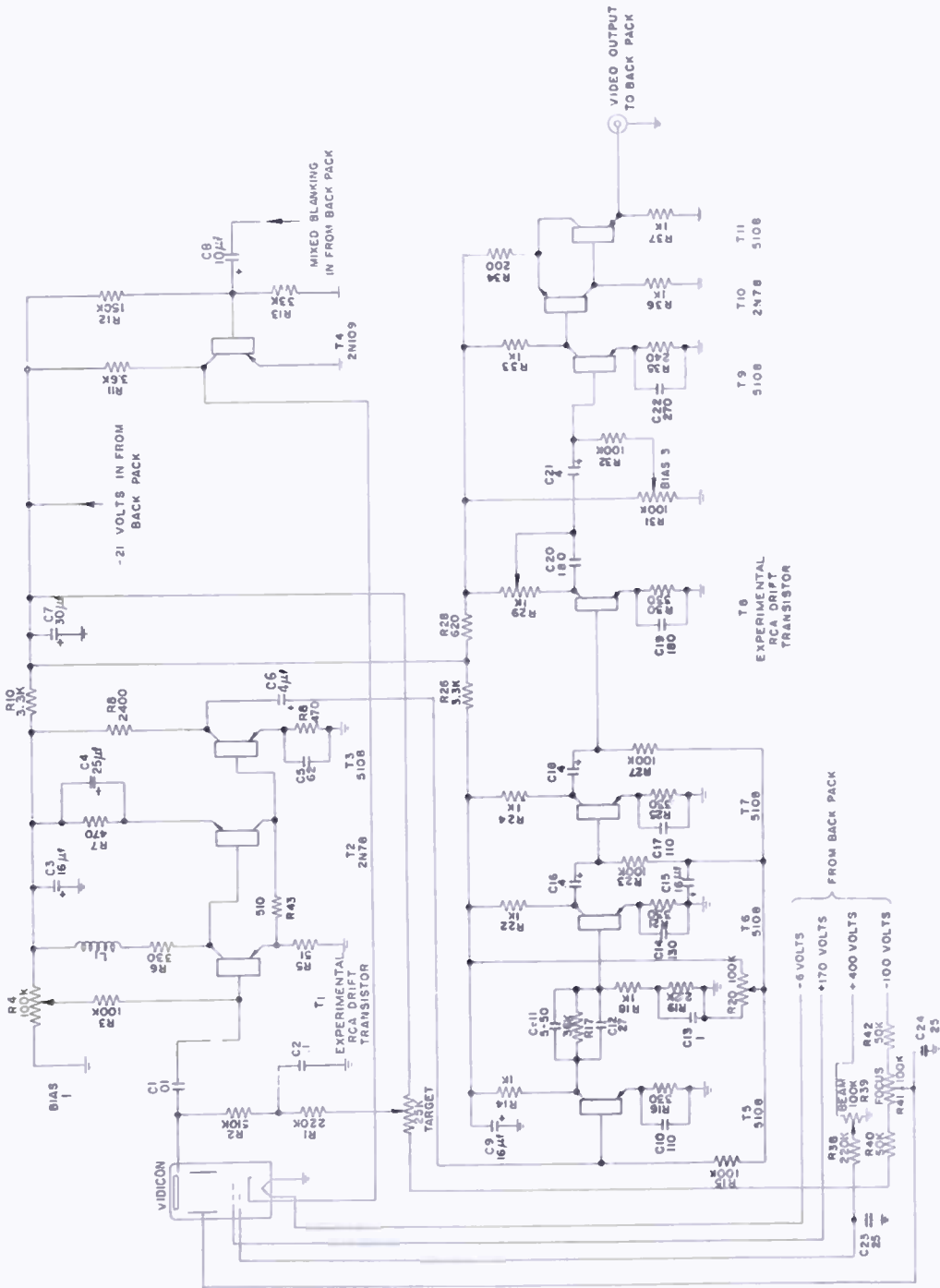


Fig. 9—Camera video and blanking circuits.

video amplifier. Basically, it has been to use a liberal number of transistors in the interests of eliminating peaking coils. The bandwidth of this amplifier is also wider (6 megacycles) than that of the TTV camera.

The input amplifier employs transistors T1, T2, and T3. Transistors T1 and T2 exemplify a type of feedback pair which has been freely used in later stages, particularly in the modulator. It consists of a pair of transistors of opposite conductivities, with feedback from the collector of the second to the emitter of the first. The arrangement is d-c stable, has high input impedance, low output impedance, and either output polarity may be derived from it. In this case the collector of the second transistor is d-c connected to the base of the third. The response of this circuit is maintained flat to 6 megacycles

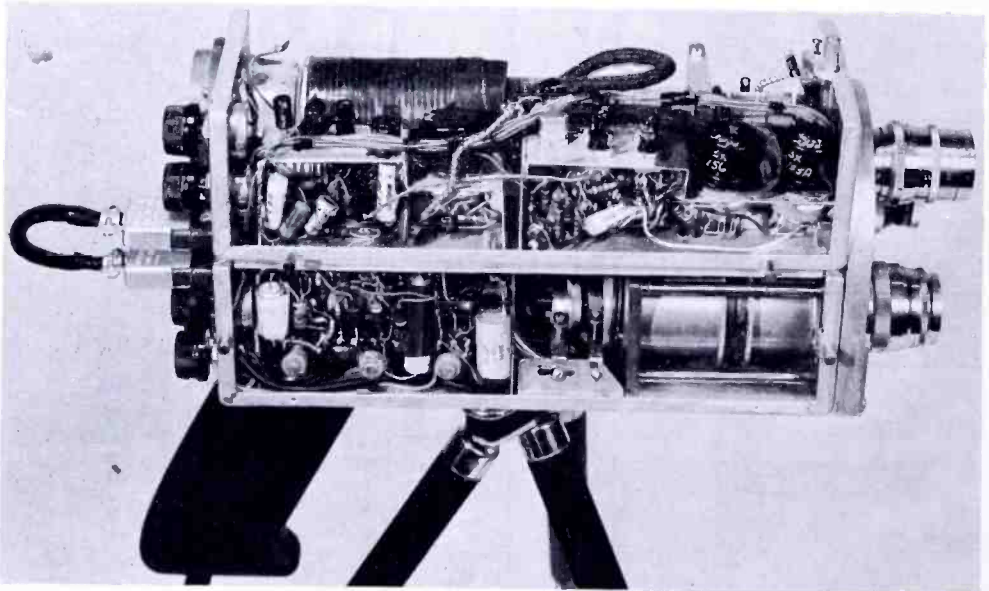


Fig. 10—Right side of camera and monitor.

by means of a peaking inductance, L1, and a capacitor, C5, shunting the emitter resistor of T3. A bias control, R4, is provided to set the operating point for this circuit. This could have been fixed, but was made variable to accommodate different types of transistors. A similar reasoning governs R20 and R31.

The next stage, T5, is an ordinary common-emitter stage which drives the high-peaker. Its high-frequency response is maintained by means of C10. The high-peaker is basically identical to that in the TTV camera with some slight differences in parameters necessitated by the increased bandwidth. Again an over-all low-frequency compensation is provided in this stage by means of C13.

The following four stages, T6 through T9, are ordinary common-

emitter amplifiers. They are, however, overcompensated as far as high-frequency response is concerned, and the cumulative effect of this overcompensation supplies the necessary aperture correction. A video gain control, R29, compensated by a small capacitor, C20, is inserted between T8 and T9. The last two transistors, T10 and T11, comprise another feedback pair which drives the cable connecting the camera and backpack. This feedback pair will deliver about 0.5 volt of 6-megacycle video signal to the 75-ohm line with good linearity. In this case, output is taken from the emitter of the second transistor of the pair.

The camera deflection circuits are shown in Figure 11. They are very similar to those of the TTV camera. The sync generator in the backpack supplies horizontal- and vertical-drive pulses to the camera. The horizontal pulses are negative and the vertical pulses positive. The negative horizontal pulses turn on transistor T31. Amplified positive horizontal pulses appear at its collector. The remainder of the horizontal-deflection circuit is identical to that of the TTV camera.

The vertical-deflection circuit is driven by the positive vertical-drive pulses. These are inverted by transistor T26 which drives a sawtooth generating circuit comprising T27 and its associated components in much the same fashion as in the TTV camera. A complementary symmetry vertical-output stage is not used, the vertical drive to the yoke being provided by two paralleled emitter followers, T29 and T30. Resistors R92 and R93 equalize the currents in these transistors. Again negative feedback is used to assist in linearizing the yoke current and circumventing the shortcomings of the necessarily small coupling capacitor, C41. Although this output circuit is less efficient than that of the TTV camera, it is more stable and exhibits less warm-up drift.

#### *Modulator, Transmitter, and Associated Accessory Circuits*

Before giving attention to the other portions of the system, it seems logical to follow the principal video chain through the equipment to its eventual destination in the transmitter. The modulator and transmitter are located in the backpack and may be seen in the photograph of Figure 17. The circuit diagram is shown in Figure 12.

The transmitter is depicted at the upper right of Figure 12. It is a self-excited cavity stabilized triode oscillator which is grid modulated. A 6442 planar triode is used. The output frequency is adjustable from 1,900 to 2,100 megacycles. The maximum output power with the voltages available in this equipment is about 0.5 watt. A video signal of 1 to 2 volts amplitude is sufficient to modulate the transmitter fully. This is supplied by transistors T12 through T16.

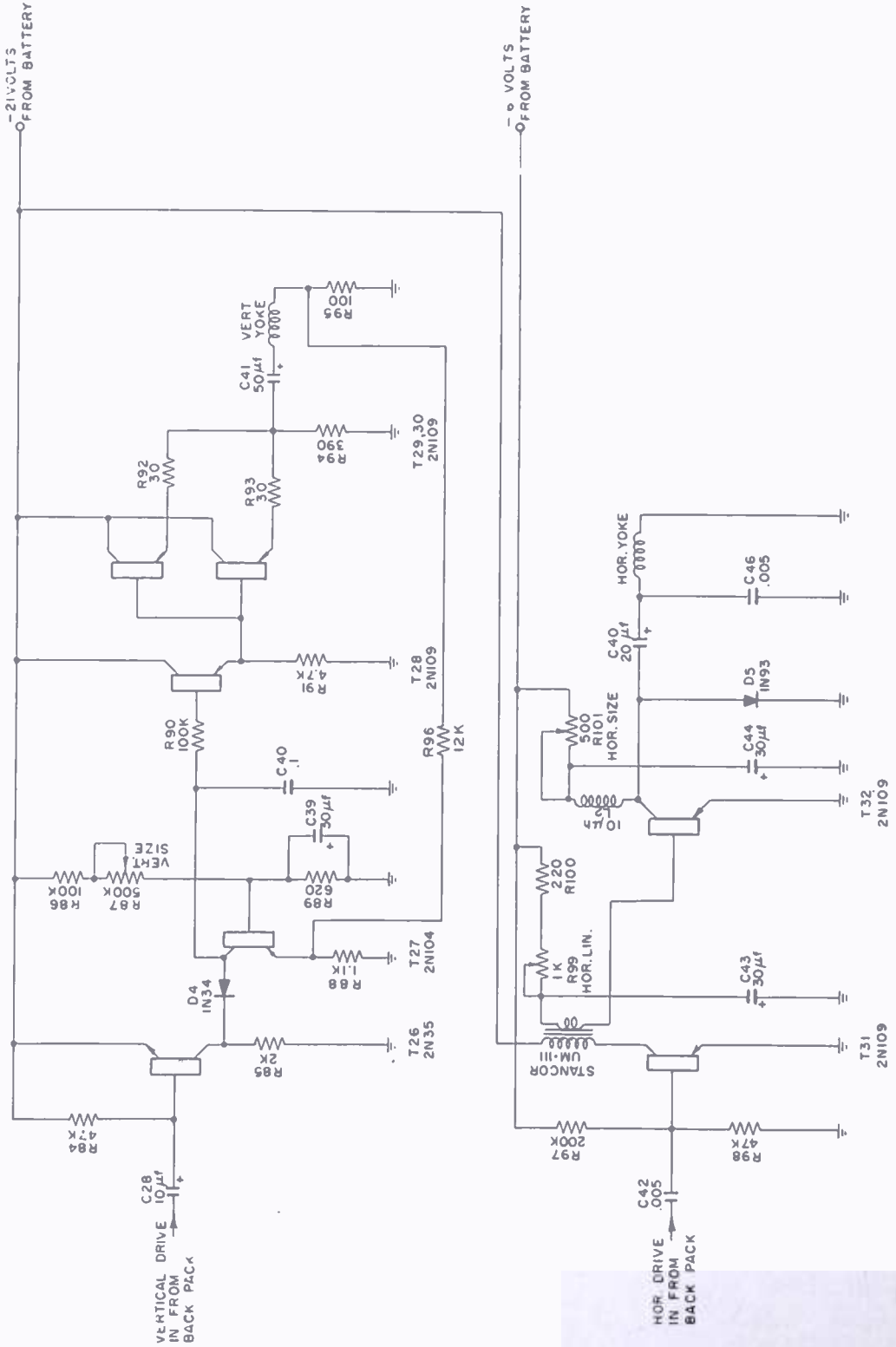


Fig. 11—Camera deflection circuits.

Video signal from the camera pre-amplifier is available across the cable termination, R43. This is coupled into the base of transistor T12 through a relatively small capacitor, C25. A keyed clamp sets the d-c level at this point at the start of each horizontal line. This action is provided by T17, which is turned on by negative mixed blanking pulses applied to its base. In somewhat unconventional fashion this also clamps the base of T12 during the entire vertical-blanking interval. The clamping potential is adjustable by means of R61, which is bypassed by a very large capacitor, C30.

Since d-c information has now been re-inserted into the signal, the following stages must be d-c coupled if this information is to appear in the output signal. By employing alternate n-p-n and p-n-p transistors, a five-stage amplifier of adequate stability has been constructed. The stage gains of this amplifier are not high; the large number of stages has been necessitated by the many other functions which must be performed in it. Mixed sync, for example, from sync amplifier T21 is inserted at the emitter of T12. Adjustable setup is inserted at the base of T14, by feeding in a small amount of mixed blanking of the correct polarity at this point.

T12 and T13 form a feedback pair similar to others previously used. This circuit is advantageous here because it presents a high impedance to the clamp circuit and thus does not discharge capacitor C25. Discharging C25 would cause horizontal shading. T14 has been included to get a low-impedance point from which to drive the auxiliary amplifiers T18 and T19 as well as the actual modulator output stage which comprises another feedback pair, T15 and T16. This stage will deliver about 1.5 volts of video signal to the transmitter.

The remaining transistors are not in the main video chain but perform various auxiliary functions. T18 is an emitter follower which drives the line to the monitor amplifier when the monitor input selector switch is in the "video" position. T19 provides an auxiliary video output if it is desired to operate the TCP into a video line rather than use the transmitter. In this case the transmitter switch may be turned to the "off" position, which removes the load of the transmitter from the various power supplies and correspondingly reduces the total load on the battery. Transistors T22 and T23 amplify the output of diode D1 which rectifies a sample of the transmitter output. When the monitor input selector switch is in the "air check" position, the output of this amplifier drives the video line to the monitor.

Transistor T20 is a special regulator which assists in maintaining the correct operating point of the transmitter as the batteries dis-

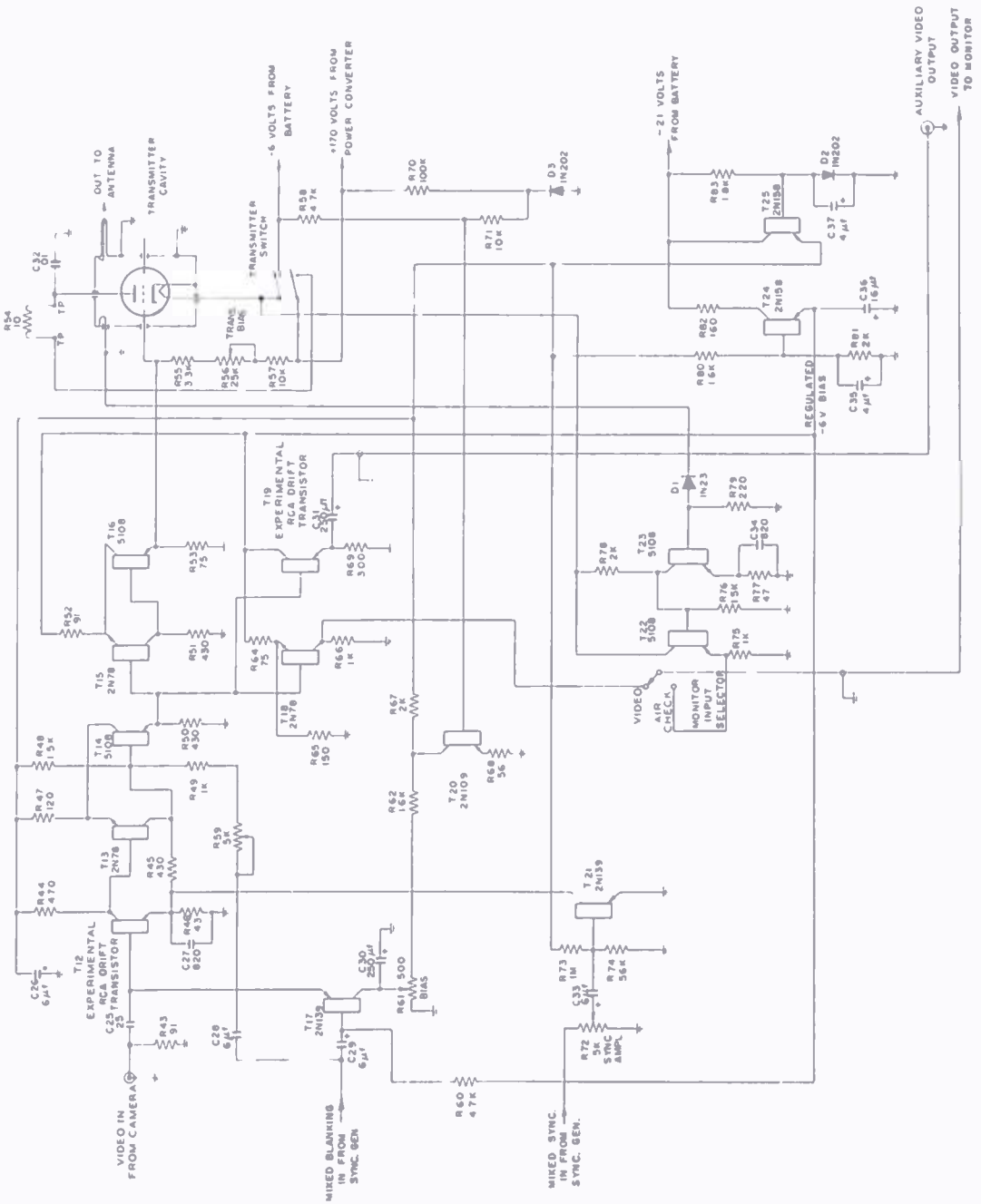


Fig. 12—Modulator circuit.

charge during operation. It was found that as the 6-volt portion of the battery discharged, the slight change in the voltage of the transmitter heater was sufficient to upset its operating point. As regulation of the 0.9-ampere current of this heater would be a difficult task, other means to correct this difficulty were sought. It was found that a slight readjustment of the transmitter bias would accomplish the necessary correction, but that the sense of the requisite bias change was opposite to the sense of the change of heater voltage causing the trouble. Transistor T20 accomplishes the necessary sense reversal. Its base is connected to the 6-volt battery through a network comprising R58, R70, R71, and D3. This network sets the base potential of T20 at the correct d-c operating point.

The collector of T20 is connected to the potentiometer which sets the clamp potential, thus inserting the required correction at this point. D-C degeneration in this compensating circuit is provided by R68, by means of which the loop gain of the circuit has been adjusted to maintain nearly perfect compensation during the useful operating life of the battery.

For stability reasons it is also necessary to regulate the supply voltages of all these amplifiers. Regulated buses of six and twelve volts are supplied. The twelve-volt regulator comprises emitter follower T25, the base potential of which is set by "zener" diode, D2. The 6-volt regulator is T24, the base potential of which is set by a potentiometer across the regulated 12-volt supply.

### *The Monitor*

The monitor is shown in Figures 10 and 14 and its circuit diagram in Figure 13. No suitable commercially available cathode-ray tube could be found for this unit, hence a special 1½-inch tube was constructed. It is magnetically deflected and electrostatically focussed. With an ultor voltage of 2,000 volts, its resolution exceeds 300 lines. It fits the standard 1-inch Vidicon yoke and about 400 milliamperes peak-to-peak horizontal-deflection current must be supplied to produce a raster of adequate size at the ultor voltage specified.

The deflection circuits are very similar to those in the TTV camera but employ larger output transistors. In the vertical circuit, complementary symmetry and negative feedback are used as before. In this circuit T37 and T38 are power transistors with rated dissipations of 1 watt each, without heat sinks.

Video signal from the backpack is amplified by transistors T42 and T43. This circuit is a transistor version of the familiar vacuum-tube "long-tailed pair." It provides a push-pull output with which the cathode and grid of the monitor are simultaneously driven in anti-

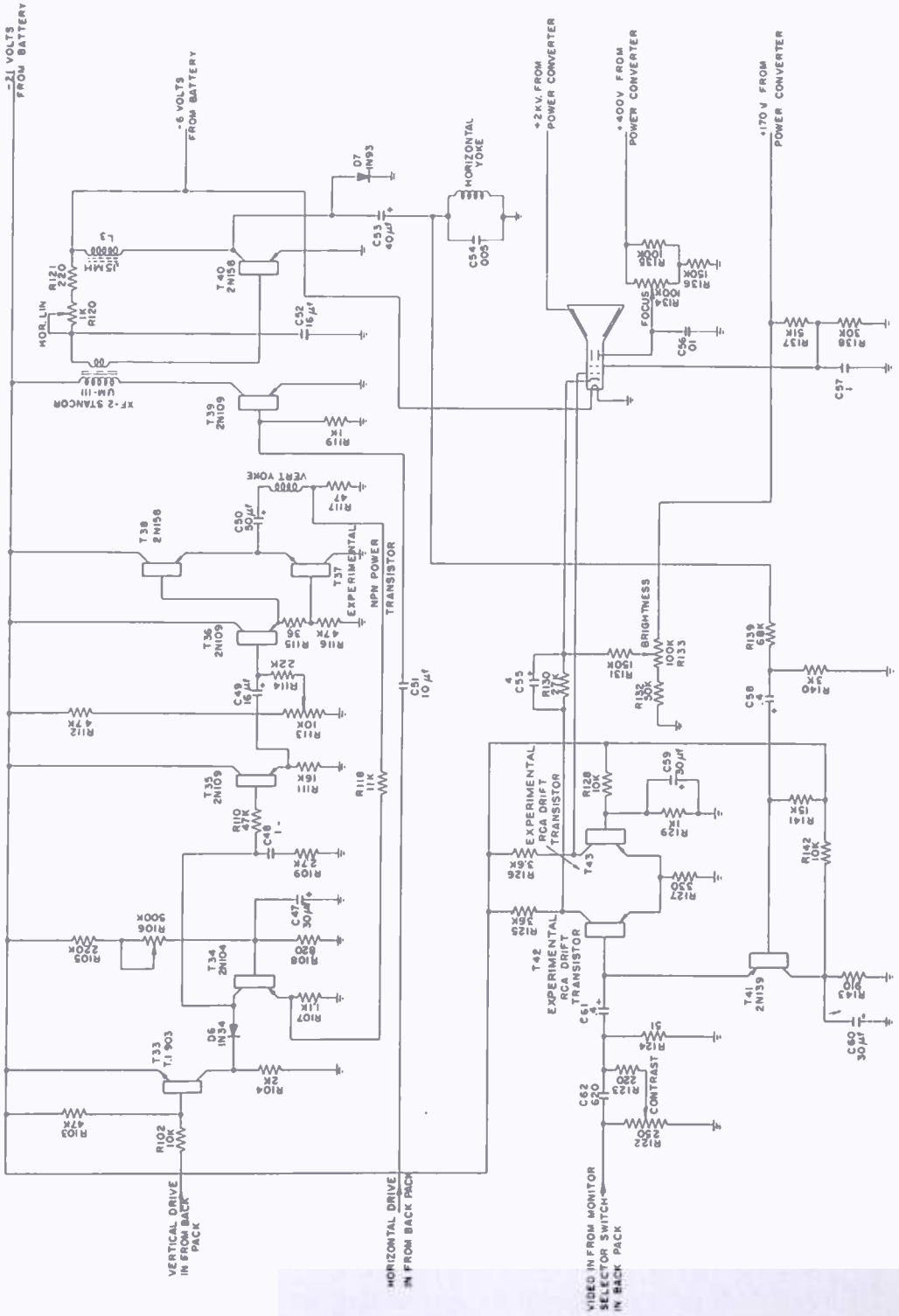


Fig. 13—Monitor circuit.

phase. By this means the effective video drive on the monitor is made about 35 volts peak-to-peak, a value difficult to achieve by other means due to the voltage and power limitations of available high-frequency transistors. T41 is a driven clamp which sets the d-c level of the monitor amplifier. It is identical to that in the modulator, except that only horizontal pulses from the monitor horizontal deflection circuit are used to drive it. Slightly better high-frequency response could have been achieved in this amplifier by incorporating peaking coils

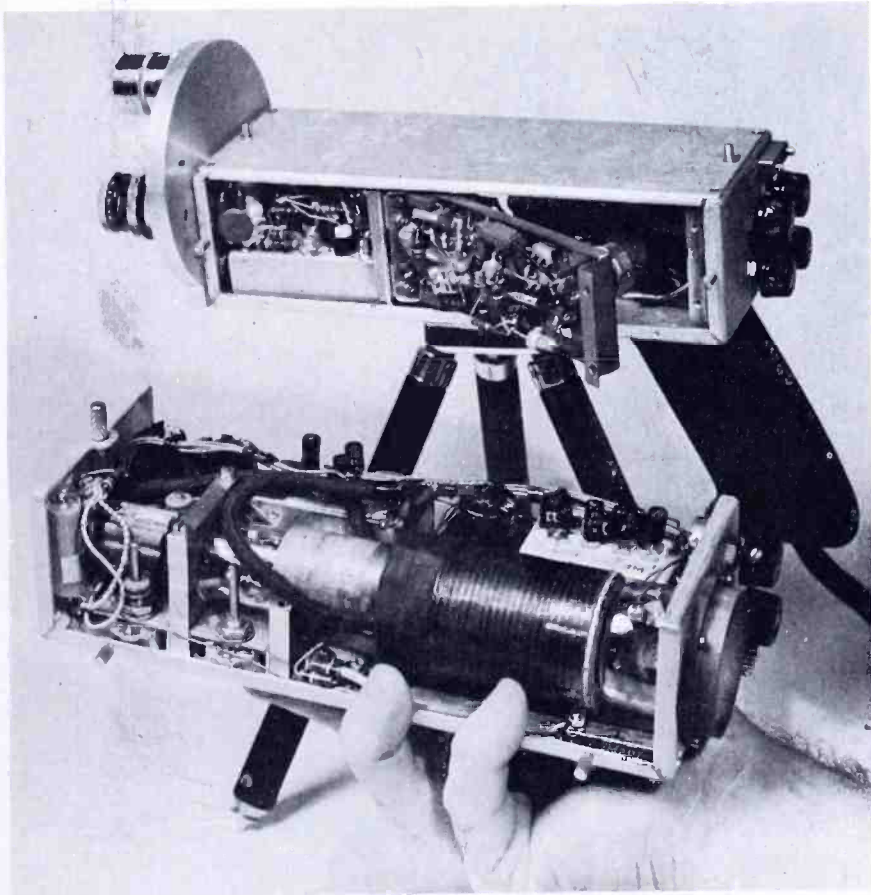
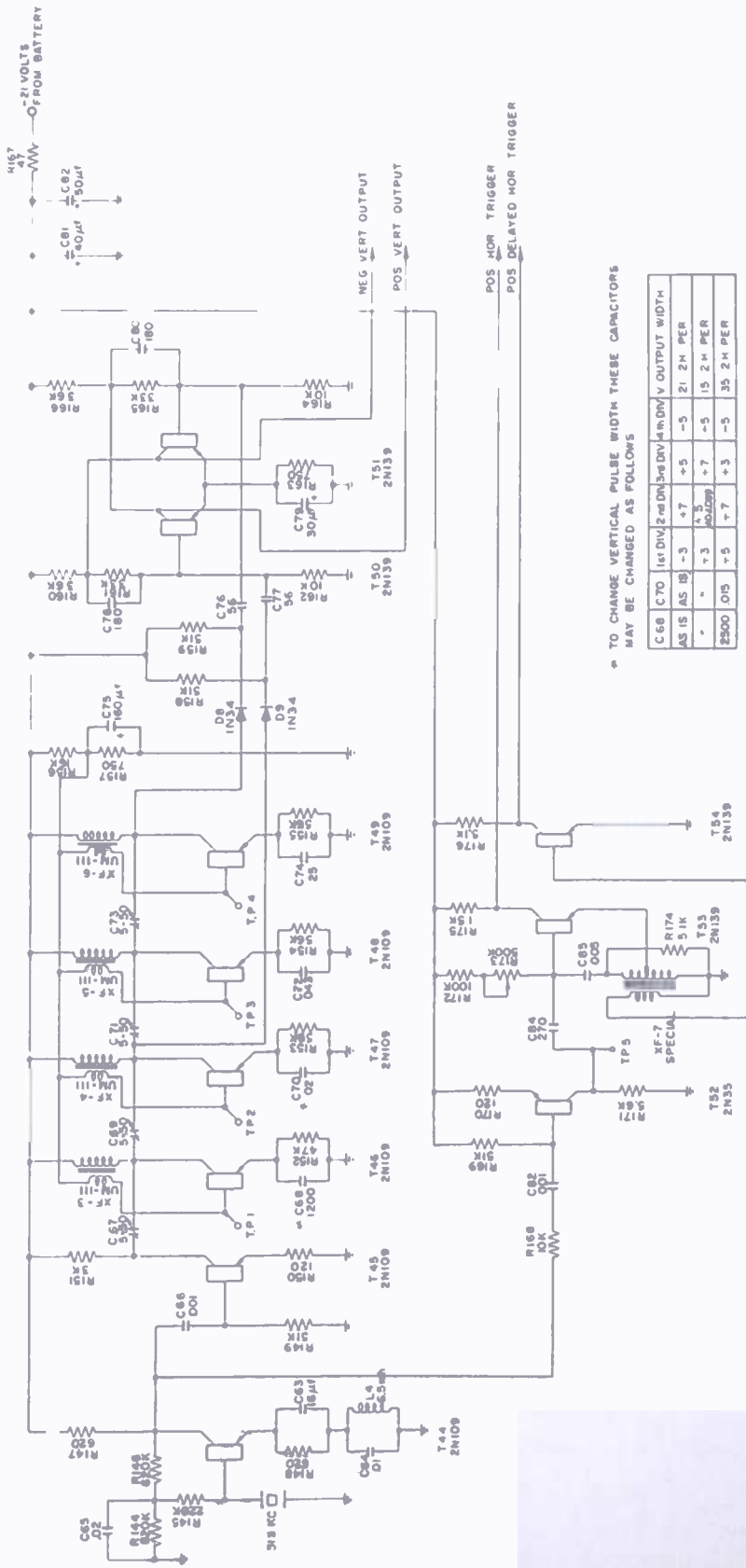


Fig. 14—Left side of camera and monitor.

in the collectors of T42 and T43, but as the response was adequate and space limited, they were omitted.

### *Synchronizing Generator*

The synchronizing generator is located in the backpack. It is in two sections, the master oscillator and divider chain comprising the first, and the waveshaping circuits and line drivers the second. Figures 15 and 16 show the circuits of these units, while the synchronizing generator may be seen in the photograph of Figure 17. Only the chassis containing the master oscillator and divider chain is visible



TO CHANGE VERTICAL PULSE WIDTH THESE CAPACITORS MAY BE CHANGED AS FOLLOWS

| C68      | C70   | 1st DIV | 2nd DIV | 3rd DIV | 4th DIV | 5th DIV | OUTPUT WIDTH |
|----------|-------|---------|---------|---------|---------|---------|--------------|
| AS IS    | AS IS | -3      | +7      | +5      | -5      | -5      | 21.2 M PER   |
| -        | -     | +3      | +5      | +7      | -5      | -5      | 15.2 M PER   |
| 2500 LOS | -5    | +7      | +3      | -5      | -5      | -5      | 35.2 M PER   |

Fig. 15—Sync generator divider schematic.

in this photograph; the waveshaper and line amplifiers are directly behind this unit.

The master oscillator, T44, is crystal controlled, and operates at 31.5 kilocycles. It is a negative-resistance oscillator. The emitter tuned circuit appears capacitive at the operating frequency. Under these conditions, a large negative resistance is developed in series with the crystal in the base circuit, and oscillation takes place at the crystal frequency.

Output from the master oscillator is taken across a small resistor, R147, in the collector circuit to drive a pair of isolation amplifiers, T 52 and T45. The horizontal divider, which divides by 2, comprises transistor T53 and associated circuits. It is a blocking oscillator using an autotransformer wound on a small toroidal ferrite core. A positive pulse of a few volts amplitude and about 1.5 microseconds duration appears at the collector of T53 each time the blocking oscillator fires. This is called the positive horizontal trigger and is used, after some processing, to initiate the leading edge of the horizontal blanking and drive pulses.

A delayed trigger pulse is derived from transistor T54. An auxiliary winding on XF-7 drives this transistor. The waveform on this winding is a considerably distorted single cycle of a sine wave, the width of each half-cycle being about 1.5 microseconds. The winding is so poled that the positive-going half cycle occurs first. T54 does not conduct during this portion of the cycle. On the following negative half-cycle, however, it does conduct, and a positive pulse is generated at its collector. This pulse is delayed with respect to the pulse from the collector to T53 by about 1.5 microseconds, and is used as the delayed horizontal trigger pulse. The leading edges of the horizontal synchronizing pulses and the serrations in the vertical synchronizing pulses are derived from this delayed trigger. This scheme will be seen to set the width of the "front porch" of the composite video output of the TCP at 1.5 microseconds, or the amount by which the delayed horizontal trigger lags the undelayed trigger.

The vertical divider chain comprises transistors T46-T49. Each of these is a blocking oscillator in which the feedback is from collector to base, and the RC circuit which controls the repetition frequency is in the emitter. The temperature stability of this circuit is superior to that of arrangements in which the frequency-determining elements are in the base circuit because it isolates these elements from the effects of the temperature-dependent base-to-collector leakage current ( $I_{co}$ ). As space is limited in the sync generator, the frequency-determining elements of each divider are fixed, and the amount of

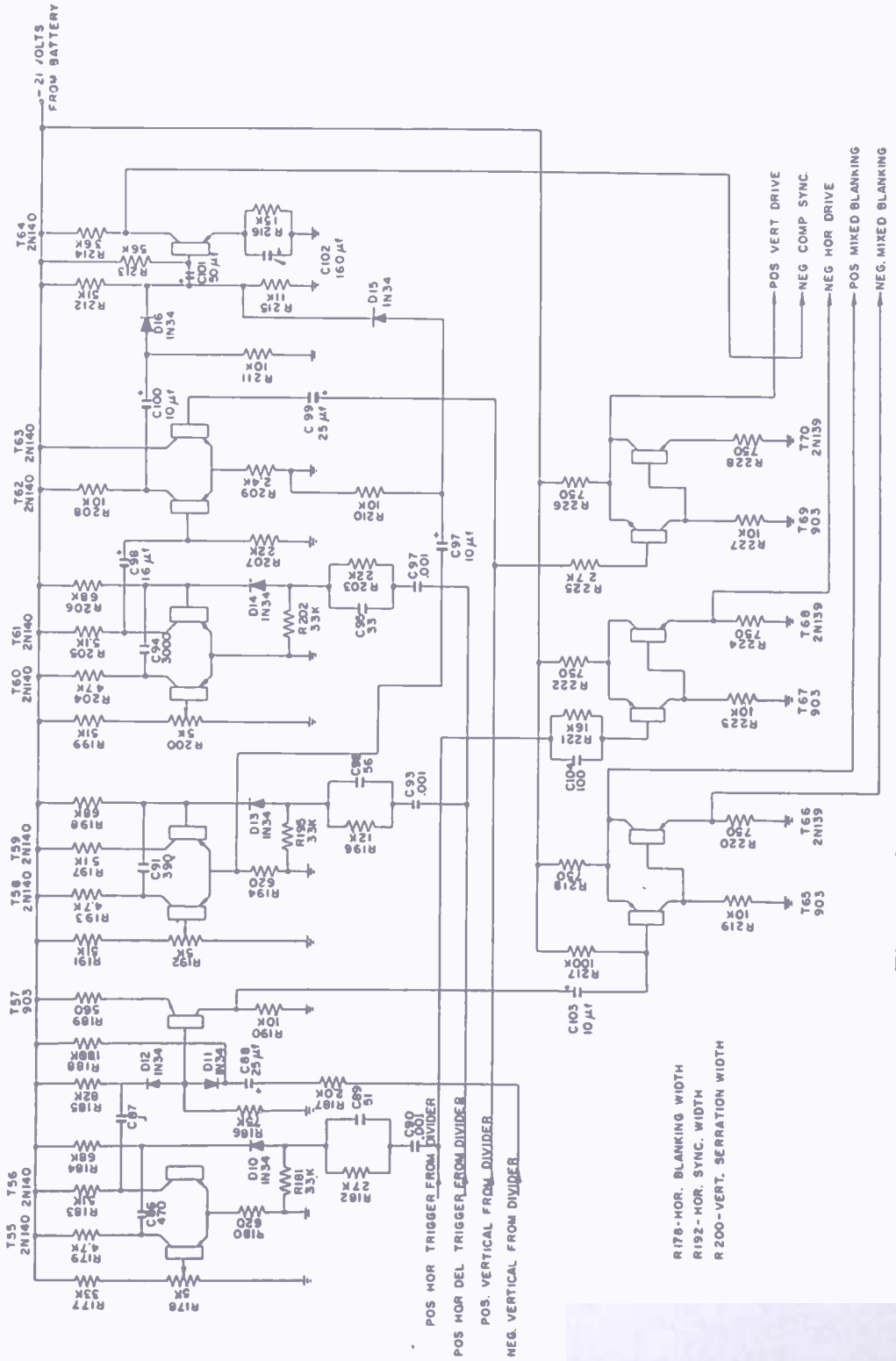


Fig. 16—Sync generator waveshaper schematic.

sync injection has been made adjustable to control the division ratio. The small capacitors C67, C69, C71, and C73 used for this purpose require appreciably less space than the adjustable potentiometers which would otherwise have to be used. A common voltage divider, R156 and R157, biases all the divider stages.

The vertical-frequency pulses at the output of the last divider, T49, are too narrow to be used directly. Vertical pulses of the desired width are generated by a bistable flip-flop comprising transistors T50 and T51. Each time T49 fires, a pulse from its collector cuts off T51. The usual regenerative action in the flip-flop assists this and, of course, turns on T50. The arrangement is such that this action may be reversed on either the 15th, the 21st, or the 35th subsequent cycle

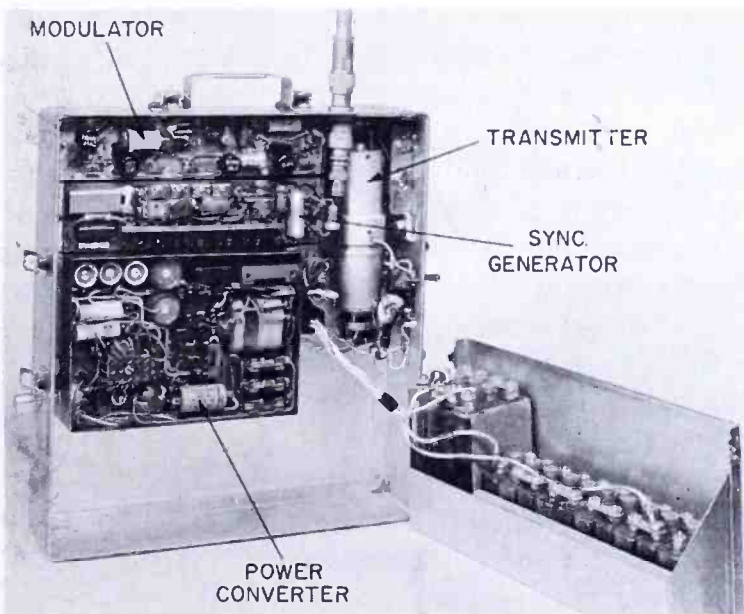


Fig. 17—Backpack opened.

of the 2H oscillator by a pulse taken from the collector of the second divider, T47, and fed to T50. This scheme causes the flip-flop to generate clean positive and negative vertical pulses the width of which can be set at  $7\frac{1}{2}$ ,  $10\frac{1}{2}$ , or  $17\frac{1}{2}$  horizontal lines by adjustment of the order in which the usual divisors of 3, 5, 5, and 7 are assigned to the various dividers. The table included as a part of Figure 15 shows the arrangement used in each case.

The output pulses from the divider chain thus consists of four kinds of pulses: positive horizontal trigger pulses, positive delayed horizontal trigger pulses, negative vertical pulses, and positive vertical pulses. The waveshaper, shown in Figure 16, synthesizes the following signals from these trigger pulses:

- (a) Positive vertical drive pulses;
- (b) Negative horizontal drive pulses;
- (c) Positive and negative mixed blanking pulses;
- (d) Negative composite sync pulses.

The formation of these signals will now be discussed.

Vertical drive pulses are formed from the positive vertical pulses at the divider output by an amplifier and line driver comprising transistors T69 and T70. These are connected in the same feedback pair configuration used in the monitor. This amplifier makes positive vertical pulses of about 5 volts amplitude available at a relatively low impedance.

Horizontal drive pulses are formed by an identical amplifier driven from the undelayed horizontal trigger pulses at the divider output. This amplifier comprises transistors T67 and T68.

The mixed blanking signals are synthesized from the undelayed horizontal trigger pulses and the negative vertical pulses from the divider by transistors T55, T56, T57, T65, and T66. T55 and T56 form a monostable emitter-coupled multivibrator which determines the horizontal blanking width. In this circuit, T55 is normally off and T56 on. Horizontal trigger pulses are applied to the base of T56 via diode D10. Each pulse turns off T56 and turns on T55 by the usual regenerative action. The circuit remains in this state for a period of time determined by the time constant, C86, R184 and the voltage at the slider of R178. It then flips back to its original state. Adjustment of R178 varies the horizontal blanking pulse width between the limits of 5 and 15 microseconds.

Negative horizontal-blanking pulses from the collector of T56 are mixed with the negative vertical pulses from the divider in an "or gate" comprising D11 and D12. The output of this gate is applied to the emitter follower, T56, and then to a line driver, T65 and T66. Both polarities of mixed blanking are available from this line driver.

It is to be noted that the three outputs from the sync generator which have just been treated must be transmitted via cable to the camera and monitor. It is for this reason that line-driving amplifiers must be provided for these signals.

The remaining transistors, T58 through T64, are employed in generating the composite sync signal. It is nonstandard in that there are no equalizing pulses, the vertical synchronizing interval is the same length as vertical blanking, and there are serrations in the vertical sync pulses at horizontal frequency. The form of this signal is shown in Figure 18.

The synchronizing signals are synthesized from the delayed horizontal-trigger pulses and the positive vertical pulses from the divider chain. A monostable multivibrator, T58 and T59, similar to that used to generate horizontal blanking pulses, generates horizontal sync pulses adjustable in width between the limits of 5 and 8 microseconds. A similar multivibrator, T60 and T61, generates serration pulses of about 40 microseconds width. The output of the serration multi-

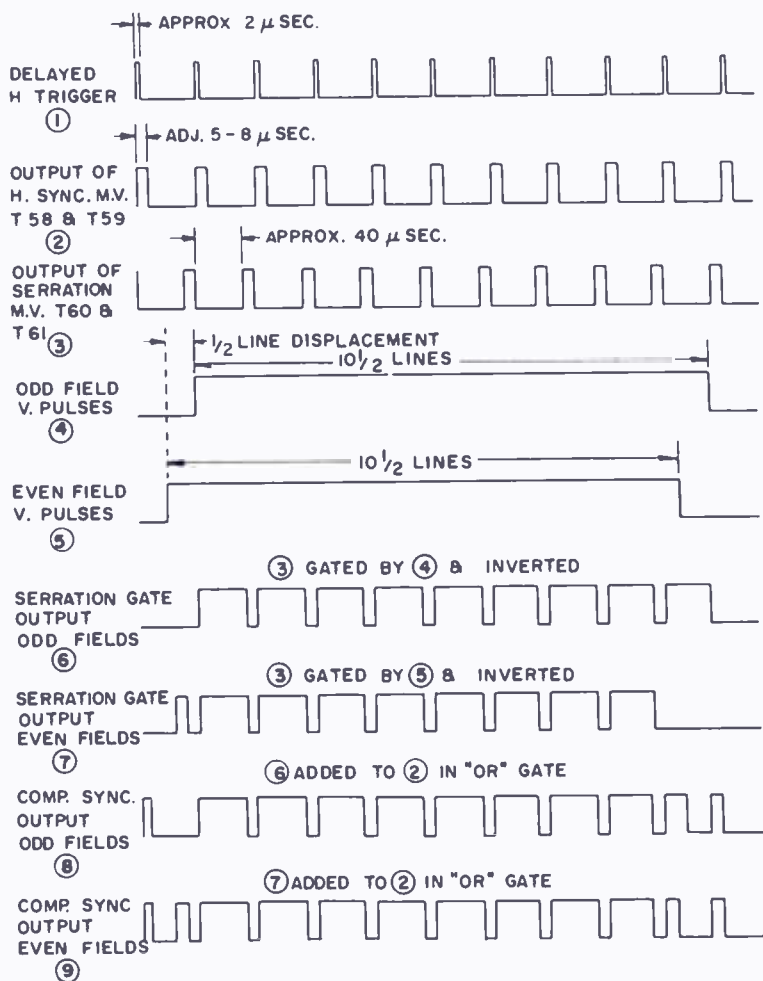


Fig. 18—Sync pulse diagram.

vibrator is gated by a serration gate comprising T62 and T63. This gate is open only during the vertical pulses from the divider. The output of the serration gate thus consists of bursts of serration pulses which are timed to occur during each vertical pulse from the divider. This signal is mixed with the output from the horizontal sync multivibrator in another "or gate" comprising diodes D15 and D16. It is then amplified and clipped by the sync output amplifier, T64. Figure 18 shows the various waveforms occurring in these circuits.



In the diagram of Figure 19, transformer XF-8 is wound on a small toroidal core and need handle only the driving power for the base circuits of the transistors. A 1,000-cycle square wave of about 90 volts peak-to-peak amplitude appears from collector to collector of transistors T71 and T72. This signal is applied to the power transformer XF-9 which steps it up to several different voltages.

Most of the power from the converter is delivered to the +170-volt bus, on which the principal load is the transmitter. The latter requires about 50 milliamperes. This is supplied by a full-wave rectifier comprising diodes D20-D23 and filtered by L6, C115, and C116. The ultor voltage for the monitor tube, 2,000 volts, is supplied by a doubler comprising D18 and D19, driven by an additional winding. The 400-volt bus which supplies accelerating and focus potentials for the Vidicon and monitor is served by a tripler comprising diodes D24-D28. The minus 100-volt bus, which is used only for bias on the Vidicon, is fed by a half-wave rectifier, D29. The over-all efficiency of this power converter is about 90 per cent.

#### *Miscellaneous*

Primary power for the entire TCP unit is supplied by a bank of silver-alkalai storage cells. Four cells are connected in series to supply the 6-volt bus which powers the heaters of the tubes and portions of the horizontal-deflection circuits. Nine additional cells of smaller size are connected in series with the 6-volt portion of the battery to power the 21-volt bus. The flat voltage characteristic of these cells during discharge is very helpful in maintaining stable operation of the more critical circuits, such as the sync generator dividers. This battery complement will run the TCP unit for about five hours before recharging becomes necessary.

#### CONCLUSIONS

Two transistorized camera equipments have been constructed and extensively operated. One is a simple camera which may be attached to any home television receiver to form a complete closed-circuit television chain. The other is, in effect, a complete portable television transmitting station which will generate a picture of adequate quality for remote broadcast purposes and transmit it for a distance of about one mile. These two units show that present-day transistors make possible operating performance in such equipment which cannot be achieved with vacuum tubes within the same limitations of weight and power. It is also of interest to note in passing that, except for the pre-production drift transistors used in the video amplifiers, com-

mercially available transistors either were used in each socket or are available for use.

Near the conclusion of the development of these cameras, the production version of the drift transistor (2N247) became available. The limited sample of 2N247's which have been tested to date worked quite well in the TCP circuits, but there are indications that some readjustments might be required if 2N247's were to be used in the TTV equipment.

The TCP unit has been used experimentally by the National Broadcasting Company in covering the recent political conventions, and has transmitted excellent pictures under difficult conditions from various sites in and around the two convention halls.

The TTV unit potentially supplies the answer to the quest for an extremely compact low power, low cost pickup unit which could convert any home receiver to a closed-circuit television system.

#### ACKNOWLEDGMENTS

The authors wish to acknowledge the direction of V. K. Zworykin in this project and the cooperation of A. D. Cope who supplied the miniature Vidicons. They wish further to mention the assistance of Lawrence A. Boyer whose skill in design and construction has contributed materially to the success of the work.

# VIEWING STORAGE TUBES FOR LARGE DISPLAYS\*

BY

H. O. HOOK,\*\* M. KNOLL,† AND R. P. STONE#

*Summary*—This paper describes two experimental viewing storage tubes which provide large displays. The first type, contained in a 15-inch metal envelope, provides a directly viewed display 10 inches in diameter with 250 foot-lamberts highlight brightness. The second is a projection storage tube which uses reflective optics to provide a four-foot-diameter radar display with 2 foot-lamberts highlight brightness. The resolution for both displays is better than 500 lines. These tubes extend the advantages of smaller viewing storage tubes to applications requiring large displays.

## INTRODUCTION

A HALFTONE VIEWING storage tube with 4-inch picture size, described in previous publications,<sup>1-4</sup> has been found particularly useful in aircraft radar for daylight operation<sup>5</sup> as well as for storage of single television frames<sup>3</sup> and oscilloscope patterns.<sup>4</sup> Because larger pictures are desirable for certain radar displays, e.g., for traffic monitoring at airports, for shipboard applications, and for certain television and telemetering applications, a 10-inch direct-view storage tube and a projection-type storage tube have been developed.

---

\* The work described in this paper was supported by a Signal Corps contract DA 36-039-sc-64572.

\*\* RCA Laboratories, Princeton, N. J.

† Formerly RCA Laboratories, Princeton, N. J.; now with the Technischen Hochschule, Munich, Germany.

# Formerly RCA Laboratories, Princeton, N. J.; now with the RCA Tube Division, Lancaster, Pa.

<sup>1</sup> M. Knoll, "Electron-Lens Raster Systems," National Bureau of Standards Circular 527, p. 329, March, 1954.

<sup>2</sup> M. Knoll and P. Rudnick, "Direct View Storage Tube," National Bureau of Standards Circular 527, p. 339, March, 1954.

<sup>3</sup> M. Knoll, P. Rudnick, and H. O. Hook, "Viewing Storage Tube With Halftone Display," *RCA Review*, Vol. XIV, p. 492, December, 1953.

<sup>4</sup> M. Knoll, H. O. Hook, and R. P. Stone, "Characteristics of a Transmission Control Viewing Storage Tube with Halftone Display," *Proc. I.R.E.*, Vol. 42, p. 1496, October, 1954.

<sup>5</sup> C. E. Reeder, "Evaluation of the Direct-View Storage Tube," presented before the PGED of the I.R.E., October 24, 1955 at Washington, D. C.

## TEN-INCH-TARGET DIRECT-VIEW STORAGE TUBE

An experimental version of the direct-view storage tube with a flat storage target and a 10-inch-diameter viewing screen is shown in Figures 1 and 2.

The metal envelope is equipped with a faceplate and neck of soft glass. Both the spread angle of the viewing beam and the total deflection angle of the writing beam are 42 degrees rather than 27 degrees as in the 4-inch flat-screen tube. The axes of the writing and viewing guns are parallel to and displaced  $\frac{1}{4}$  inch from the tube axis. After the image-amplifier section is mounted on the chrome-iron cone, the envelope is closed by heliarc-welding the top cap in place. Supported



Fig. 1—Direct-view storage tube with 10-inch-diameter target.

within the conical section of the envelope is a conical electrode which forms a double-condenser lens.

The target structure consists of two grids and a luminescent screen supported by a cold-rolled steel ring. The collector grid ( $G_1$ ) composed of 230-mesh woven stainless steel is welded directly to the support ring. The storage grid ( $G_2$ ), which consists of 100-mesh electro-formed nickel formed on a stainless-steel ring, and the Pyrex-plate luminescent screen are secured to the principal support by machine screws and ceramic spacers.

The storage grid is prepared by evaporating magnesium fluoride from three platinum "boats" onto the heated nickel mesh in a vacuum of approximately  $10^{-4}$  mm Hg. These boats are arranged in a triangle with their centers about three inches from the center of the array,

the top of which is about 14 inches below the mesh. The thickness of the evaporated layers is uniform to within 10 per cent.

Such large direct-view tubes are capable of reproducing at least 4 halftones with a highlight brightness of 300 foot-lamberts at 10-kilovolt phosphor potential. The resolution is at least 400 lines per target diameter, although picture uniformity is poorer than in the smaller tubes. Because of the wide divergence angle of the viewing beam, strong electron lenses are required to make the beam arrive normal to the storage grid; the aberrations of these lenses (Figure 11a) account for much of the 10 to 15 per cent variation in storage-

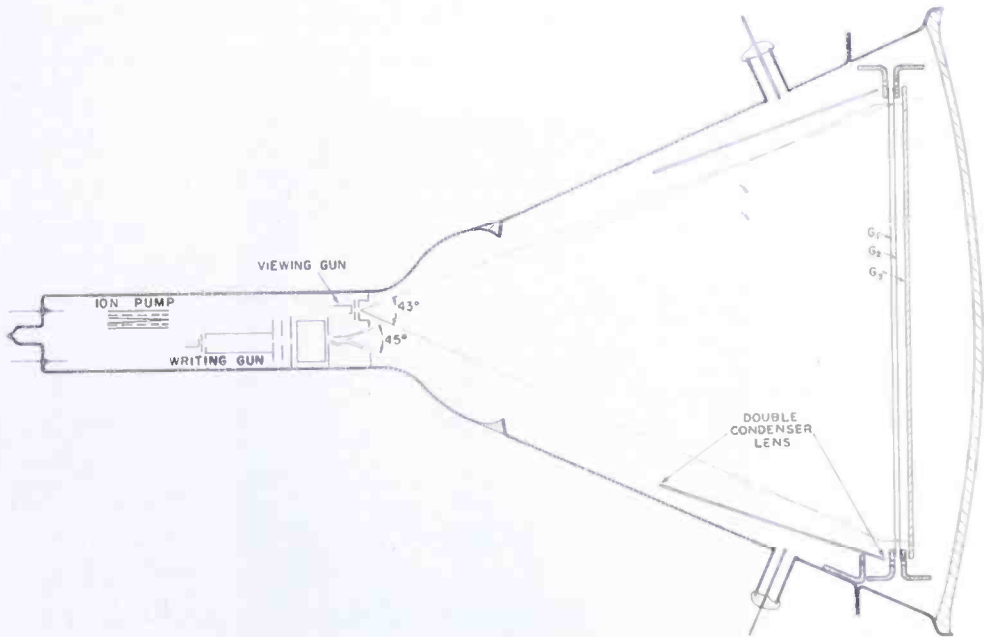


Fig. 2—Large-screen storage tube.

grid cutoff voltage.\* This variation can be reduced to 5 to 8 per cent by operating with an 8-inch display (Figure 11b) instead of a 10-inch display. This not only reduces lens strength but also the area of the lens used. (The 4-inch tubes showed a variation of 8 to 10 per cent.) Figure 3 is a photograph of a test-pattern display 10 inches in diameter.

Although satisfactory results have been achieved with the flat target structure, experience with 4-inch tubes indicates that curved screens will give better uniformity and higher brightness as well as improved mechanical and thermal stability. These results should apply to larger tubes also. The reasons for this assumption are discussed more fully in the following section.

\* The difference between the cutoff voltages for the darkest and brightest areas of the viewed pattern without a written picture expressed as a percentage of their mean is used as a measure of nonuniformity.

## STORAGE TUBE WITH SPHERICAL IMAGE AMPLIFIER

*Description*

Figure 4 is a schematic representation of the experimental projection storage tube. To match the reflective optical system of the 5TP4 projection kinescopes, which was used for the experiment, a curved luminescent screen with a 7.1-inch radius of curvature was employed. In addition, a curved storage target and an approximately concentric collector grid were used; these permit normal incidence of the viewing beam without an electron condenser lens or with a very weak one. The crossover of the viewing gun was near the center of curvature of the collector and storage grids. Minor electron-optical corrections may be achieved by making the curvature of the grids non-concentric with

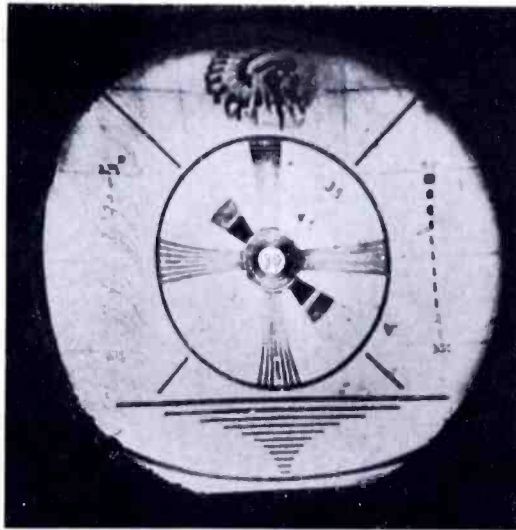


Fig. 3—Photograph of test pattern on 10-inch direct-view storage tube.

the curvature of the luminescent screen. In general, the functions of the collector grid, storage grid, and the luminescent screen (final anode) as well as the functions of the writing, viewing, and erasing guns are similar to those already described for the viewing storage tube with a flat-image amplifier.<sup>4</sup> Also, the electron paths in the electron lens raster system are similar to those in flat-image amplifier systems. However, the electron-optical condenser system of the image amplifier is different.

Figure 5 shows an experimental projection storage tube which may also be used for very bright direct-view applications. The ion pump and the writing and erasing guns, both of which are parallel to the tube axis, are in the tube neck. The viewing gun, which is quite short, is located on the tube axis between the writing and erasing guns.

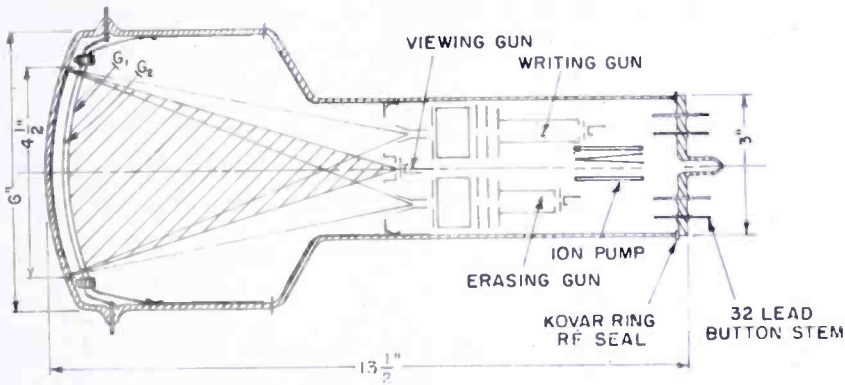


Fig. 4—Design for spherical-screen projection storage tube.

### Construction

The storage-grid mesh is made of electroformed nickel, and the collector grid of woven stainless-steel wire screen (both about 250 mesh per inch). It was found that both kinds of mesh could be formed by cold drawing between soft aluminum sheets. The mesh was completely annealed before drawing; the work-hardening during the drawing process provided sufficient stability and negligible spring-back.\*

An aluminized phosphor screen which can withstand gradients of about 30 kilovolts per centimeter between it and the storage grid is required. Under such gradients, ordinary phosphor screens such as used in television kinescopes, where practically no gradient is present at the phosphor surface, disintegrate.

Satisfactory phosphor screens can be produced by settling a fine-grained phosphor and rinsing it with a silicate solution. After the phosphor is baked it is firmly bound to the curved glass support. Then

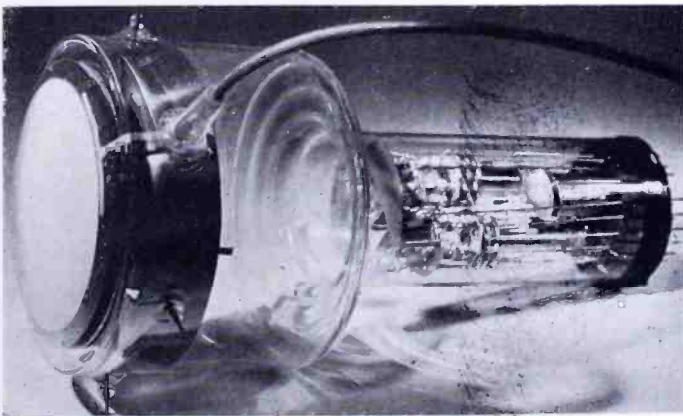


Fig. 5—Projection storage tube.

\* Because of its simplicity and positive results, this technique can be employed for the design of large electron optical mesh lenses.

a very thin collodion film is deposited; this permits phosphor particles to protrude through and bond directly to the aluminum layer which is evaporated on the collodion.

Such a phosphor screen has an "egg shell" appearance, and it can be rubbed lightly with a finger tip without damage. Spark-overs produce a shiny spot on the aluminum, but no damage to the phosphor screen.

### *Projection Arrangement*

Figure 6 shows the projection arrangement which was designed for an 88-inch throw when used with a 5TP4 projection kinescope. A magnification of 12 times gives a 4-foot-diameter display from a 4-inch display on the face of the tube. Curtains placed about the display

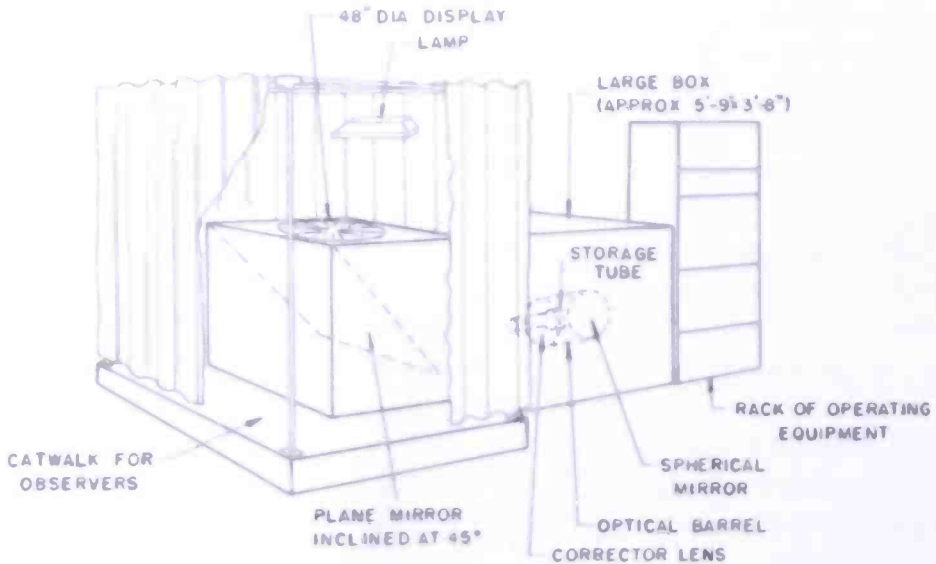


Fig. 6—Storage tube projection display.

were used to darken the viewing area, as shown in Figure 7. The ambient light level from an overhanging incandescent lamp was controlled by varying the lamp voltage.

### *Brightness, Halftones, and Resolution*

Tube-face brightness at 20 kilovolts (applied to the luminescent anode) measures approximately 5,000 foot-lamberts. The optical efficiency of the reflective optics projection system is estimated to be about 15 per cent, and the gain of the projection screen (a piece of drafting vellum) varies from about 0.25 to 2, compared to a perfect diffuser depending on the angle of observation. From these figures, and assuming a magnification of 12, one should expect a brightness at the center of the projection screen of 1 to 10 foot-lamberts. Be-

cause of the properties of the light optical system, there is a decrease in brightness from center to edge of the display.

Actual measurements made with a Luckiesh-Taylor light meter held normal to the projection screen slightly away from center indicated a highlight brightness of 3 to 4 foot-lamberts, which is within the predicted interval. About two foot-candles of ambient light on the projection screen were necessary to cause any visible deterioration of picture contrast; about 10 foot-candles of ambient light caused enough deterioration to make the picture unusable.

The tolerance to ambient light is due partly to the screen (P1) phosphor which provides color contrast with the reddish incandescent

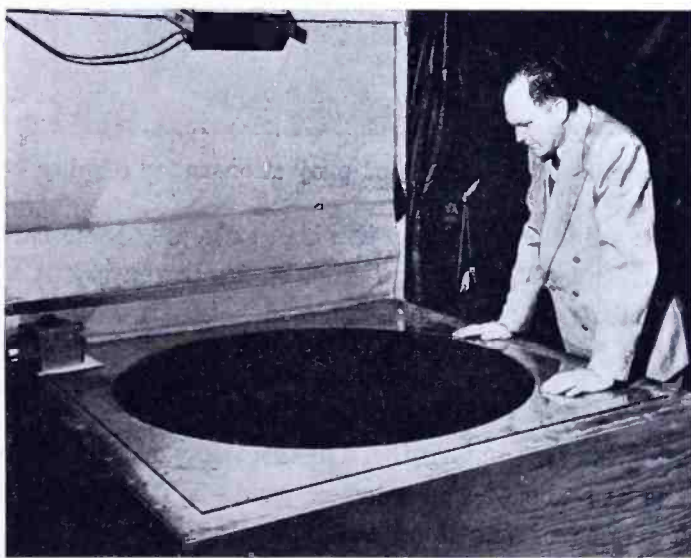


Fig. 7—Viewer's position at projection radar display.

ambient light. Better tolerance can be expected by using a green filter over the projection screen, and a higher directivity screen.

In the photograph of the radar display (Figure 8) the erasing beam is not visible, although in the display itself it is visible as a faint strobe line. The writing beam (invisible) follows 10 to 15 degrees behind it. Because most of the targets are buildings in the metropolitan Philadelphia-Camden area, the picture is rather cluttered. The course of the Delaware River appears as a dark streak, nearly devoid of targets, running along the dotted line from about 6 o'clock to the center, and then curving out toward 3 o'clock. The erased sector is slightly to the right of the lower part of the Delaware River.

Figure 9 (an enlarged picture of the area enclosed by the white lines on Figure 8) shows details of the structure of the projected radar picture. The small grey spots distributed at random between

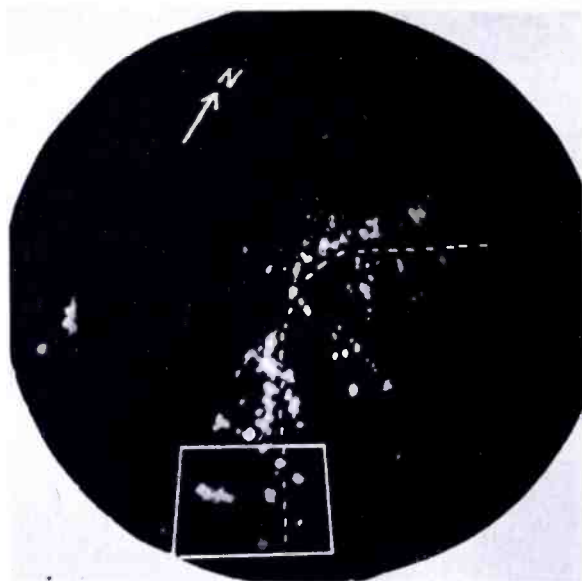


Fig. 8—Photograph of projection radar display.

the targets are noise pulses from the input stages of the radar receiver. The targets are not only distinguished by their shape but also by their brightness because of antenna beam-width integration at the storage grid.

#### *Selective Erasure and Condenser Lens Design*

For ideal picture uniformity, the viewing electrons must arrive normal to the surface of the storage grid. With a *flat* storage grid and a point source of the flood beam, a single strong condenser lens may be used (Figure 10a). One electrode of this lens is formed by the collector grid, the other by a conducting wall coating (at viewing-



Fig. 9—Photograph of portion of projected radar display showing stored noise.

gun anode potential). To keep the viewing beam angle of divergence as small as possible, and thus decrease spherical aberration, this lens should be close to the collector grid. In such an arrangement, two sources of concentric nonuniformities are variations in the angle of incidence of viewing electrons approaching the storage grid, and spherical aberration of the condenser lens (as in Figure 10a). These nonuniformities disappear as the viewing-beam diameter decreases (Figure 10b). Still other nonuniformities, usually asymmetric, are caused by magnetic poles in the storage or collector grid frames (Figure 10c). Although demagnetizing helps reduce the latter, both types of nonuniformity can be reduced by increasing the ratio of the voltage gradients on the phosphor side to that on the gun side of the storage grid. This uniformity improvement probably occurs because viewing-beam electrons with non-normal incidence (which at lower gradient ratios would be reflected) are collected by the field of the elementary lenses. Thus, for a uniform picture background, a low

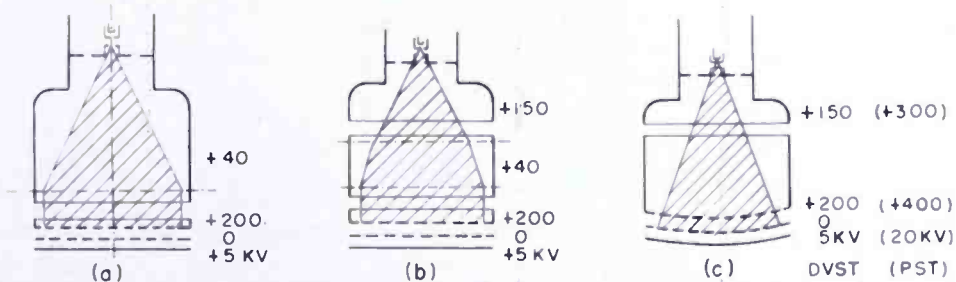


Fig. 10—Condenser-lens configurations for viewing storage tubes.

collector-grid voltage ( $< 100$  volts) or a high phosphor-screen voltage is desirable for lens-raster-type image amplifiers. On the other hand, to prevent positive ions from landing on the storage grid, the collector grid must be at higher positive potential than any electrode between it and the viewing or erasing beam cathodes. Also, a higher collector-grid voltage ( $> 100$  volts) is desirable to obtain optimum gun voltage for a well-focused erasing beam. As a result, there must be a compromise between concentric background patterns, and a poor erasing-beam resolution for a viewing storage tube with a flat storage target and a single condenser lens. Such a system, however, may be tolerated if over-all (flooding) erasure with the viewing beam is used.

One way to improve selective erasure in a viewing storage tube with flat-image amplifier is the introduction of a *double* condenser lens (Figure 10b). There are three advantages:

- (1) The erasing (and viewing) gun anode voltage may be as much

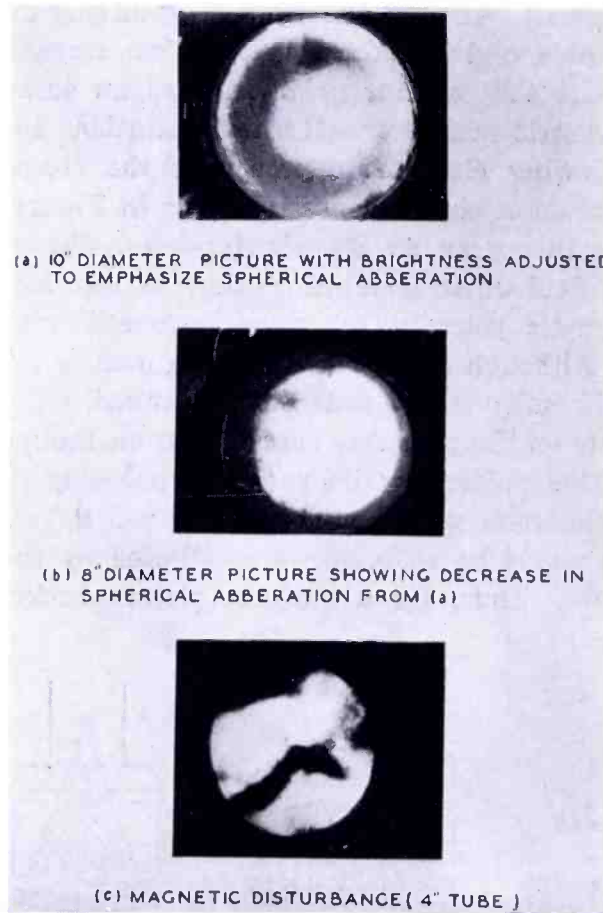


Fig. 11—Nonuniformity due to lack of normal incidence of viewing beam at storage grid.

as 70 per cent of the collector voltage instead of less than 20 per cent for the single condenser lens; this permits more viewing-beam and erase-beam current and better erase-beam spot with the electron guns used.

(2) Less spherical aberration.

(3) Less space-charge defocusing of the erasing beam in the condenser-lens region.

However, although selective erasing is possible with the double condenser lens, the low voltage available for the erasing gun makes possible a well-focused beam with sufficient current only for the slow erasing speeds (e.g., as in radar). Therefore, the alternative is between concentric background patterns and slow or poorly focused selective erasing for the double condenser lens as well as for the single condenser lens.

This compromise is much less severe for *spherical* image amplifier systems (Figure 10c). In this case, normal incidence can be obtained by simply placing the viewing-beam crossover near the center of curvature of the storage grid. Thus, only a weak condenser lens is needed for small corrections of the angle of incidence and for repelling positive ions which would otherwise land at the storage target. Because such a weak condenser lens has a small spherical aberration, it permits a higher collector voltage (in the order of 500 volts if needed) and also higher voltages for the anodes in the viewing and erasing guns. These higher voltages are essential for a small erasing beam spot and high current of the viewing beam.\*

For proper tube operation, the viewing beam must arrive normal to the storage grid, whether flat or curved. In the first case, a condenser lens is required close to the grid. However, in the curved-grid tube, normal incidence is obtained with a diverging beam. Thus, the condenser lens can be placed nearer the viewing-beam cathode without increasing the viewing-beam angle. By using a smaller portion of this lens, spherical aberration is reduced further and a larger viewing screen may be used for the same envelope size.

### CONCLUSIONS

Two new experimental versions of viewing storage tubes have been developed for use where larger stored pictures are required.

The first version is a tube with a large, flat (10-inch diameter) viewing screen which is bright enough to be used in a well lighted place such as a laboratory or a ship's bridge. It has adequate writing speed for radar and similar displays, at least one minute viewing duration, and approximately 500 lines resolution (television standards).

The second version is a projection storage tube with a  $4\frac{1}{4}$  inch spherical luminescent screen. It provides more than 5,000 foot-lamberts brightness at 20 kilovolts, when the image is projected to a 48-inch diameter display, the brightness is high enough for use with room illumination of 3 to 5 foot-candles. Such tubes have high maximum writing speed, (up to  $10^8$  spots per second), good line-by-line erasing, adequate storage for radar displays, and 500-line resolution.

The investigation of curved-image amplifier systems for this projection storage tube revealed several important advantages of curved screens which are applicable for direct view storage tubes. Curved screens make it easier to achieve normal arrival of viewing

---

\* With conventional gun structures.

electrons at the storage grids, thus eliminating background nonuniformity caused by spherical aberration of the condenser lens. Also, higher voltages may be used on the collector grid and viewing and erasing guns; this results in better focus of a separate erasing beam and more current in both the viewing and erasing beams.

# THE APPARENT CONTACT POTENTIAL OF A PSEUDO-ABRUPT P-N JUNCTION

BY

HERBERT KROEMER

RCA Laboratories  
Princeton, N. J.

*Summary*—The capacitance-voltage relationship is studied for junctions which have constant impurity densities on both sides of the junction but where the transition from the density value on the *n* side to that on the *p* side is not an abrupt one. Instead, it is assumed that the transition takes place over a finite region all of which lies inside the space-charge region. It is found that the inverse square of capacitance,  $C$ , of such a "pseudo-abrupt" junction varies linearly with voltage,  $V$ , as in the case of a truly abrupt junction:

$$\frac{1}{C^2} \sim V + V_c^*$$

However, the constant term,  $V_c^*$ , is no longer the contact potential as in a truly abrupt junction. The difference between the true contact potential and this "apparent" contact potential can be utilized to obtain detailed information about the internal structure of the junction; for example, about the amount of any diffusion that has taken place.

## INTRODUCTION

THE variation of the transition capacitance,  $C$ , of an abrupt p-n junction with voltage follows the relation

$$\frac{1}{C^2} = \text{const} \cdot (V + V_c), \quad (1)$$

where  $V$  is the applied reverse bias and  $V_c$  is the contact potential.

$$V_c = \frac{kT}{q} \ln \frac{NP}{n_i^2}, \quad (2)$$

where  $N$  and  $P$  are the impurity densities on the two sides of the junction, and  $n_i$  is the intrinsic carrier concentration.

In many practical cases some diffusion has taken place at the junction, so that the junction is not really abrupt. If the region of deviation from abruptness is narrow enough, it will lie entirely inside the depletion region, at least above a certain critical voltage,  $V_A$ . Such

a junction will be called a "pseudo-abrupt" junction. The purpose of this paper is to show that, for a pseudo-abrupt junction and for  $V > V_A$ ,

- (a) The capacitance still follows an equation like Equation (1).
- (b) The value of the constant is the same as in a truly abrupt junction.
- (c)  $V_c$  has to be replaced in Equation (1) by a quantity  $V_c^*$  which is no longer the true contact potential, but differs from it in accordance with the manner in which the transition from  $p$  to  $n$  takes place.

The difference between this "apparent contact potential,"  $V_c^*$ , as deduced from capacitance measurements, and the true contact potential,  $V_c$ , as calculated from the impurity densities of the two sides of the junction, can yield some important quantitative information about the internal structure of the junction, such as the amount of the diffusion that has taken place.

#### MATHEMATICAL ANALYSIS

The electrostatic potential,  $\phi$ , inside a depletion layer obeys Poisson's equation

$$\frac{d^2\phi}{dx^2} = -\frac{4\pi}{\epsilon} \rho(x), \quad \rho(x) = qN(x), \quad (3)$$

where  $\epsilon$  = dielectric constant and  $N(x)$  = donor density minus acceptor density. If  $x_p$  and  $x_n$  are the  $p$ - and  $n$ -side limits of the depletion layer, the boundary conditions are (Figure 1)

$$\phi'(x_p) = \phi'(x_n) = 0, \quad (4)$$

$$\phi(x_n) - \phi(x_p) = V + V_c, \quad (5)$$

where  $V$  is the applied reverse bias and  $V_c$  the true contact potential. Integrating Equation (3) and observing the boundaries specified by Equations (4) and (5) gives

$$0 = -\frac{4\pi q}{\epsilon} \int_{x_p}^{x_n} N(x) dx, \quad (6)$$

$$V + V_c = -\frac{4\pi q}{\epsilon} \int_{x_p}^{x_n} dx \int_{x_p}^x N(s) ds = \frac{4\pi q}{\epsilon} \int_{x_p}^{x_n} N(x) x dx. \quad (7)$$

For a truly abrupt junction,

$$N(x) = N_A(x) = \begin{cases} -P_0 & \text{for } x < x_0 \\ +N_0 & \text{for } x > x_0 \end{cases} \quad (8)$$

Substituting these values in Equations (6) and (7) yields the well-known expressions:

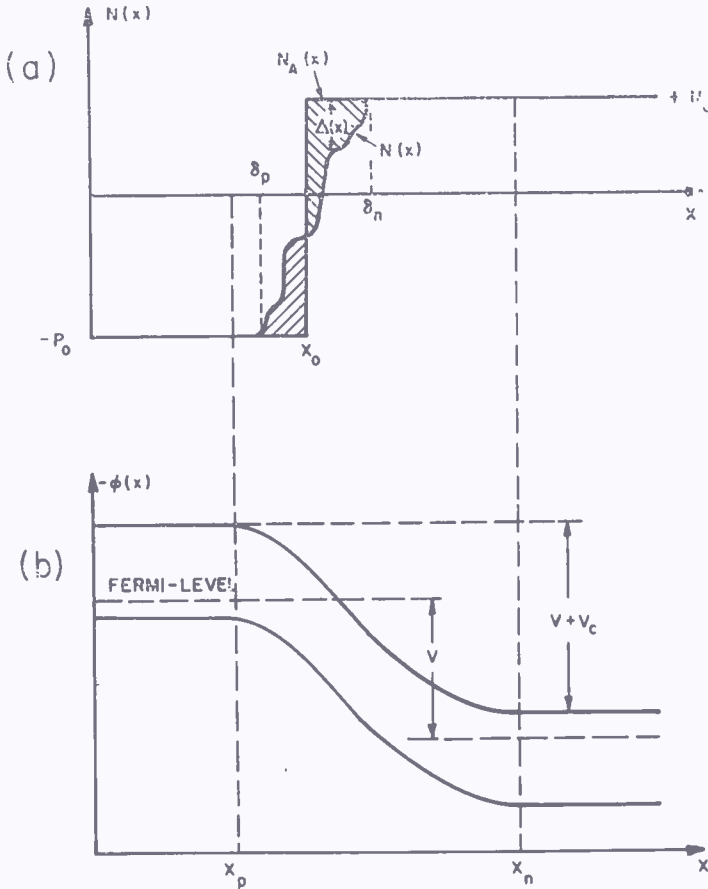


Fig. 1—Pseudo-abrupt junction; impurity and potential distribution.

$$P_0 (x_0 - x_p) = N_0 (x_n - x_0), \quad (9)$$

$$\begin{aligned} V + V_c &= \frac{2\pi q}{\epsilon} [P_0 (x_0 - x_p)^2 + N_0 (x_n - x_0)^2] \\ &= \frac{2\pi q}{\epsilon} \frac{P_0 N_0}{P_0 + N_0} (x_n - x_p)^2, \end{aligned} \quad (10)$$

$$\frac{1}{C^2} = \left( \frac{4\pi}{\epsilon} \right)^2 (x_n - x_p)^2 = \frac{8\pi}{\epsilon q} \frac{P_0 + N_0}{P_0 N_0} (V + V_c). \quad (11)$$

In the case of a pseudo-abrupt junction we split the mathematical representation of the actual impurity density into two parts, an abrupt distribution plus a deviation:

$$N(x) = N_A(x) - \Delta(x), \quad (12)$$

where we choose the arbitrary transition coordinate,  $x_0$ , of the abrupt distribution in such a way that the integral over the deviation part vanishes, i.e., that the two shaded areas in Figure 1 are equal:

$$0 = \int_{\delta_p}^{\delta_n} \Delta(x) dx = -P_0(x_0 - \delta_p) + N_0(\delta_n - x_0) - \int_{\delta_p}^{\delta_n} N(x) dx. \quad (13)$$

Therefore,

$$x_0 = \frac{1}{P_0 + N_0} \left[ P_0 \delta_p + N_0 \delta_n - \int_{\delta_p}^{\delta_n} N(x) dx \right] \quad (14)$$

If one inserts  $N(x) = N_A(x) - \Delta(x)$  in Equations (6) and (7), this again leads to the expressions (9, (10) and (11), except that now  $V_c$  is replaced by the "apparent" contact potential

$$V_c^* = V_c + \Delta V_c, \quad (15)$$

where

$$\Delta V_c = \frac{4\pi q}{\epsilon} \int_{\delta_p}^{\delta_n} \Delta(x) x dx = \frac{2\pi q}{\epsilon} \left[ -P_0(x_0^2 - \delta_p^2) + N_0(\delta_n^2 - x_0^2) - \int_{\delta_p}^{\delta_n} N(x) x dx \right]. \quad (16)$$

The interpretation of the additional term  $\Delta V_c$  is simple. It is the potential difference across the dipole layer consisting of the impurity difference,  $\Delta(x)$ .

If  $1/C^2$  is plotted against voltage, a straight line results parallel to the line for the abrupt case, but displaced to the left by  $\Delta V_c$ .

In Figure 1 the deviation of  $N(x)$  was in the direction of flattening

the junction, that is,  $-P_0 < N(x) < N_0$ . In this case  $\Delta V_c$  is always positive, and the capacitance is decreased as though a greater voltage had been applied.

#### APPLICATION TO SPECIAL CASES

When the way in which a junction deviates from abruptness is qualitatively known, a measurement of the apparent contact potential and comparison with the true contact potential may give quantitative information about the actual dimensions of the deviation. This is illustrated here through two practical examples.

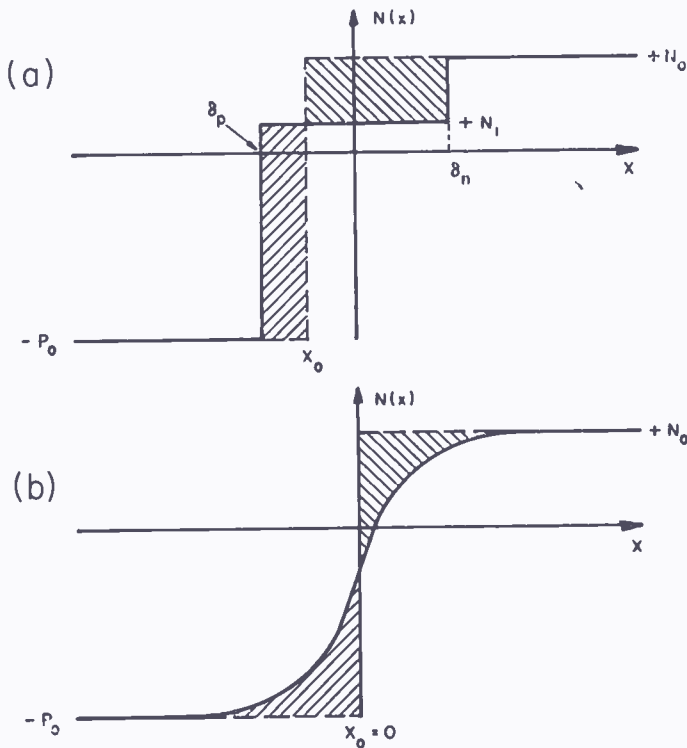


Fig. 2(a)—P-I-N junction; (b) symmetrically diffused junction.

#### (a) P-I-N Junction and P+N-N+ Junction (Figure 2a)

In the P-I-N junction, an intrinsic region has been sandwiched between the n and the p regions. In practical cases the central region always contains some remaining impurities so that the junction had best be treated as a P+N-N+ junction (Figure 2a). If these remaining impurities have a sufficiently high density, the critical voltage,  $V_A$ , referred to previously, may be no longer negligible, and may actually become rather high. If we restrict ourselves to low values of  $N_1$  and/or to  $V > V_A$ , we have

$$N(x) = N_I \text{ for } \delta_p < x < \delta_n, \quad (17)$$

$$x_o = \frac{P_o \delta_p + N_o \delta_n - N_I (\delta_n - \delta_p)}{P_o + N_o} = \frac{(P_o + N_I) \delta_p + (N_o - N_I) \delta_n}{P_o + N_o}, \quad (18)$$

$$\begin{aligned} \Delta V_c &= \frac{2\pi q}{\epsilon} [- (P_o + N_I) (x_o^2 - \delta_p^2) + (N_o - N_I) (\delta_n^2 - x_o^2)] \\ &= \frac{2\pi q (P_o + N_I) (N_o - N_I)}{\epsilon (P_o + N_o)} (\delta_n - \delta_p)^2. \end{aligned} \quad (19)$$

From this formula if either  $N_I$  or  $(\delta_n - \delta_p)$  is known, the other quantity can be determined. ( $P_o$  and  $N_o$  are always assumed to be known.)

The maximum value of  $\Delta V_c$  occurs for  $N_I = \frac{1}{2} (N_o - P_o)$ :

$$\Delta V_{c \text{ max}} = \frac{\pi q}{2\epsilon} (P_o + N_o) (\delta_n - \delta_p)^2. \quad (20)$$

Numerical example:  $\epsilon = 16$ ,  $P_o = N_o = 10^{16} \text{ cm}^{-3}$ ,  $\delta_n - \delta_p = 10^{-4} \text{ cm}$ . This results in  $\Delta V_{c \text{ max}} \approx 2.8$  volts. This is not a negligible quantity. Equation (19) also covers the case where either  $N_I > N_o$  or  $N_I < -P_o$ , that is the case of impurity pileup inside the junction.  $\Delta V_c$  then becomes negative. The practical importance of this case may be rather limited because such a structure could have a rather high critical voltage,  $V_{A1}$ .

(b) *Junction with Symmetrical Diffusion (Figure 2b)*

A grown junction is treated with a P-type background doping  $-P_o$ , which has been over-compensated by a donor density,  $N_o + P_o$ , so that the net donor density is  $N_o$ . If the donor density has flattened out through diffusion, then  $x_o = 0$ , and

$$N(x) = \frac{1}{2} (-P_o + N_o) + \frac{1}{2} (P_o + N_o) \operatorname{erf} \left( \frac{x}{2\sqrt{Dt}} \right), \quad (21)$$

$$\Delta(x) = \mp \frac{1}{2} (P_o + N_o) \operatorname{erfc} \left( \frac{|x|}{2\sqrt{Dt}} \right), \text{ for } x \begin{matrix} < 0, \\ > \end{matrix} \quad (22)$$

Here  $D$  and  $t$  are the diffusion constant of the impurity and the diffusion time, respectively. If  $\sqrt{Dt} \ll |x_p|$  and  $\ll x_n$ ,  $\Delta(x)$  has decreased to a very low value at the ends of the depletion layer and the junction can be considered to be pseudo-abrupt. The integral in Equation (16) can be extended from  $-\infty$  to  $+\infty$  with only negligible error, resulting in

$$\begin{aligned} \Delta V_c &= \frac{4\pi q}{\epsilon} (P_o + N_o) \int_0^\infty \operatorname{erfc} \left( \frac{x}{2\sqrt{Dt}} \right) \cdot x dx \\ &= \frac{16\pi q}{\epsilon} (P_o + N_o) \cdot Dt \cdot \int_0^\infty \operatorname{erfc}(s) \cdot s ds. \end{aligned} \quad (23)$$

The integral is equal to 1/4, and

$$\Delta V_c = \frac{4\pi q}{\epsilon} (P_o + N_o) \cdot Dt. \quad (24)$$

This equation could be utilized for the measurement of diffusion constants under conditions where the total amount of diffusion is so small that none of the conventional methods can be applied.

With  $\epsilon = 16$ ,  $P_o = N_o = 10^{15} \text{ cm}^{-3}$ ,  $\sqrt{Dt} = 10^{-4} \text{ cm}$ ;  $\Delta V_c$  would become 1.1 volts.

In cases where the diffusion is not symmetrical, similar results can easily be obtained by inserting the proper distributions in Equations (14) through (16).

# BIGRADIANT UNIAXIAL MICROPHONE

BY

HARRY F. OLSON, JOHN PRESTON, AND JOHN C. BLEAZEY

RCA Laboratories,  
Princeton, N. J.

*Summary*—A second-order unidirectional microphone has been developed consisting of two uniaxial microphones connected in series opposition. This system has been termed the bigradient uniaxial microphone. The directional efficiency, that is, the energy response to random sounds is one-ninth. The high discrimination which this microphone exhibits to sounds which originate from the sides and rear makes it particularly suitable for long distance sound pickup in radio, television, sound motion pictures, phonograph recording, and sound reinforcing systems.

## INTRODUCTION

**D**IRECTIONAL microphones are employed in sound reproducing systems to discriminate against undesired sounds, and thereby obtain a satisfactory pickup of the desired sound. It has been established that a directional system in which the directivity does not vary materially with frequency is the most desirable because there will be no frequency discrimination in either the direct or generally reflected sound or noise. The order of directivity required in a microphone will depend upon the application. The greater the directivity the larger the pickup distance that can be used. For sound motion picture and television applications where the microphone must be kept out of the picture, a large pickup distance is a requirement. These applications require a directional microphone with a high order of directivity in order to obtain a reasonable ratio of desired to undesired sound.

A unidirectional microphone with the maximum sensitivity along the cylindrical axis of the microphone was developed some time ago. This was termed the uniaxial microphone.<sup>1</sup> The commercial version<sup>2</sup> of the uniaxial microphone is designated the BK-5A. The features of the uniaxial microphone are a high ratio of electrical output to size, a sharper directivity pattern than a cardioid, a directivity pattern

---

<sup>1</sup> H. F. Olson, J. Preston, and J. C. Bleazey, "The Uniaxial Microphone," *RCA Review*, Vol. XIV, p. 47, March, 1953.

<sup>2</sup> J. W. O'Neil and R. M. Carrell, "The BK-5A Uniaxial Microphone," *Broadcast News*, Vol. 83, p. 44, May, 1955.

that is independent of the frequency, and a blast-proof vibrating system. The high discrimination which this microphone exhibits to sounds which originate from the sides and the rear makes it particularly suitable for long-distance sound pickup in radio, television, sound motion pictures and sound reinforcing systems.

Since the uniaxial microphone has demonstrated that a high order of directivity is of great value in sound pickup applications, it appeared desirable to examine the possibilities of microphones with even greater directivity. The simplest solution to the problem of increased directivity is the combination of two first-order gradient directional microphones to form a second-order gradient unidirectional microphone. A

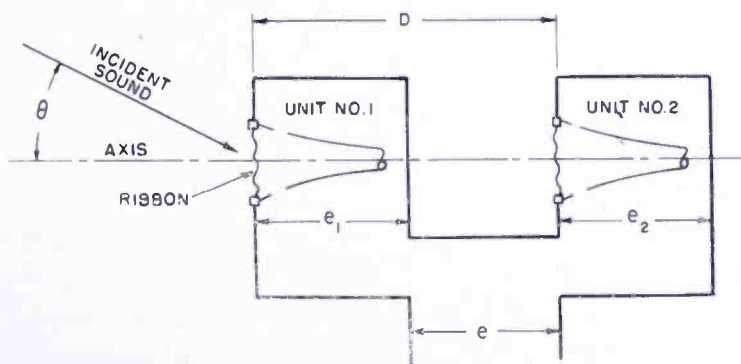


Fig. 1—A schematic diagram of a second-order gradient unidirectional microphone consisting of two first-order gradient microphones connected in series opposition.

microphone of this type has been developed employing the uniaxial microphone as the basic element. It is the purpose of this paper to describe a second-order gradient uniaxial microphone.

#### THEORETICAL CONSIDERATIONS INVOLVING A SECOND-ORDER GRADIENT UNIDIRECTIONAL MICROPHONE

A second-order gradient unidirectional microphone<sup>3,4</sup> may be developed from two first-order gradient unidirectional microphones connected in series opposition. A schematic view of the arrangement is shown in Figure 1. The first-order microphones have cardioid directional patterns.

Since the two units are connected in opposition, the response with

<sup>3</sup> H. F. Olson, *Elements of Acoustical Engineering*, D. Van Nostrand Co., Princeton, N. J.

<sup>4</sup> H. F. Olson and J. Preston, "Directional Microphone," *RCA Review*, Vol. X, p. 339, September, 1949.

respect to frequency and the absolute output are important considerations. The performance of the arrangement of Figure 1 will now be deduced from the equations which govern the system.

The voltage output is given by

$$e = e_1 - e_2 = e_{01} (.5 + .5 \cos \theta) \left[ \sin \left( \omega t - \frac{\pi D}{\lambda} \cos \theta \right) \right] - e_{02} (.5 + .5 \cos \theta) \left[ \sin \left( \omega t + \frac{\pi D}{\lambda} \cos \theta \right) \right], \quad (1)$$

where  $e$  = instantaneous output of the combination, in volts,  
 $e_1$  = instantaneous output of unit No. 1,  
 $e_2$  = instantaneous output of unit No. 2,  
 $e_{01}$  = peak amplitude of the output of unit No. 1,  
 $e_{02}$  = peak amplitude of the output of unit No. 2,  
 $\omega = 2\pi f$ ,  
 $f$  = frequency, in cycles per second,  
 $t$  = time, in seconds,  
 $D$  = distance between the units, in centimeters,  
 $\lambda$  = wavelength of the sound, in centimeters, and  
 $\theta$  = angle between the direction of the incident sound and the axis of the system.

In Equation (1), the point of zero phase is considered to be midway between the two units.

If the outputs of the two units are the same, Equation (1) may be written

$$e = -2e_{01} (.5 + .5 \cos \theta) \cos \omega t \sin \left( \frac{\pi D}{\lambda} \cos \theta \right). \quad (2)$$

If the harmonic term with respect to time is omitted, then Equation (2) becomes

$$e = -2e_1 (.5 + .5 \cos \theta) \sin \left( \frac{\pi D}{\lambda} \cos \theta \right). \quad (3)$$

The response frequency characteristic for a second-order gradient unidirectional microphone obtained from Equation (3) for  $\theta = 0$  is

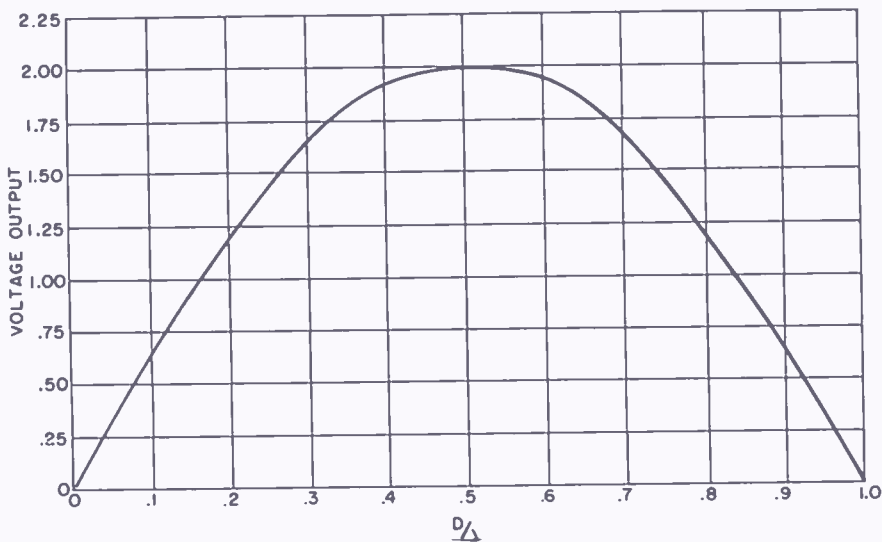


Fig. 2—The response of a second-order gradient unidirectional microphone as a function of the ratio of the distance  $D$ , between the units, to the wavelength,  $\lambda$ , for sound incident along axis.

shown in Figure 2. It will be seen that the upper limit of the useful frequency range is  $D/\lambda = 1$ . It will be also seen that the response falls off 6 decibels per octave in the low-frequency range.

The polar directional characteristic of a second-order gradient unidirectional microphone obtained from Equation (3) is shown in Figure 3. In this case the upper limit of unidirectional pickup is  $D/\lambda = 3/4$ . The directivity patterns below  $D/\lambda = 3/4$  can be improved by means of the electrical networks. The dividing electrical network alters the amplitude contribution of the two units and the phase relations as contrasted to the direct series opposition connection. This will be evident later in the paper where the experimental results are

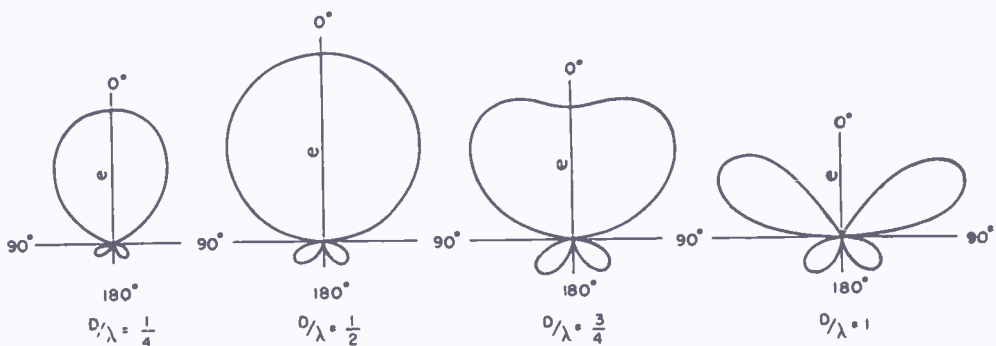


Fig. 3—The polar directional characteristics of a second-order gradient unidirectional microphone for various ratios of the distance  $D$  between the units, to the wavelength,  $\lambda$ .

shown for the working model of the bigradient uniaxial microphone.

A general consideration of the factors of frequency response and directivity indicates that second-order operation could be maintained to 1,500 cycles and still retain adequate response in the low-frequency range. It also appeared that a high order of directivity is not required in the high-frequency range. Furthermore, if directivity is required in the high-frequency range, it can be obtained by diffraction.

Since gradient systems depend upon the difference of the output of two units, there are two major problems, namely, similarity of frequency response and high sensitivity of the units. Similarity of frequency response of the units is required in order to obtain a high order of discrimination. High sensitivity is required because larger pickup distances can be used when the directivity is increased. The first-order unidirectional microphone, termed the uniaxial microphone, fulfills these requirements. Accordingly, uniaxial microphones were selected as the microphone units in the second-order gradient microphone. Since the maximum pickup of the system is along the cylindrical axis, the second-order gradient microphone employing two first-order gradient uniaxial microphone units has been termed the bigradient uniaxial microphone.

A sectional view and acoustical network of the first-order gradient uniaxial microphone<sup>1</sup> is shown in Figure 4.

The polar directional characteristic of the uniaxial microphone is shown in Figure 5. The directional characteristic of the uniaxial microphone is given by

$$e = K_1 \left( .3 + .7 \cos \frac{\theta}{3} \cos \theta \right) \quad (4)$$

where  $K_1$  = voltage sensitivity constant of the microphone, in volts,  
and  
 $\theta$  = angle between the direction of incident sound and the  
cylindrical axis of the microphone.

Referring to Figure 5 and Equation (4), it will be seen that the directivity pattern of the uniaxial microphone is sharper than a cardioid pattern. Since the directivity of the bigradient uniaxial microphone is the product of the directivity patterns of the individual units and the cosine function, the resultant characteristic will exhibit a higher order of directivity by the use of the uniaxial microphone units as contrasted to microphone units with a cardioid directivity pattern.

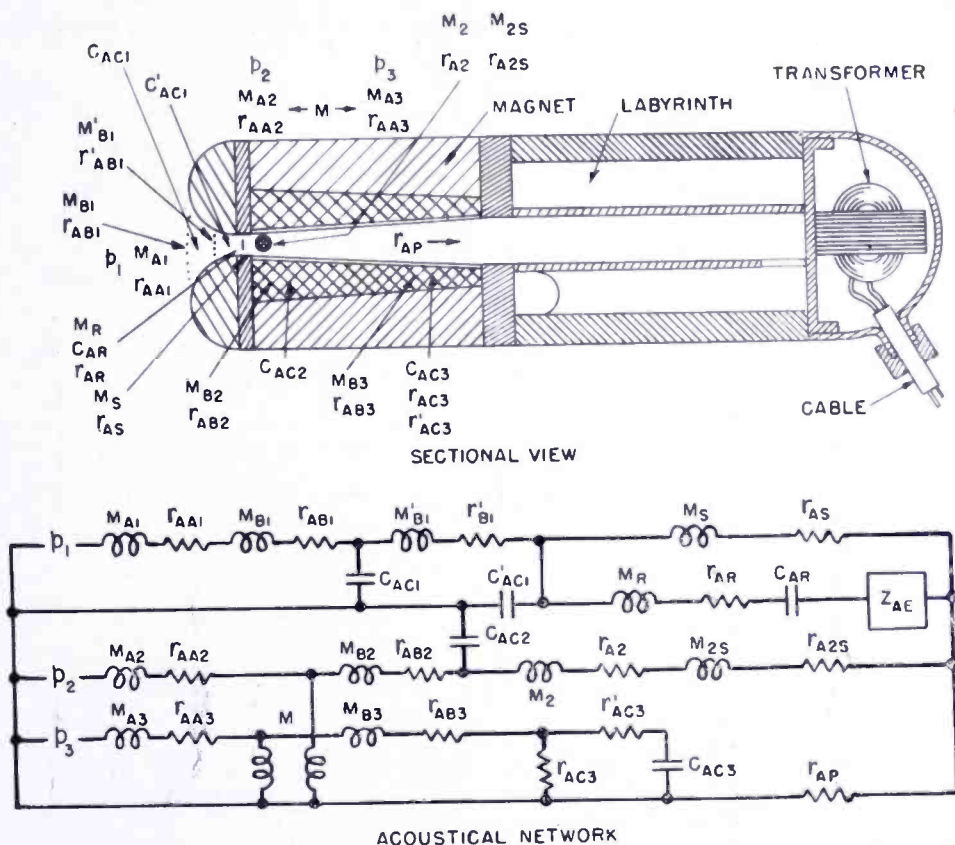


Fig. 4—A sectional view and the acoustical network of a uniaxial microphone. In the acoustical network  $p_1$  is the sound pressure on the front of the microphone;  $M_{A1}$  and  $r_{AA1}$  are the inertance and acoustical resistance of the air load on the front of the microphone;  $M_{B1}$ ,  $r_{AB1}$ ,  $M'_{B1}$ , and  $r'_{AB1}$  are the inertances and acoustical resistances of the blast baffles on the front of the microphone;  $C_{AC1}$  and  $C'_{AC1}$  are the acoustical capacitances of the volumes between the blast baffles;  $M_S$  and  $r_{AS}$  are the inertance and acoustical resistance of the slit between the ribbon and pole pieces;  $M_R$ ,  $r_{AR}$ , and  $C_{AR}$  are the inertance, acoustical resistance, and acoustical capacitance of the ribbon;  $Z_{AE}$  is the acoustical impedance due to the electrical circuit;  $p_2$  is the sound pressure at the apertures in the labyrinth connector;  $M_{A2}$  and  $r_{AA2}$  are the inertance and acoustical resistance of the air load at the apertures of the labyrinth connector;  $M_{B2}$  and  $r_{AB2}$  are the inertance and acoustical resistance of the blast baffles on the side of the microphone;  $C_{AC2}$  is the acoustical capacitance of the volume behind the blast baffle;  $M_{2S}$  and  $r_{A2S}$  are the inertance and acoustical resistance of the screen covering the hole in the labyrinth connector;  $M_2$  and  $r_{A2}$  are the inertance and acoustical resistance of the hole in the labyrinth connector;  $r_{AP}$  is the acoustical resistance of the labyrinth;  $p_3$  is the sound pressure at the damped cavity between the magnets;  $M_{A3}$  and  $r_{AA3}$  are the inertance and acoustical resistance of the air load upon the damped cavity;  $M_{B3}$  and  $r_{AB3}$  are the inertance and acoustical resistance of the blast baffle over the damped cavity;  $C_{AC3}$ ,  $r_{AC3}$ , and  $r'_{AC3}$  are the acoustical capacitance and acoustical resistances of the cavity between the magnets; and  $M$  is the coupling between the cavity and the apertures.

Following the procedures outlined in deriving Equation (3), the directional pattern of the bigradient uniaxial microphone in the region of second-order gradient operation is given by

$$e = K_2 \left( .3 + .7 \cos \frac{\theta}{3} \cos \theta \right) \cos \theta, \quad (5)$$

where  $K_2$  = voltage sensitivity constant of the microphone, in volts, and

$\theta$  = angle between the direction of the incident sound and the cylindrical axis of the microphone.

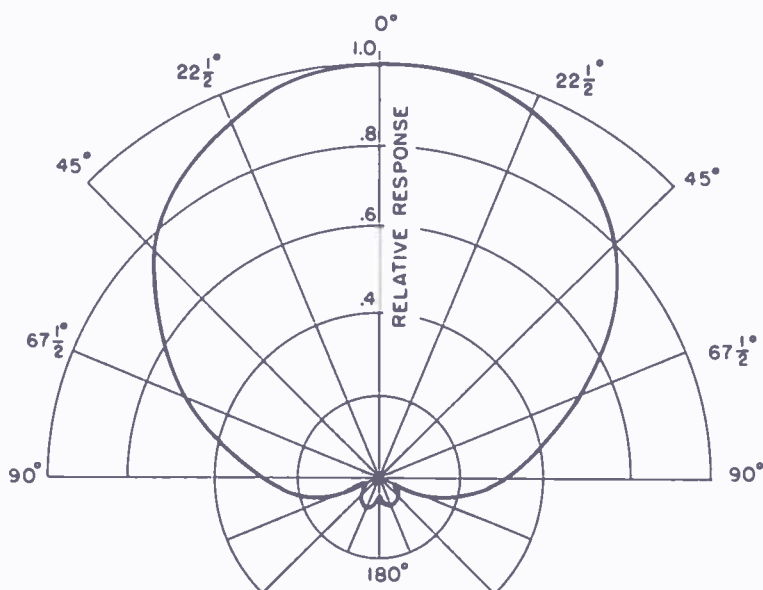


Fig. 5—The theoretical polar directional characteristic of the uniaxial microphone.

The polar directional characteristic obtained from Equation (5) is shown in Figure 6.

The directional efficiency of the bigradient uniaxial microphone is given by

$$\text{D.E.} = \frac{2\pi \int_0^\pi \left( .3 + .7 \cos \frac{\theta}{3} \cos \theta \right)^2 \cos^2 \theta \sin \theta d\theta}{4\pi} \quad (6)$$

$$\approx \frac{1}{9}$$

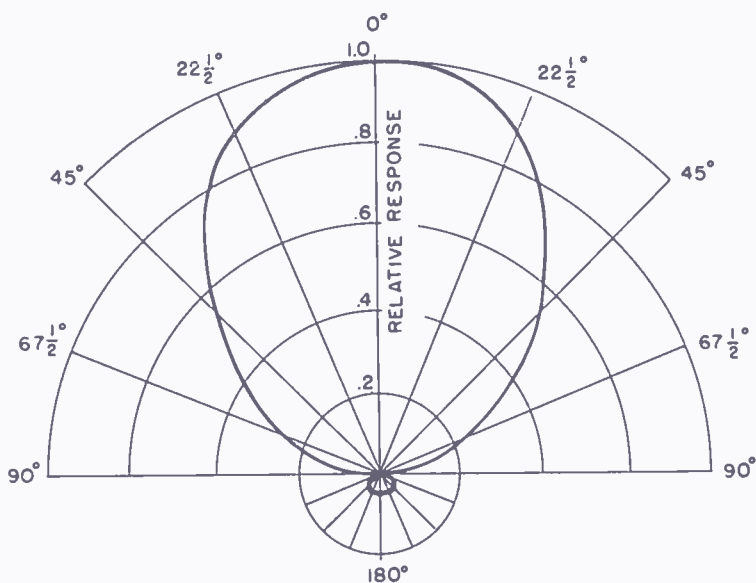


Fig. 6—The theoretical polar directional pattern of the bigradient uniaxial microphone.

The response of the bigradient uniaxial microphone to random sounds is  $1/9$  that of a nondirectional microphone. The increased directional efficiency of the bigradient uniaxial microphone makes it possible to use a pickup distance three times that of a nondirectional microphone.

#### DESCRIPTION OF THE MICROPHONE

The elements of the experimental bigradient uniaxial microphone are shown in Figures 7 and 8. The front and rear uniaxial units are mechanically connected by a perforated cylindrical shell. The transformers are housed behind the labyrinth in each uniaxial unit. The electrical network is housed in the enlarged housing behind the rear unit.

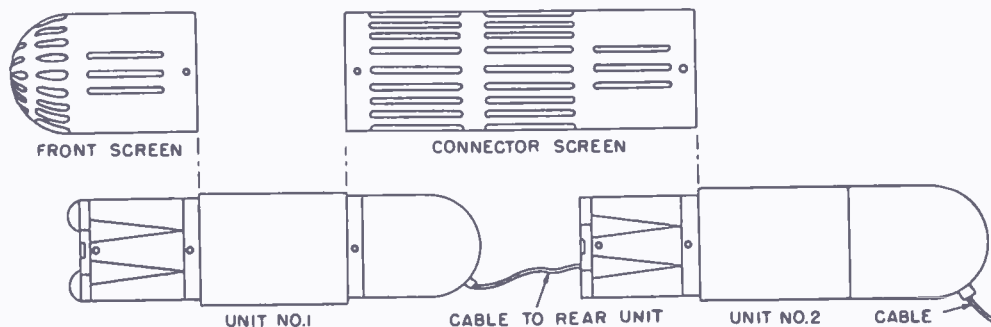


Fig. 7—A schematic view of the elements of an experimental bigradient uniaxial microphone.

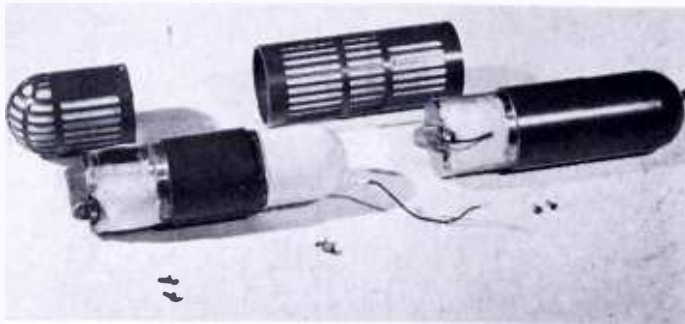


Fig. 8—A photographic view of the elements of a bigradient uniaxial microphone.

The electrical system is shown in Figure 9. Transformers are used to raise the impedance of the ribbon to that suitable for transmission over a line. An electrical network is provided to transfer the output of the two units in series opposition in the frequency range below 1,500 cycles to the single front unit in the frequency range above 4,000 cycles. Suitable electrical compensation circuits are used to obtain uniform response in the bigradient operation frequency range.

The complete bigradient uniaxial microphone mounted in a cradle suitable for boom operation is shown in Figure 10. The over-all length of the microphone is  $11\frac{1}{2}$  inches. The weight is 1.9 pounds.

#### PERFORMANCE CHARACTERISTICS

The response frequency characteristics for sound incident at angles of  $0^\circ$ ,  $45^\circ$ ,  $67\frac{1}{2}^\circ$ ,  $90^\circ$  and  $180^\circ$  with respect to the axis of the microphone, are shown in Figure 11. These characteristics show that there is very little frequency discrimination over the useful pickup angle of the microphone.

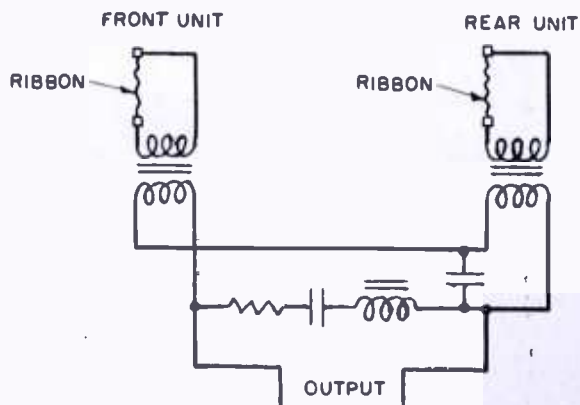


Fig. 9—The electrical network of the bigradient uniaxial microphone.

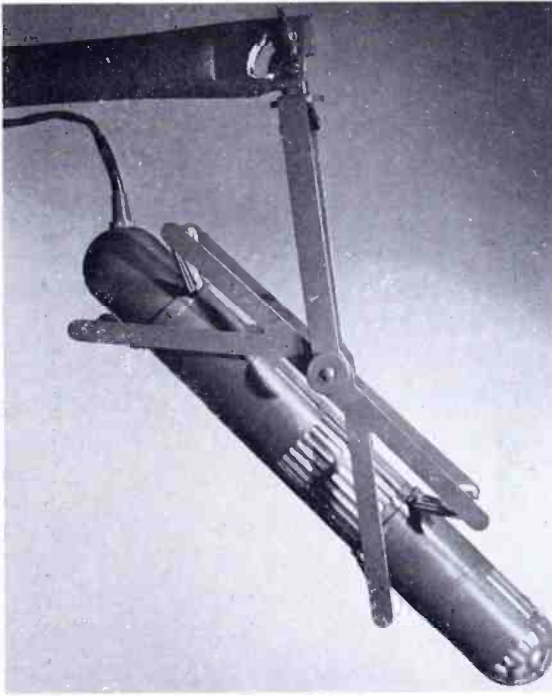


Fig. 10—The bigradient uniaxial microphone mounted in a cradle for boom operation.

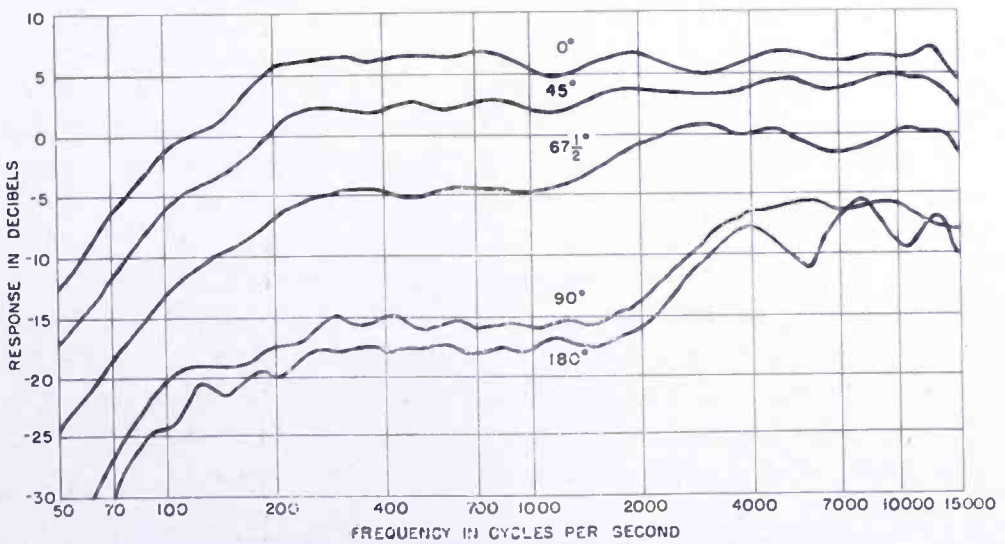


Fig. 11—The response frequency characteristics of the bigradient uniaxial microphone for sound incident at angles of  $0^\circ$ ,  $45^\circ$ ,  $67\frac{1}{2}^\circ$ ,  $90^\circ$  and  $180^\circ$  with respect to the axis of the microphone.

The polar directional patterns for 200, 1,000 and 4,000 cycles are shown in Figure 12. These directivity patterns and the response frequency characteristics of Figure 11 show a high order of discrimination for the sides and the rear hemisphere in the mid- and low-frequency ranges. It is in the region below 2,000 cycles that practically all of the difficulty due to reverberant and other undesirable sounds occurs. The operation shifts from the two uniaxial microphones in second-order gradient operation to the single uniaxial microphone in first-order operation in going from the low-frequency range to the high-frequency range. By the use of diffraction phenomena, it would be a comparatively simple task to develop a microphone with a sharper directivity pattern in the high-frequency region for use in the front

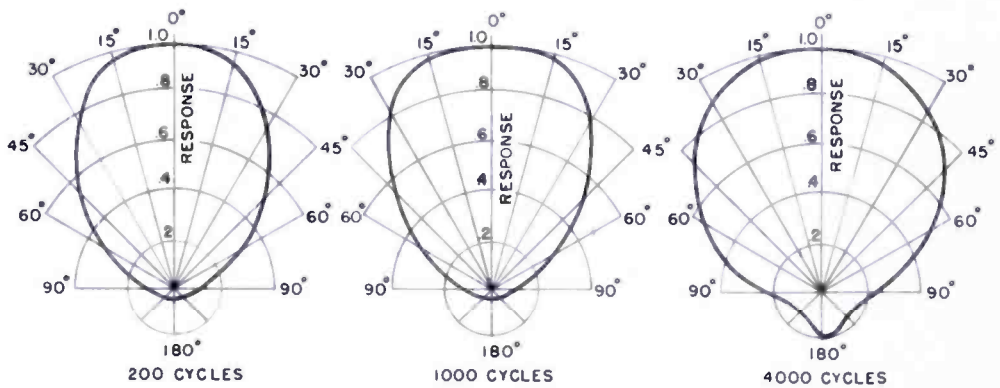


Fig. 12—The polar directional characteristics of the second order gradient uniaxial microphone for 200, 1,000 and 4,000 cycles.

uniaxial microphone if this appeared desirable. In this connection, in actual operation the broader directivity pattern in the high frequency range does not appear to be an objectionable feature. As a matter of fact, it appears to be desirable because it adds a tinge of brightness in the reproduced sound.

The measured response of the bigradient uniaxial microphone to random sounds in the frequency range below 2,000 cycles is  $1/9$  that of a nondirectional microphone. The increased directional efficiency makes it possible to employ a pickup distance three times that of a nondirectional microphone and 1.7 times that of a unidirectional microphone with a cardioid directional pattern.

#### APPLICATIONS OF A BIGRADIENT UNIAXIAL MICROPHONE

A microphone with a small angle of sound pickup and high discrimination against undesirable sounds is useful in recording sound

motion pictures and sound pickup in television where the microphone must be kept out of the picture. The size and weight of the microphone are such that it may be mounted on a conventional boom, Figure 10. The cradle designed for this microphone provides adequate shock mounting. In addition, the microphone is underslung so that the microphone is the lowest part of the system. The larger pickup distance provided by this microphone makes it possible to allow greater freedom of operation of the action.

In the pickup of orchestras and other distributed sound sources, it has been established that as the pickup distance is increased the balance is improved because the ratios of the distances from the various sound sources and the microphone are closer to the same values. The larger pickup distance is only possible if the microphone provides sufficient discrimination against reverberation and other undesirable sounds. Thus it will be seen that the bigradient uniaxial microphone is also useful in radio broadcasting, recording of phonograph records, and sound reinforcing. In the latter application, because of the large ratio of response of direct to reflected sound, it provides the possibility of fixed microphone locations and locked amplifier gain controls, thereby providing unattended operation. In such use, an automatic-gain-control system might be desirable as an added refinement.

# ANALYTICAL APPROACHES TO LOCAL OSCILLATOR STABILIZATION

BY

W. Y. PAN AND D. J. CARLSON

RCA Victor Television Division,  
Camden, N. J.

*Summary*—The behavior of local oscillator tubes and associated circuit elements under complex conditions of heat flow can be treated analytically. By means of such an analytical treatment, local oscillators operating at frequencies up to and beyond 1,000 megacycles may be stabilized methodically with conventional temperature-sensitive elements. The resultant frequency stability is satisfactory for most practical purposes.

The analytical approaches to local oscillator stabilization in general, and special considerations at UHF, are demonstrated by application to two types of commercial television tuners. After two minutes of operation, the VHF tuner exhibited a maximum residual frequency deviation of  $\pm 50$  kilocycles, while that of the UHF tuner was  $\pm 100$  kilocycles.

It is believed that the same general approaches and considerations can be utilized to stabilize local oscillators for other applications.

## INTRODUCTION

OSCILLATOR-FREQUENCY deviations caused by an oscillator tube or any associated circuit element under complex conditions of heat flow have been treated analytically.<sup>1</sup> Such frequency deviations may be represented by a simple mathematical expression:

$$\Delta f = \alpha (1 - e^{-\beta t}), \quad (1)$$

where  $\Delta f$  = instantaneous frequency deviation of the local oscillator,

$\alpha$  = maximum frequency deviation,

$\beta$  = a constant determined by the rate of change of oscillator frequency with respect to time,  $t$ , or the rate of temperature rise of the local oscillator elements.

A normalized graphical illustration of Equation (1) is shown in Figure 1 for various values of  $\beta$  and a unity value of  $\alpha$ . When plotted on a linear scale, this exponential function becomes essentially a straight line for  $\beta < 0.01$ . Conversely, it stabilizes within a relatively short interval of time for  $\beta > 0.1$ . These curves clearly explain the

<sup>1</sup> W. Y. Pan, "Frequency Characteristics of Local Oscillators," *RCA Review*, Vol. XVI, p. 379, September, 1955.

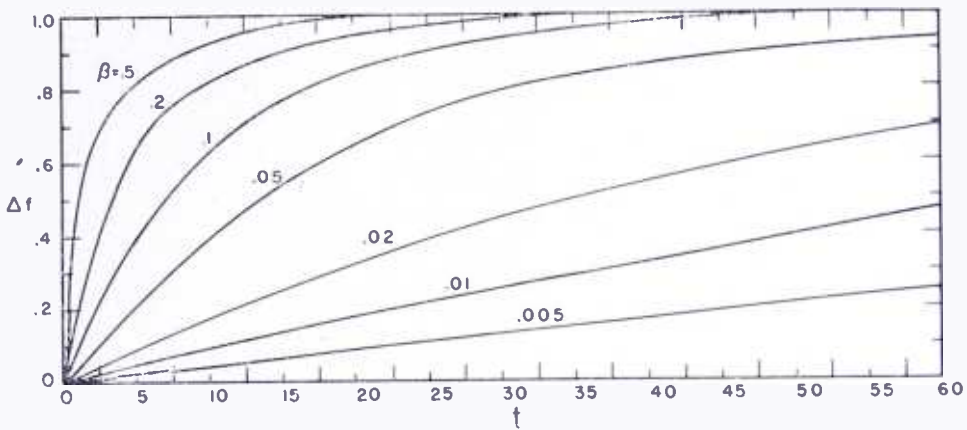


Fig. 1—Normalized frequency characteristics of oscillator circuit elements under the conditions of heat flow  $\Delta f = 1 - e^{-\beta t}$ .

fact that the stability of any local oscillator depends upon the rate of heat flow to the temperature-sensitive elements in the circuit.

The foregoing analytic treatise can be utilized conveniently and accurately to stabilize local oscillators at frequencies up to and including the ultra-high-frequency (UHF) band. To illustrate this, the local oscillators of two representative commercial television receivers have been stabilized.

- (1) Very-high-frequency (VHF) local oscillator—oscillator frequency varies from 101 megacycles at channel 2 to 257 megacycles at channel 13.
- (2) UHF local oscillator—oscillator frequency varies continuously from 517 megacycles at channel 14 to 931 megacycles at channel 83.

### STABILIZATION OF A VHF TELEVISION LOCAL OSCILLATOR

The original or uncompensated VHF television oscillator circuit is indicated in Figure 2. At channel 13 the inductances  $L_2$  and  $L_3$  are short-circuited; under this condition the inductance  $L_1$  and the circuit capacitances constitute the frequency-determining elements. At chan-

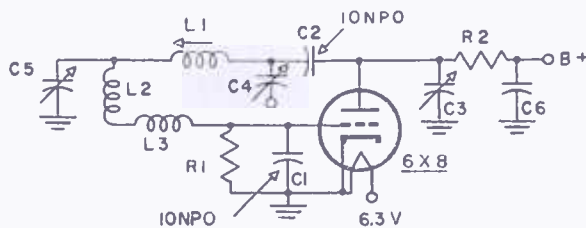


Fig. 2—Original oscillator circuit VHF television tuner.

nel 7, however, only  $L_3$  is short-circuited. Consequently,  $L_2$  tunes through the upper VHF television channels (channels 7 to 13 inclusive), whereas  $L_3$  tunes from channel 2 to channel 6, inclusive.

All capacitances in the original oscillator circuit are not temperature-sensitive. Functionally,  $C_1$  is a part of the "limiter device" which controls the level of oscillation;  $C_2$  is essentially for blocking purposes, and  $C_3$  equalizes the variation of tube capacitances;  $C_4$  and  $C_5$  are for oscillator-injection and fine-tuning controls, respectively.

#### *Analysis of the Original Frequency-Deviation Characteristics*

Figure 3 shows the frequency characteristics of the local oscillator

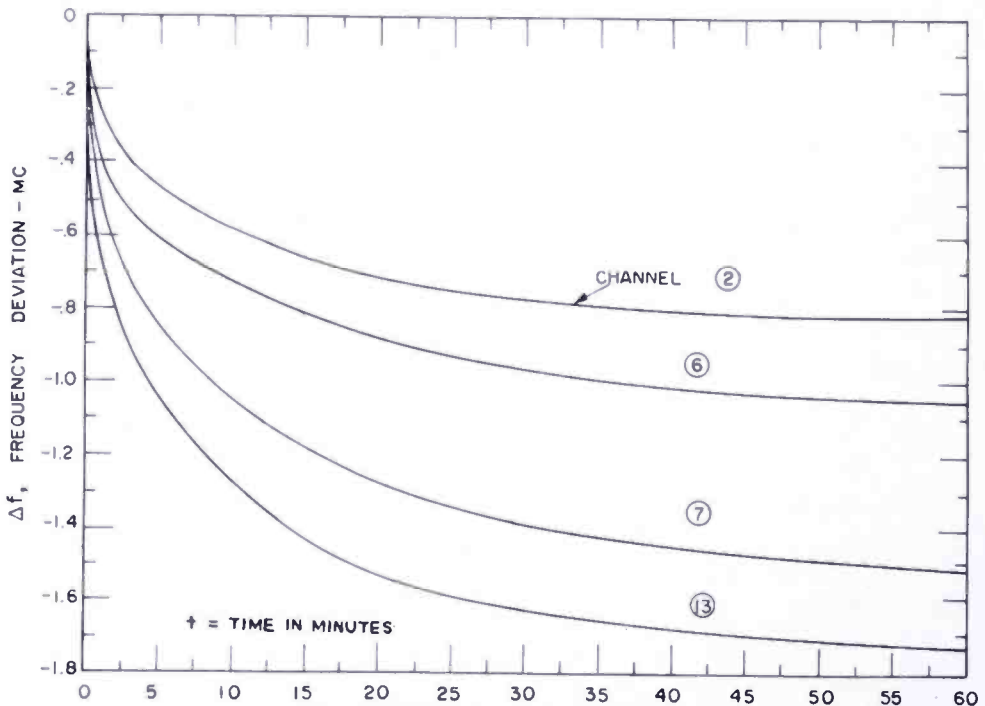


Fig. 3—Frequency characteristics of the original VHF television local oscillator.

of a commercial VHF color television receiver for channels 2, 6, 7, and 13.

Each curve exhibits two distinct changes in slope. Accordingly, there are at least two major components of frequency deviations—a fast-acting component,

$$\Delta f_1 = \alpha_1 (1 - e^{-\beta_1 t}), \quad (2)$$

and a slow-acting component,

$$\Delta f_2 = \alpha_2 (1 - e^{-\beta_2 t}). \quad (3)$$

The fast-acting component is caused by the change of tube capaci-

tances, while the slow-acting component is caused by the associated circuit elements. The over-all instantaneous frequency deviation,  $\Delta f$ , is the sum of the fast-acting and the slow-acting components, or

$$\Delta f = \Delta f_1 + \Delta f_2. \tag{4}$$

**The Fast-Acting Component**

To evaluate the fast-acting component, all associated circuit elements of the original local oscillator were replaced with a single inductance  $L_o$ , made of "Milvar" wire having an extremely low coefficient of thermal expansion.  $L_o$  and the tube capacitances then constituted the frequency-determining elements. The corresponding

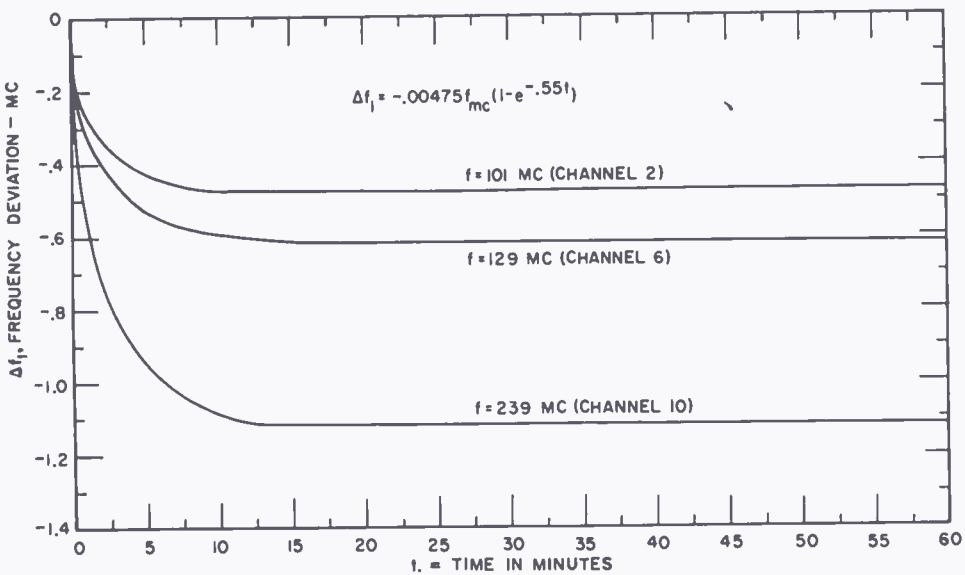


Fig. 4—Frequency deviation resulting from changes of oscillator-tube capacitances in the VHF television tuner.

frequency-deviation characteristics are given in Figure 4 at channels 2 (101 megacycles), 6 (129 megacycles), and 10 (239 megacycles):

| Oscillator Frequency<br>(megacycles) | $\alpha_1$<br>(megacycles) | $\beta_1$<br>(megacycles) |
|--------------------------------------|----------------------------|---------------------------|
| 101                                  | -0.48                      | 0.55                      |
| 129                                  | -0.62                      | 0.55                      |
| 239                                  | -1.13                      | 0.55                      |

It is evident that the frequency deviation,  $\Delta f_1$ , or the constant  $\alpha_1$ , is directly proportional to the oscillator frequency. Thus the instantaneous values under these operating conditions can be expressed by

$$\Delta f_1 = -0.00475 f (1 - e^{-0.55t}), \quad (5)$$

where  $t = 0$  when the oscillator has been energized for a period of exactly 30 seconds. Since the  $\beta_1$  value is 0.55, the oscillator frequency according to Equation (1), is substantially stabilized after 10 minutes. Therefore, any frequency deviation of the original oscillator circuit shown by Figure 2 after  $t = 10$  minutes is caused by circuit elements other than the oscillator tube.

### The Slow-Acting Component

The difference between the over-all frequency deviation,  $\Delta f$ , of Figure 3 and the fast-acting component,  $\Delta f_1$ , represented by Equation (5), gives the slow-acting component,  $\Delta f_2$ , or

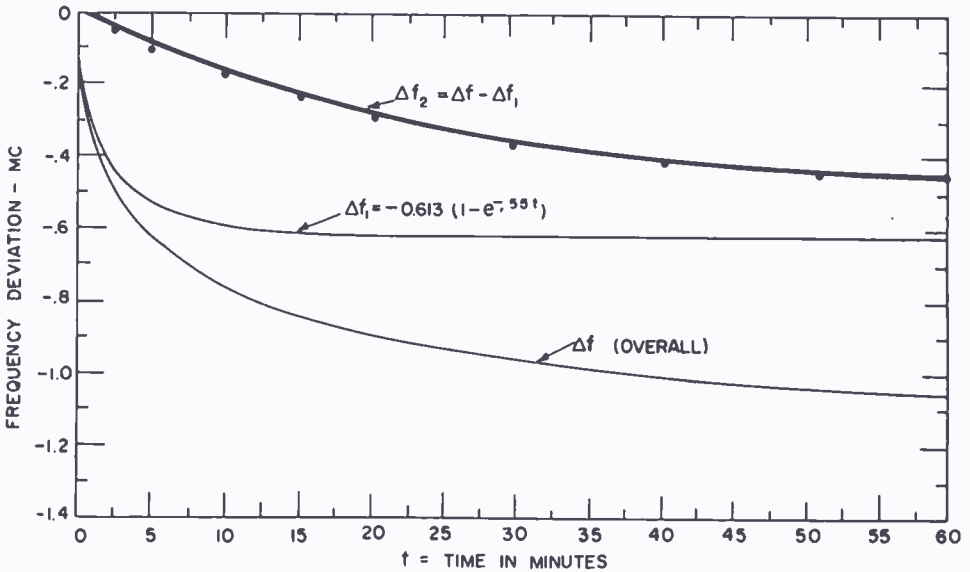


Fig. 5—Slow-acting component at channel 6.

$$\Delta f_2 = \Delta f - \Delta f_1. \quad (6)$$

At channel 6, for instance, the slow-acting component is as plotted in Figure 5:

$$\Delta f_2 = -0.500 (1 - e^{-0.04t}). \quad (7)$$

Stabilization had not been reached at the end of a 60-minute period which would explain the finite slopes of the curves shown in Figure 3 after one hour of continuous operation in a color television receiver.

A close inspection of the  $\Delta f_2$  curve in Figure 5 discloses slight deviations from the mathematical formula of Equation (7). The

points which are calculated according to Equation (7) do not exactly coincide with the observed curve. In fact, the slow-acting component may consist of many sub-components:

$$\Delta f_2 = \Delta f_{21} + \Delta f_{22} + \Delta f_{23} + \dots \quad (8)$$

The factors contributing to the  $\Delta f_2$  sub-components are the inductance  $L_1$ , the injection circuit, the fine-tuning device  $C_5$ , the inductances  $L_2$  and  $L_3$ , the switching mechanism, etc. In this particular circuit one of these factors is more pronounced than the others. Therefore, if it is assumed that  $\Delta f_2$  follows the general expression of Equation (1), the resulting error is small. This approximation is satisfactory for most practical purposes.

#### *Requirements for Frequency Stabilization*

To obtain good frequency stabilization of the local oscillator at any particular VHF television channel, the following is necessary:

(a) At least two compensating elements are needed, one to compensate for the fast-acting component,  $\Delta f_1$ , and the other to compensate for the slow-acting component,  $\Delta f_2$ .

$$\begin{aligned} \Delta f'_1 &= \alpha'_1 (1 - e^{-\beta'_1 t}) \\ &= -\Delta f_1, \end{aligned} \quad (9)$$

$$\begin{aligned} \text{and } \Delta f'_2 &= \alpha'_2 (1 - e^{-\beta'_2 t}) \\ &= -\Delta f_2. \end{aligned} \quad (10)$$

(b) These two compensating elements must be so situated that  $\beta'_1$  approaches the value of  $\beta_1$  of  $\Delta f_1$ , and  $\beta'_2$  approaches the value of  $\beta_2$  of  $\Delta f_2$ .

(c) The compensating elements must exhibit negative temperature sensitivities to raise the oscillator frequency with temperature.

(d) The magnitudes of  $\alpha'_1$  and  $\alpha'_2$  must approach those of  $\alpha_1$  of  $\Delta f_1$  and  $\alpha_2$  of  $\Delta f_2$ , respectively.

Furthermore, it is desirable that the spread between channels 7 and 13 and between channels 2 and 6 shown by Figure 3 be minimized so that a minimum number of compensating elements may be used.

#### *Stabilized Oscillator Circuit*

The stabilized oscillator circuit is indicated in Figure 6. When

compared with the original oscillator circuit of Figure 2, it is noted that  $C_1$  (10NPO) of the original oscillator circuit is replaced with 10N330 and a lead length of  $\frac{5}{8}$  inch;  $C_2$  (10NPO) of the original oscillator circuit is moved to a position between  $L_1$  and  $L_2$  and is changed to 10N330; and a new temperature-sensitive capacitance,  $C_8$  (47N750), is added between  $L_2$  and  $L_3$ .

The capacitance values, temperature sensitivities, and placements of  $C_1$ ,  $C_2$ , and  $C_8$ , and the lead length of  $C_1$ , are determined as follows:

### Capacitance $C_1$

Capacitance  $C_1$  compensates for  $\Delta f_1$ , according to Equations (2) and (9). To make  $\beta'_1 = \beta_1$ ,  $C_1$  must be located as close as possible to the source of heat flow. Therefore, it is placed at the grid pin of the oscillator tube. The resultant  $\beta'_1$  value is 0.29 as compared to  $\beta_1$  of 0.55. The discrepancy between  $\beta'_1$  and  $\beta_1$  unavoidably introduces a compensation error,  $\epsilon$ , where

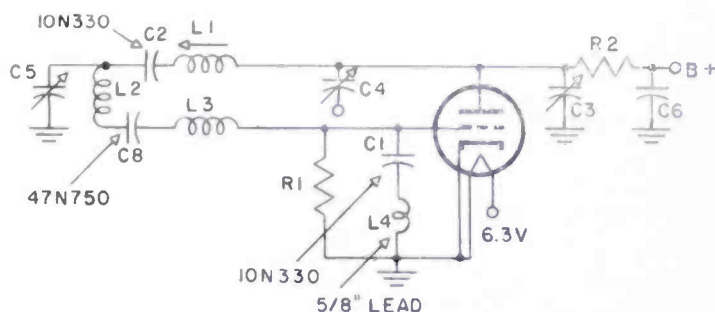


Fig. 6—Modified oscillator circuit VHF television tuner.

$$\begin{aligned}\epsilon &= \Delta f'_1 + \Delta f_1 \\ &= \alpha'_1 (1 - e^{-0.29t}) + \alpha_1 (1 - e^{-0.55t}),\end{aligned}\quad (11)$$

The compensation error expressed in Equation (11) is evaluated in Figure 7 for  $\alpha'_1/\alpha_1 = 0.4, 0.6, 0.8,$  and  $1.0$ . The error is minimum with  $\alpha'_1 = 0.6\alpha_1$  after a period of two minutes, which is usually allowed to make the initial adjustments of a color television receiver. According to Figure 4 or Equation (5),  $\alpha_1 = -1.13$  megacycles at channel 10. The corresponding compensation error, after two minutes, is  $0.04\alpha_1$  or  $.045$  megacycles, and the corresponding  $\alpha'_1 = 0.6\alpha_1$  or  $0.678$  megacycles. A compensating capacitor of 10N330 produces these results approximately.

### Inductance $L_4$ ( $\frac{5}{8}$ -inch lead of $C_1$ )

Inductance  $L_4$  is used to reduce the spread between channels 7 and

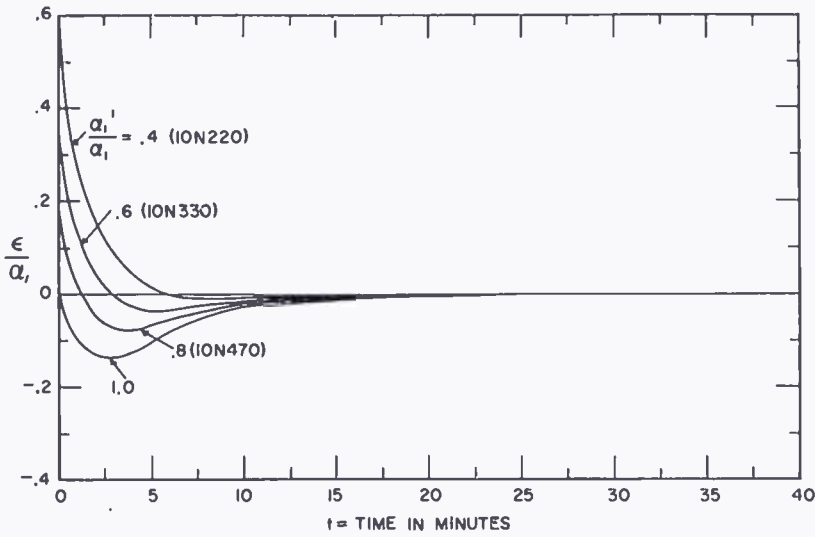


Fig. 7—Compensation error.

13 substantially, and between channels 2 and 6 to a lesser extent. The action can be explained by referring to Figure 8, which shows the self-resonance frequencies,  $f_c$ , of a 10-micromicrofarad capacitor with varying lead lengths. With a  $\frac{5}{8}$ -inch lead,  $f_c = 450$  megacycles. This self-resonance frequency is closer to 257 megacycles (channel 13) than 221 megacycles (channel 7). For this reason, the "equivalent temperature sensitivity" of  $C_1$  is higher at channel 13 than at channel 7. The spread between curves (7) and (13) of Figure 3 for the original local oscillator will thereby be significantly decreased. The same effect takes place insofar as the spread between channels 2 and 6 is concerned, but the effectiveness is much less, due to high ratios of

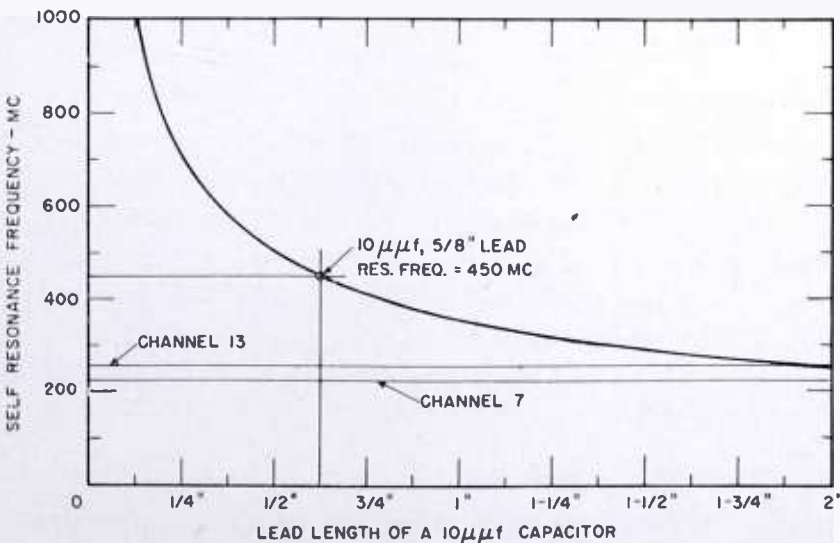


Fig. 8—Self resonance frequency of a 10-micromicrofarad capacitor.

$f_c$  to the oscillator frequencies at the lower VHF television channels. However, the initial spread between channels 2 and 6 is usually not serious enough to warrant special attention.

### Capacitance $C_2$

Capacitance  $C_2$  compensates for the slow-acting component of the frequency deviations for channels 7 to 13 inclusive, according to Equations (10) and (3). At these upper VHF television channels, the inductance  $L_3$  and capacitance  $C_1$  are short-circuited.  $C_2$  is situated among the associated circuit elements of the local oscillator where the rate of temperature rise is relatively slow. Therefore, the value  $\beta'_2$  is approximately equal to the value  $\beta_2$ . The capacitance and temperature-sensitivity of  $C_2$  (10N330) is determined in an analogous manner as for  $C_1$ , and the corresponding  $\alpha'_2 = \alpha_2$  at all upper VHF television channels.

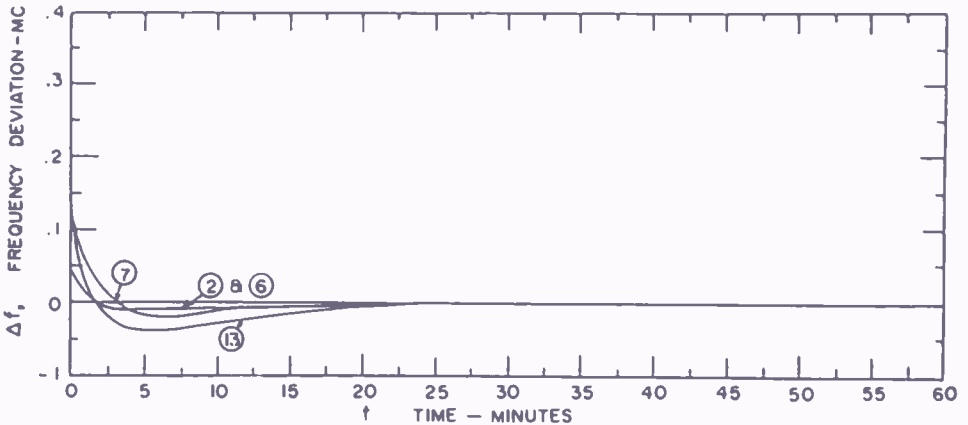


Fig. 9—Frequency characteristics of the compensated VHF television local oscillator (4 channels).

### Capacitance $C_8$

At the lower VHF television channels, both  $C_2$  and  $C_8$  are effective in frequency stabilization. Owing to the difference in  $L/C$  ratios at the lower oscillator frequencies,  $C_2$  is not sufficient to compensate for the frequency deviations at channels 2 to 6 inclusive. The addition of  $C_8$  makes  $\alpha'_2$  (at the lower VHF television channels)  $= \alpha_2$ . The  $\beta'_2$  value of  $C_8$  is approximately equal to the  $\beta'_2$  value of  $C_2$  because the locations of these two elements are equally distant from the heat sources.

### Residual Frequency Deviations

A typical production VHF television tuner incorporating these compensating elements behaves according to the curves of Figure 9

at channels 2, 6, 7, and 13. The maximum residual frequency deviation is less than  $\pm .05$  megacycle after a period of two minutes, and all channels become almost completely stabilized within 30 minutes. The residual frequency deviation is caused by the discrepancy between the  $\beta'_1$  value of the  $C_1$  capacitance and the  $\beta_1$  value of the fast-acting component.

For local oscillators in other applications, where a greater degree of frequency stability is required, the compensation error can be further minimized by special means.

a. The capacitance  $C_1$  may be mounted inside the oscillator tube, thereby facilitating the rate of heat flow to the compensating element. Thus, the  $\beta'_1$  value of Equation (9) may be made to equal or approximately equal the  $\beta_1$  value of Equation (2).

b. The  $\beta'_1$  value may also be raised by an artificial heat source<sup>2</sup> closely coupled to the compensating capacitance  $C_1$ . Such artificial source device can be standardized readily in terms of dissipation and heat coupling coefficient.

c. A junction diode or transistor may be used as a frequency-sensitive device of an automatic frequency-control system<sup>3</sup> which is capable of stabilizing a VHF local oscillator to within  $\pm .005$  megacycle and a UHF local oscillator to within  $\pm .01$  megacycle.

#### STABILIZATION OF A UHF TELEVISION LOCAL OSCILLATOR

The same approach utilized to stabilize a VHF television local oscillator applies equally well to the stabilization of a UHF oscillator. Appropriate compensating elements can again be secured by analyzing the original frequency-deviation characteristics of the oscillator with the aid of the basic relationship expressed in Equation (1).

The stabilization procedure at UHF, however, is usually further complicated by the fact that (1) the frequency-deviations of the original local oscillator may exhibit rather inconsistent characteristics between receivers and between frequencies; (2) some of the associated circuit elements of the local oscillator may have electrical lengths comparable to  $\frac{1}{4}\lambda$  of the oscillator frequency.

For these reasons, additional practical aspects of UHF oscillator stabilization have been considered. To illustrate such considerations, a typical commercial UHF local oscillator is shown schematically in

<sup>2</sup> Initial work was done by H. L. Donley and E. O. Keizer of RCA Laboratories in 1949.

<sup>3</sup> W. Y. Pan and O. Ramanis, "Automatic Frequency Control of Television Receivers Using Junction Diodes," *Transistors I*, RCA Laboratories, Princeton, N. J., 1956, p. 598.

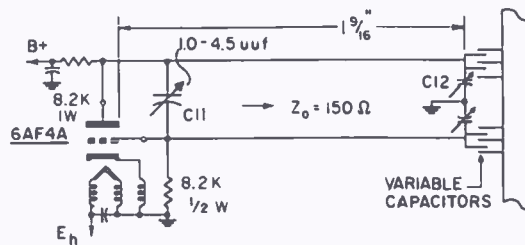


Fig. 10a—Original oscillator circuit of the UHF television tuner.

Figure 10a. This oscillator circuit has been commonly used in UHF television receivers which cover continuously a frequency range from 517 to 931 megacycles by means of a variable gang capacitor. The variable gang capacitor is coupled to the 6AF4A oscillator tube by a transmission line having a characteristic impedance of approximately 150 ohms. The plate-to-grid trimmer,  $C_{11}$ , extends the frequency tuning range and, at the same time, provides an adjustment for the low-end (517 megacycles) coverage, while the trimmer,  $C_{12}$ , insures the high-end (931 megacycles) coverage.

#### *Inconsistency of Frequency-Deviation Characteristics*

Among many other factors contributing to the inconsistency of frequency-deviation characteristics of the oscillator shown in Figure 10a, the factor of primary importance is the construction of the variable gang capacitor, indicated in Figure 10b.

When the local ambient temperature rises, the brass shaft expands more than the stator assembly. Consequently, the rotor plates are displaced relative to the stator plates. This relative displacement, represented by  $\Delta d$  of Figure 10b, exhibits an equivalent temperature sensitivity insofar as oscillator frequency is concerned.

The magnitude of this equivalent temperature sensitivity depends upon the ratio  $d_1/d_2$ . It is positive when  $d_1 < d_2$  and negative when  $d_1 > d_2$ , if the rotor plates were displaced in the direction of reducing  $d_1$  or increasing  $d_2$ . Under these conditions, the capacitance  $C$  between the rotor and stator is given by

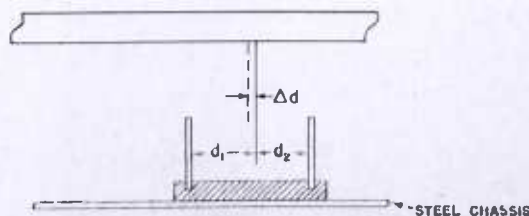


Fig. 10b—Variable gang capacitor.

$$C = KA \left( \frac{1}{d_1} + \frac{1}{d_2} \right),$$

and

$$C + \Delta C = KA \left( \frac{1}{d_1 - \Delta d} + \frac{1}{d_2 + \Delta d} \right) - 1, \quad (12)$$

or

$$\frac{\Delta C}{C} = \frac{1}{1 + \frac{\Delta d}{d_2} - \frac{\Delta d}{d_1} - \frac{(\Delta d)^2}{d_1 d_2}},$$

where  $K = \text{constant},$

$A = \text{effective projected area between the rotor and stator plates},$

$\Delta C = \text{change of capacitance due to the rise of local ambient temperature}.$

The change in capacitance,  $\Delta C$ , is minimum when

$$\frac{\partial \left( \frac{\Delta C}{C} \right)}{\partial d_1} = 0,$$

which gives  $d_1 = d_2$ , or the rotor plates are initially set at exactly equal distances from the adjacent stator plates at room temperature.

When  $d_1 = d_2 = d$

$$\frac{\Delta C}{C} = \frac{1}{\left( \frac{d}{\Delta d} \right)^2 - 1}. \quad (13)$$

When  $d_1 < d_2$

$d = 1/2 (d_1 + d_2)$  — the mean value of the spacing between adjacent rotor and stator plates.

Let

$$\frac{d}{d_1} = \delta,$$

$$\frac{\Delta d}{d} = \psi,$$

where  $\delta$  is a factor which takes into account the position of the rotor plates relative to the stator plates, and  $\psi$  is a factor which takes into account the difference in coefficients of thermal expansion between the shaft and the stator assembly, and also the rise in local ambient temperature.

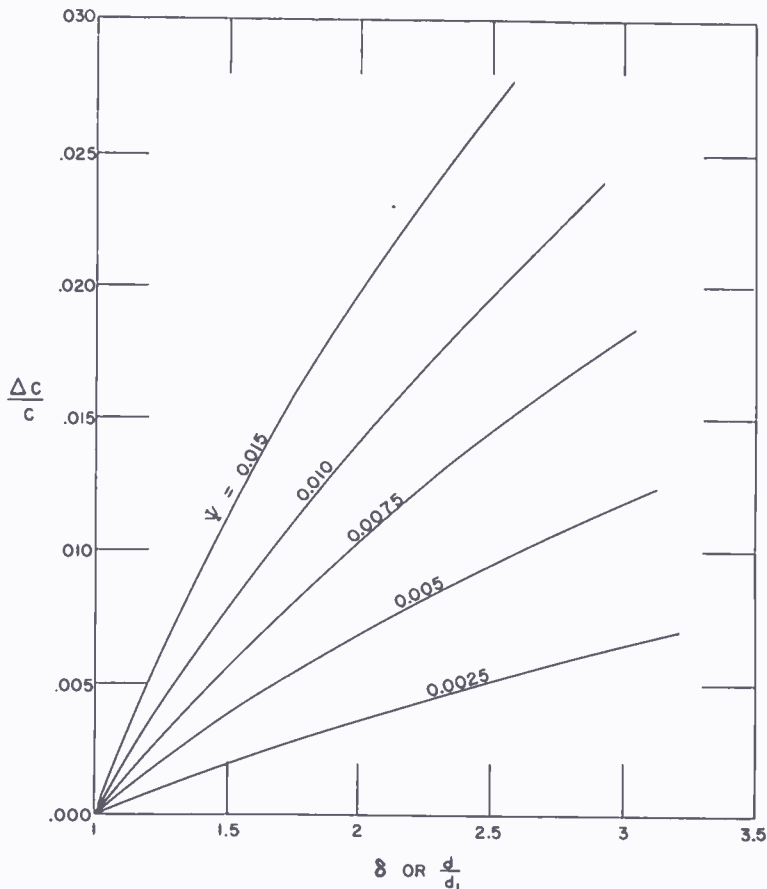


Fig. 11—Change of gang capacitance as a function of  $\delta$ .

$$\frac{\Delta C}{C} = \frac{1}{1 - \delta\psi + \frac{\delta\psi(1 - \delta\psi)}{2\delta - 1}} - 1. \quad (14)$$

Equation (14) is plotted in Figure 11 as a function of  $\delta$  for various values of  $\psi$ . It is noted that the change of capacitance is nearly proportional to  $\delta$ . In order to minimize the effect of relative position of rotor and stator plates on oscillator frequency characteristics,  $d_1$  must be equal to  $d_2$ , or the coefficient of thermal expansion of the shaft must be equal to that of the stator assembly. Therefore, a silver-

plated steel shaft is highly desirable for more consistent frequency drift characteristics.

### Experimental Verification

The brass shaft of the gang capacitor exhibits a coefficient of thermal expansion of 18.9 PPM/°C, whereas that of the steel chassis is in the order of 12 PPM/°C. The difference between these two coefficients and the temperature rise determine the magnitude of  $\psi$ . For a temperature rise of 50°C,  $\psi = 0.005$ . When  $\delta = 1.5$ ,

$$\frac{\Delta C}{C} = 0.004,$$

or the frequency deviation at 600 megacycles is

$$\left( \sqrt{\frac{C + \Delta C}{C}} - 1 \right) \times 600 = 1.2 \text{ megacycles.}$$

The relative position of the rotor and stator plates is adjustable by a set screw which fastens the shaft to the tuner chassis. The frequency characteristics at 600 megacycles with the set screw in the middle position are plotted by the solid curve marked (1) in Figure 12; by displacing the rotor plates  $\pm .005$  inch relative to the stator plates or, by turning the set screw 90° clockwise or 90° counter-clockwise, the frequency characteristics are substantially different as shown by the solid curves marked (2) and (3) respectively. The position of the set screw changes the  $\alpha$  value, although  $\beta$  remains constant. At a period of 10 minutes, the difference in frequency deviation amounts to .83 megacycle. Because of this variation, the tuners are extremely inconsistent in frequency-drift characteristics. By replacing the brass shaft with a steel shaft, the corresponding variations are much less, as shown by the dotted curves in Figure 12.

### *The "Null Points" Along the Oscillator Line*

At the socket pins of the 6AF4A tube, Figure 10a, the oscillator voltage between the plate and grid falls to a minimum value at approximately 1,000 megacycles. Any temperature-sensitive element placed across these two points would affect the oscillator frequencies either above or below that frequency. At 1,000 megacycles the effect is theoretically zero. Since the oscillator line is  $1\frac{9}{16}$  inches long, the voltage minimum or null point at the other end of the line corresponds approximately to 500 megacycles.

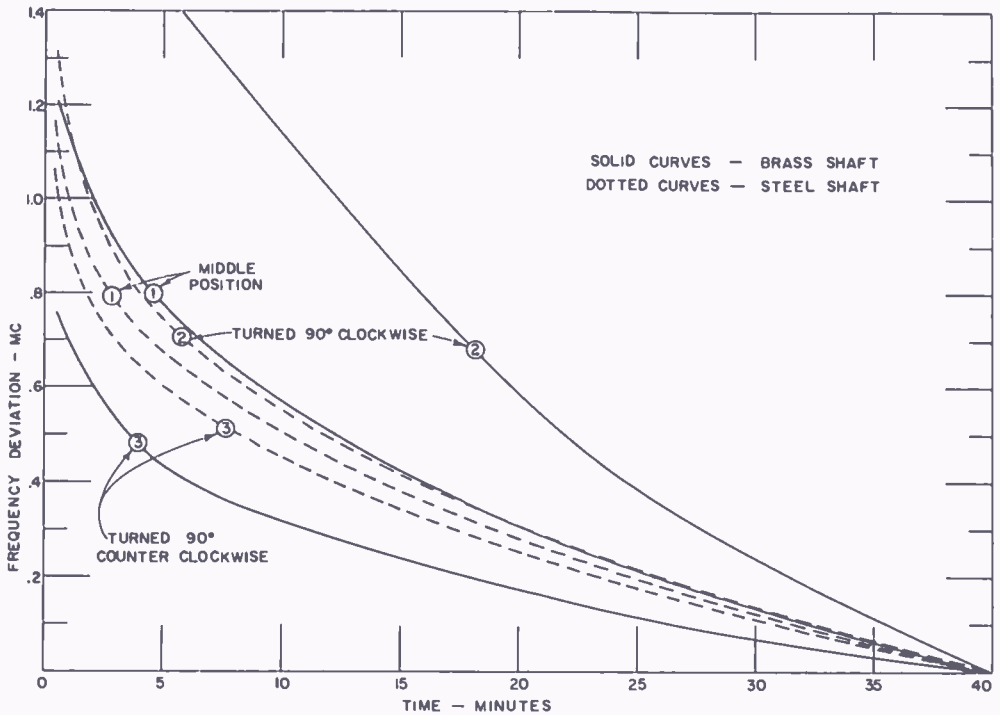


Fig. 12—Effect of relative spacing (rotor and stator plates) on local-oscillator frequency deviation at 600 megacycles.

Let the distance at the junction between the oscillator line and the stator assembly be zero; the null points along the line are illustrated in Figure 13. For instance, the 725-megacycle null point occurs at  $\frac{7}{8}$  inch.

After substituting a steel shaft for the brass shaft of the variable gang capacitor and determining the null points along the oscillator line, the UHF local oscillator can be stabilized in a similar manner as was the VHF local oscillator.

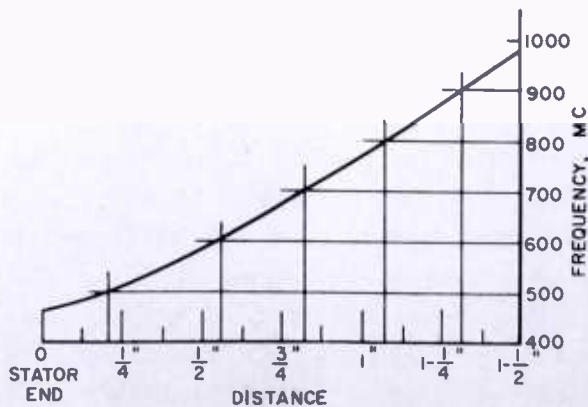


Fig. 13—Null points along the oscillator line.

One-Point Compensation

By placing an appropriate temperature-sensitive capacitor at any point ( $x$ ) along the oscillator line, the relative effectiveness of frequency compensation  $P_x$  at an oscillator frequency  $f$  is determined by

$$P_x = 1 - |\sin \theta_x|, \tag{15}$$

where

$$\theta_x = \frac{1}{2} \frac{\pi f}{f_x}$$

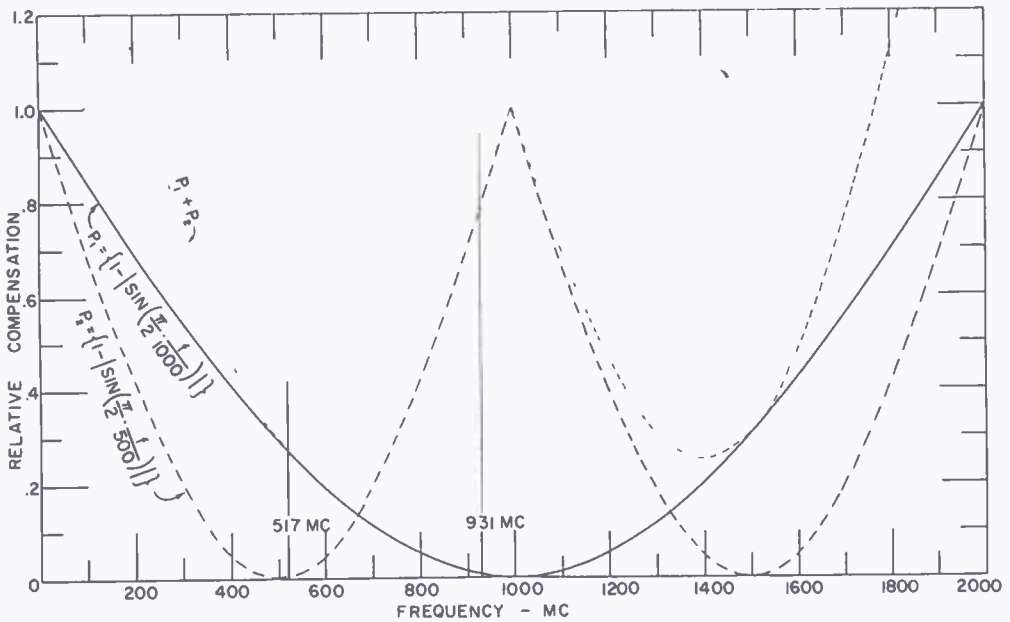


Fig. 14—Relative effectiveness of one-point and two-point oscillator-frequency compensations.

and  $f_x =$  null frequency corresponding to point  $x$ .

The solid curve of Figure 14 shows the  $P_1$  function for  $C_1$  placed at the socket pins where  $f_x = 1,000$  megacycles, while the dashed curve shows the  $P_2$  function for  $C_2$  placed at the stator junction where  $f_x = 500$  megacycles. It is obvious that one-point compensation is adequate only at one frequency or for a very narrow frequency spectrum. The position of such a compensating capacitor is dictated by the oscillator frequency at which the compensation is intended.

### Two-Point Compensation

To compensate for a band of frequencies, more than one temperature-sensitive capacitor must be employed. By placing  $C'_1$  at the socket pins and  $C'_2$  at the stator junction, the relative compensation throughout the UHF television band is the sum of  $P_1$  and  $P_2$  which is shown dotted in Figure 14, assuming that the maximum effectiveness of  $P_1$  is the same as that of  $P_2$ .

However, a maximum effectiveness of either  $P_1$  or  $P_2$  can be varied independently by (1) using a capacitor of different temperature sensi-

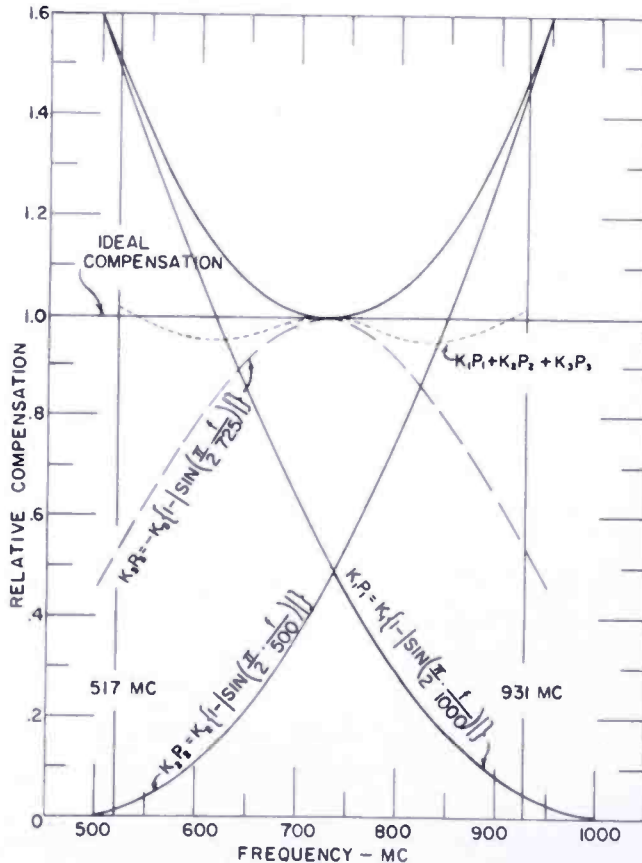


Fig. 15—Three-point compensation.

tivity, or (2) a different value of capacitance. The  $K_1P_1$  and  $K_2P_2$  curves of Figure 15 are derived from the  $P_1$  and  $P_2$  curves of Figure 14 respectively, where  $K_1 = 1.85$  and  $K_2 = 5.5$ . The  $K_1P_1 + K_2P_2$  curve indicates good compensation at 725 megacycles, but over-compensation at all other frequencies, particularly at 517 and 931 megacycles. Conversely, if the values of  $K_1$  and  $K_2$  were so selected that the oscillator was properly compensated at 517 and 931 megacycles, the oscillator would be under-compensated at all other frequencies, particularly at 725 megacycles.

This method of frequency compensation is analogous to the two-point frequency tracking of radio receivers. The tracking error can be minimized by properly selecting the two tracking frequencies, but such error may still exceed the acceptable limits.

*Three-Point Compensation*

The need for a third compensating capacitor,  $C'_3$ , is rather apparent from the above discussion. For best results, the third compensating capacitor must fulfill the following conditions:

- a. It must exhibit a positive temperature sensitivity.

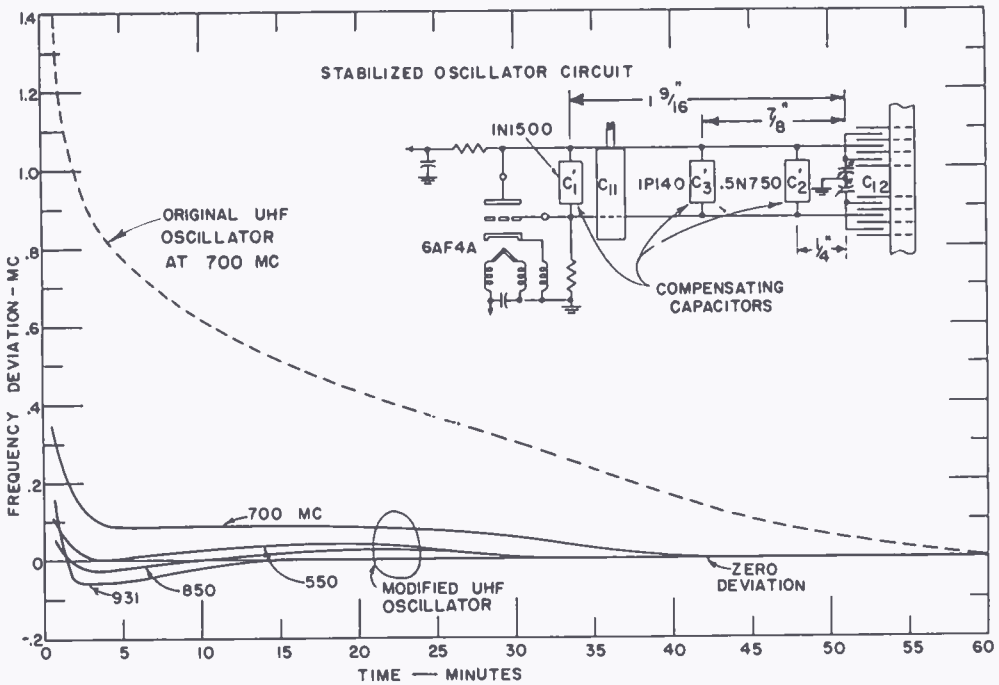


Fig. 16—Frequency characteristics of the UHF tuner installed in color receiver.

- b. It must be least effective at 725 megacycles, i.e., it must be located at the null point of 725 megacycles, which is  $\frac{7}{8}$  inch from the stator.

The positive temperature sensitivity of the third capacitor does not affect the oscillator frequency at 725 megacycles because it is located at the null point of that frequency. However, it brings down the  $K_1P_1 + K_2P_2$  curve of Figure 15 at frequencies other than 725 megacycles by an amount represented by the  $K_3P_3$  curve. The dotted curve,  $K_1P_1 + K_2P_2 + K_3P_3$ , is the final result of three-point compensation. It does not depart much from ideal compensation at all UHF television channels.

Six commercial UHF television tuners have been stabilized using the three-point compensation. The stabilized oscillator circuit together with the residual frequency deviation characteristics are illustrated in Figure 16. After an initial period of two minutes, the frequency deviation does not exceed  $\pm .1$  megacycle at any UHF television channel. The local oscillator is almost completely stabilized in 40 minutes.

#### CONCLUSIONS

According to a prior investigation on requirements of local oscillator stability for color television programs under standard conditions, a frequency deviation of  $\pm .05$  megacycle is quite acceptable, and that of  $\pm .1$  megacycle may satisfy most television viewers. Such requirements can be fulfilled by commercial local oscillator circuits employing conventional compensating elements.

# TEST SIGNAL FOR MEASURING "ON-THE-AIR" COLOR-TELEVISION SYSTEM PERFORMANCE

BY

RALPH C. KENNEDY

National Broadcasting Company, Inc.,  
New York, N. Y.

*Summary*—The National Broadcasting Company has been using a special test signal which is inserted for a duration of three lines in the vertical blanking interval of color television transmissions. This signal provides a reference level for proper adjustment of sync, burst, chroma and white amplitudes as well as permitting the measurement of the differential gain and phase distortion.

## INTRODUCTION

THE task of maintaining the adjustments necessary for the proper operation of a television broadcast system could be simplified by the addition to the broadcast signal of a suitable waveform. The need for such an addition has increased considerably with the introduction of color television.

This paper describes a waveform which, when added to the transmitted signal, greatly facilitates the setting of sync, burst, chroma, and white amplitudes and, in addition, permits measurement of the differential gain and phase distortion characteristics of the system while the system is carrying a color television program. The addition of the waveform does not affect the picture as viewed on a receiver.

## DESCRIPTION OF THE TEST SIGNAL

Figures 1a, 1b, and 1c show the test signal as it appears when inserted into a composite color-bar signal. Figure 1a shows, from left to right, the end of one field followed by the standard vertical sync interval. Next appear the flag bursts. Four lines prior to the end of vertical blanking the test waveform appears. As can be seen, the test signal lasts for three lines which leaves one line separating the test signal from the top of the picture. This means that the waveform will not be visible in the picture as viewed on a conventional receiver or monitor. This location was chosen since retrace lines appear in some receivers and monitors if the proposed waveform signal occurs earlier in time or nearer the vertical sync pulses.

Figures 1b and 1c are views of Figure 1a expanded in time. As may be seen, each line of the proposed waveform is the same and con-

sists of three pedestals or levels. Approximately 1 microsecond after horizontal sync and flag burst, a pedestal having a duration of 20 microseconds and an amplitude of 50 IRE units appears. Centered and superimposed on this pedestal is 10 microseconds of 3.579-megacycle sine wave phased  $180^\circ$  from the program flag burst.

After the bar, 2 microseconds of sync level (0 IRE units) appears

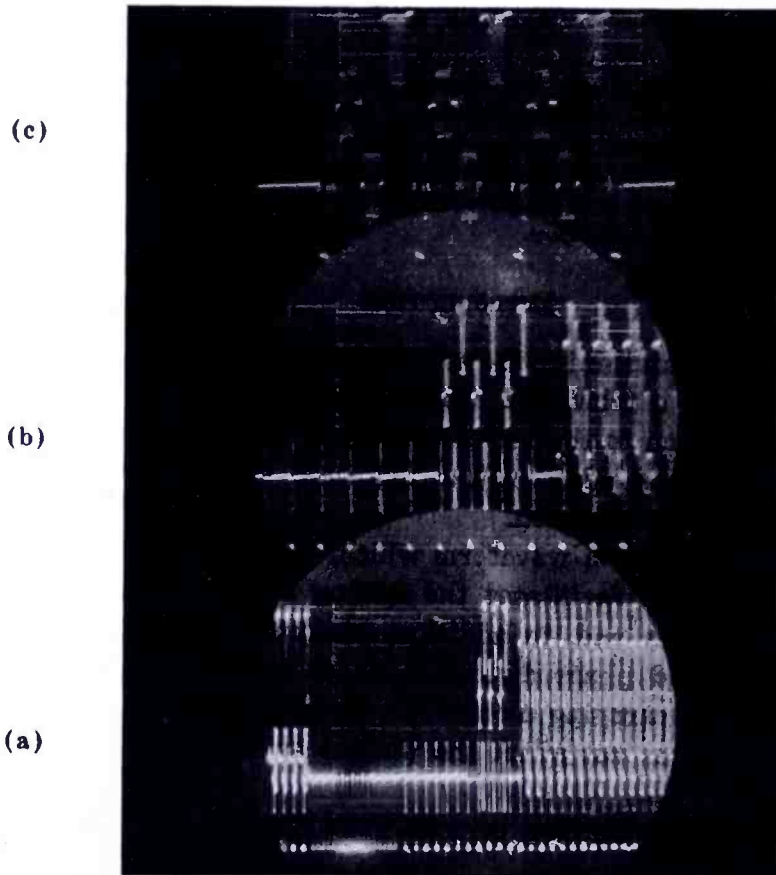


Fig. 1—Oscilloscope display showing the vertical blanking interval of a color-bar signal with the test signal inserted. Figures 1b and 1c are expanded presentations of the test signal.

followed by 10 microseconds of 3.579-megacycle sine wave phased to magenta.

Two microseconds of 0 IRE level follows the magenta sine wave at which time a bar having a duration of 20 microseconds and an amplitude of 100 IRE units appears. Centered in the bar appears 10 microseconds of 3.579-megacycle sine wave phased to cyan. The positive crests of the sine waves are at a level of 100 IRE units. This is necessary to comply with FCC requirements regarding transmitter modulation.

The amplitudes of all three sine-wave portions of the test signal are equal to 40 IRE units peak to peak. This is the peak-to-peak value for flag burst and also the amplitude of sync.

The amplitudes of the pedestals and the amplitude and phase of the sine-wave components are all very accurately maintained.

### MONOCHROME USES

For monochrome transmissions, the 3.579-megacycle sine waves are removed and the  $\frac{1}{2}$  white, pedestal, and white levels remain. It is necessary that the system have a transmission characteristic such that the  $\frac{1}{2}$ -white bar is undistorted. This level closely approximates the signal a-c axis. If slight compression of white occurs, the white pedestal will have an amplitude something less than twice the  $\frac{1}{2}$ -white amplitude.

### COLOR USES

For color transmissions, the 3.579-megacycle sine waves are added to the signal. The amplitudes of the three sine-wave signals are the same as the flag or color burst in the video signal. These are also the same as sync amplitude. Thus sync, burst, and chroma as well as white levels are all established by the test signal.

By passing the waveform through a 1-megacycle high-pass filter, all the low-frequency components are removed and as a result, the a-c axis of color burst and the three sine waves of the test signal are on the same a-c axis. If no differential gain distortion is present in the system, these should all have the same amplitudes.

Figures 2a and 2b show the display seen on a vectorscope. In 2a, the test signal appears in conjunction with a color slide. The normal flag burst appears horizontally to the left of the origin while the vector representing the sine wave phased  $180^\circ$  from burst appears horizontally to the right of the origin. The magenta vector appears  $30^\circ$  to the right of the vertical axis and above the horizontal axis. The cyan vector appears  $13^\circ$  to the right of the vertical axis and below the horizontal axis. Figure 2b shows the test signal as it appears in conjunction with a conventional monochrome test pattern slide. No flag burst is present but the three vectors of the test signal are clearly visible. The presence of any differential phase distortion in a system causes the vectors to rotate and it is easy to measure the number of degrees of such shift on the vectorscope. The choice of cyan and magenta in the signal was dictated by the fact that the eye is most sensitive to these colors. However, means are readily available to change these colors to others.

Another characteristic of the system which may be evaluated with the test signal is the amount of low-frequency tilt present. This creates smear in a picture and an apparent loss in resolution. The  $\frac{1}{2}$ -white and white pedestals, since they have durations 20 microseconds each and rise times of the order of 0.1 microsecond, quite clearly indicate the presence of low-frequency distortion.

It should be pointed out that by suitably adjusting either the vertical centering or the vertical hold control in a receiver, the three bars of color on their respective pedestals may be made to appear in the middle of the screen. These signals could aid in adjusting a color receiver. The use of a plastic translucent card for color comparison or a transparent color card for interference cancellation may be of further aid.

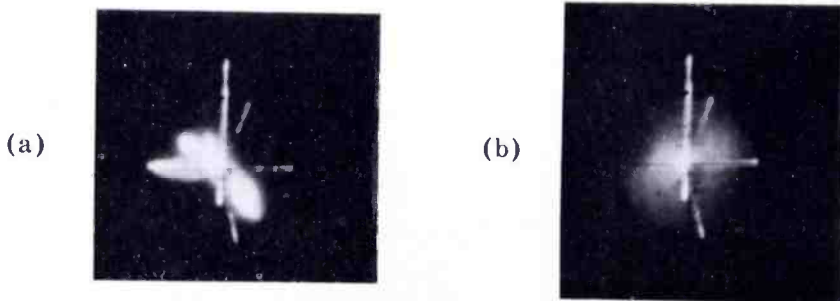


Fig. 2—(a) Vectorscope display of a color slide signal with the test signal inserted; (b) Vectorscope display of a monochrome slide signal with the test signal inserted.

It is expected that the waveform will be inserted in the colorplexer; this means that the effects of each stage of the entire system from the camera through the transmitter may be measured. With this test signal it is possible to monitor the system performance continuously, and to make necessary corrective adjustments when the need arises. The nature of the information obtainable from the test signal is such that many of the adjustments could be made automatically through the use of feedback techniques.

#### CONCLUSION

Several on-the-air tests of the signal have been made and it has been determined the test signal can be used without causing adverse effects in receivers and monitors. The signal has been in experimental use during the last few months following FCC authorization.

It appears that the signal will be able to make local and network operations much simpler and more consistent. The modulation charac-

teristics of transmitters should be more accurately determined. There may be some usefulness found in adjusting monitors and receivers.

ACKNOWLEDGMENTS

The author is indebted to A. L. Hammerschmidt and H. C. Gronberg of the NBC Engineering Department for valuable suggestions and encouragement offered during this investigation.

# A VIDEO AUTOMATIC-GAIN-CONTROL AMPLIFIER

BY

JOHN O. SCHROEDER

National Broadcasting Company, Inc.,  
New York, N. Y.

*Summary*—This paper discusses some of the considerations which are involved when automatic-gain-control systems are used to hold the peak-to-peak level of a television video signal constant. The design of a satisfactory video automatic-gain-control amplifier is described and measured performance data is shown by means of curves and oscillograms.

## INTRODUCTION

AUDIO automatic-gain-control amplifiers or "limiters" have attained widespread use in the broadcasting and recording fields wherever it is desired to maintain a given output signal level more or less constant in the presence of varying input levels. There has, however, been little use of similar techniques for handling video signals in television transmission systems.

This paper discusses some of the problems involved in designing AGC (automatic-gain-control) equipment suitable for television broadcast purposes and describes a video AGC amplifier which has been used by the National Broadcasting Company for some time with very gratifying results. This device has made it possible to transmit signals originating from all over the country with relative ease and freedom from level fluctuations. Shows such as "Wide Wide World" have depended heavily on video AGC equipment to maintain the level of the signal fed to the transmitter and network lines within acceptable limits despite wide variations in the level of the signals as they are received from the incoming telephone company lines.

## FUNCTION OF VIDEO AGC

Just as in audio transmission, whenever the video signal is transmitted from one location to another, there exists a standard level which the transmission engineer attempts to maintain rather closely in order to utilize the transmission facilities involved properly and to provide a picture on the home viewer's screen having the proper brightness and contrast. This level is currently standardized at 1 volt peak-to-peak as measured from the tip of sync to the peak white picture components, this composite signal being composed of 0.7 volt of video and 0.3 volt of sync.

There are several reasons why both the total peak-to-peak amplitude and the ratio of sync to video must be held at the proper values:

1. Video amplifiers in general cannot readily be designed as conservatively as audio amplifiers. Usually a 100 per cent increase in level will be easily tolerated by most audio equipment whereas serious picture degradation would result if double-level video signals were fed to most video distribution amplifiers. This is especially significant in connection with color television signals since the requirements imposed on the video amplifiers are extremely severe with regard to differential gain and differential phase distortion.
2. Clamp circuits are apt to perform unsatisfactorily and cause severe damage to the signal.
3. Unless white peak clipping is installed at the transmitter, the carrier will be over-modulated and cause audible "sync buzz" as well as adverse effects upon the picture as seen on the home screen. Improper sync-to-video ratio can cause faulty sync separation and incorrect picture brightness since most receivers employing d-c restoration use the sync tips as black reference level.

#### FUNDAMENTAL DESIGN CONSIDERATIONS

In designing video AGC equipment, it must first be decided whether the system is to handle composite signals (video plus sync) or non-composite signals (video only). If only composite need be handled, some of the design problems may be eased by employing keyed clamps whose keying pulses can be derived from the sync portion of the incoming composite signal. However, such a system would be completely useless for handling non-composite signals. Conversely, if the system is designed to handle non-composite signals, keyed clamps cannot be used because properly timed horizontal drive pulses may not be available.

It is therefore apparent that the most flexible system will result if the video AGC amplifier is designed to handle non-composite video. The AGC amplifier is then preceded by a television stabilizing amplifier such as the TA-5C which will deliver a "video-only" signal and a sync signal when fed a composite input signal. The video-only output is fed to the AGC amplifier and after it has been "gain-controlled," the sync from the TA-5C can be reinserted to form a composite signal again. By means of a simple relay switching arrangement, the video

AGC system can then handle both composite and non-composite signals.

Another factor which must be considered is the maximum deviation from standard level which is likely to be presented to the AGC equipment. Although audio equipment can be, and generally is, designed to control over a fairly wide range of input levels, this is not practical for television purposes because when the director wished the picture to fade to black level, the AGC equipment would attempt to maintain a normal 100 per cent output level and in so doing, would cause the picture as seen on the television screen to fade to a bright grey instead of black. For this reason it is necessary to limit the amount of gain increase provided by the AGC equipment; operating tests have indicated that good results are produced if this increase is limited to 6 decibels.

#### REQUIREMENTS

The functions which the video AGC amplifier will be called upon to perform can now be enumerated:

1. Accept a non-composite video input signal at a nominal level of 0.7 volt and deliver a video output signal at a level of 0.7 volt regardless of input level variations between 0.35 and 1.4 volts. After the input signal reaches 0.35 volt, the output signal should linearly follow any decrease.
2. Automatic video gain control must be achieved without the use of keyed clamp circuits. This means that special attention must be given to the reduction of "bounce" or d-c shift in the output signal.
3. There should be no appreciable differential gain or differential phase distortion introduced by the equipment. Also, frequency response should remain flat regardless of the amount of gain reduction taking place.
4. 60-cycle square wave tilt must be essentially zero and constant regardless of the amount of gain reduction. This indicates the need for extended low-frequency response which multiplies the importance of (2) above manyfold.
5. Facilities should be provided to add sync to the video output signal if desired.
6. A method of remotely switching the video AGC equipment from non-composite operation to composite operation with a TA-5C stabilizing amplifier should be provided to allow complete flexibility of use.

GENERAL DESIGN

It is now possible to block out a method of achieving the desired results. Referring to Figure 1, it can be seen that a scheme very similar to that which is used in audio practice has been employed. The input is split into a push-pull signal which is gain-controlled by a pair of balanced variable gain amplifiers whose bias is obtained from a delay-biased rectifier. This rectifier is fed from the output signal through a side amplifier to achieve the required amount of loop gain. The push-pull signals, after being gain-controlled, are combined in a differential amplifier stage, and the resulting signal is fed to two 75-ohm outputs by means of a very stable negative feedback output

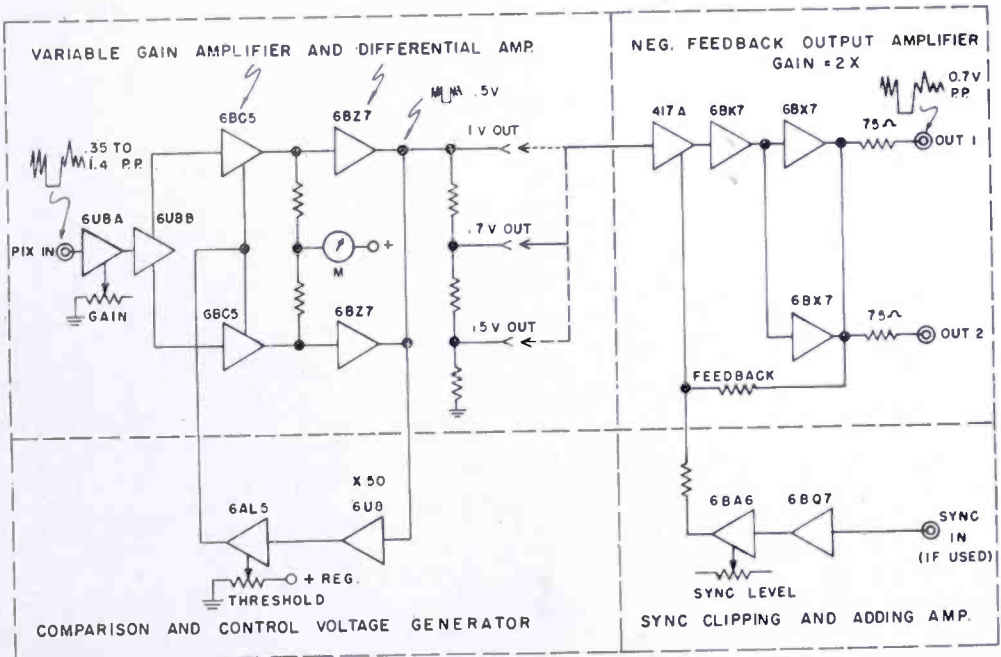


Fig. 1—Video automatic-gain-control amplifier block diagram.

amplifier which is also provided with sync-mixing facilities. Since the amplitude of the signal at the output of the differential amplifier is accurately controlled by AGC action, which is a negative feedback process, it is highly desirable that the gain of all following circuits be rigidly stabilized so as not to destroy the inherent self-regulating action of the device.

CIRCUIT DESCRIPTION

The complete schematic diagram of the video AGC amplifier is shown in Figure 2.

The non-composite video signal is first applied to the input amplifier, the pentode section of V1, whose gain is adjustable by means of

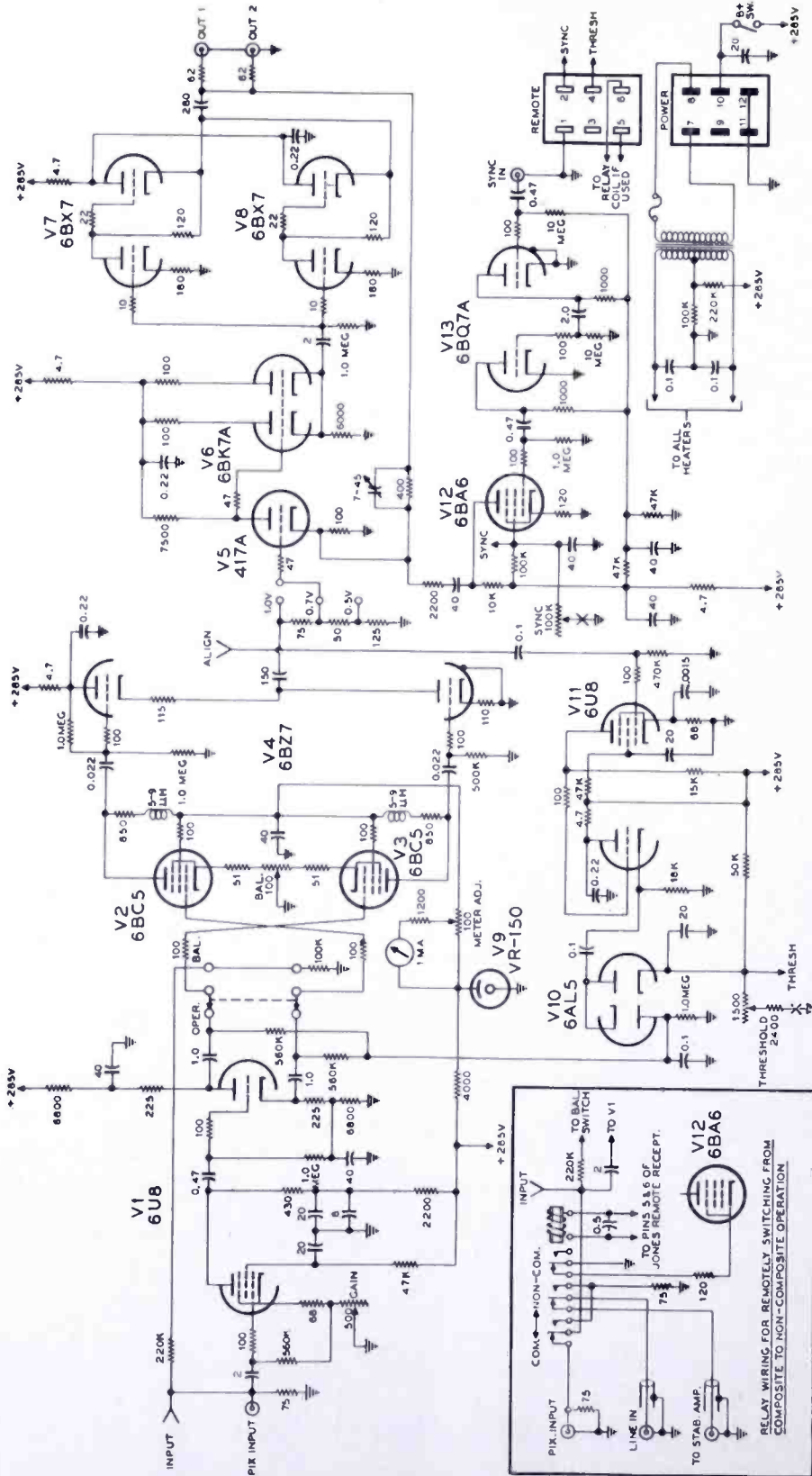


Fig. 2—Video automatic-gain-control amplifier.

a variable cathode degeneration potentiometer. The signal at its plate is coupled to the grid of the triode section, the coupling circuit constants being chosen so as to produce a controlled rising low-frequency response starting at about 14 cycles. This is done in order that complimentary low-frequency roll-off can be employed following the gain-controlled stages so as to reduce low-frequency "bounce" and d-c shift in the final output signal. The method of staggering the responses of the various circuits which affect low-frequency response so as to obtain an over-all flat and tilt-free amplifier is shown in idealized form in Figure 3.

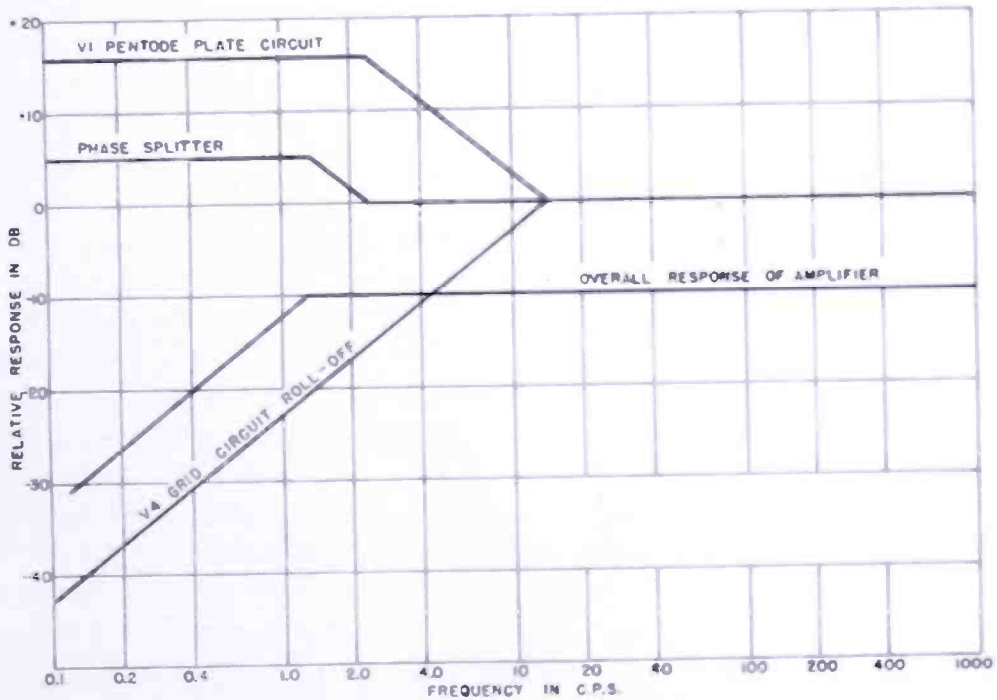


Fig. 3—Staggering of low-frequency characteristics.

By means of the triode section of V1, balanced push-pull signals are obtained at its cathode and plate since equal impedances form the load for both elements. These push-pull signals are coupled to the grids of variable-gain stages V2 and V3, a pair of 6BC5 pentodes, whose grid biases are derived from rectification of the output signal as described later. Both plate and screen voltages are regulated so as to minimize d-c shift at the output of these tubes while a d-c milliammeter is included in the circuit to indicate the total current of V2 and V3, the scale on the meter being calibrated so as to read actual gain reduction in decibels. The inclusion of this meter facilitates initial adjustment of the AGC amplifier and also provides a continuous visual indication of proper automatic-gain-control performance.

The push-pull signals at the plates of V2 and V3 are coupled to the control grids of a series-connected type of differential amplifier comprised of the dual triode V4, a type 6BZ7, with proper low-frequency roll-off provided by the choice of interstage coupling time constant. The differential amplifier serves the same function that a push-pull to single-ended transformer does since it provides an output which is proportional to the two grid signals as long as they are in push-pull but provides zero output for grid signals which are in phase. Due to this action, the distortion which is normally produced by the variable-gain tubes operating at high grid bias and relatively high grid signal swings is greatly reduced, and the "bounce" components which appear in-phase at the two grids of the differential amplifier are cancelled out.

The video signal from the differential amplifier is fed to two places — the output and sync-mixing amplifier, and the side-amplifier and rectifier circuits. Considering first the side amplifier, the pentode section of V11, a 6U8, is utilized as a restricted bandwidth video amplifier stage with a circuit gain of about 45. This amplifies the 0.5 volt peak-to-peak signal at its grid to a level of about 22 volts. High-frequency response is rolled off starting at little under 1.0 megacycle by the stray circuit capacitance in shunt with the relatively high value of the plate load resistor so that video signal components of very short duration and high-frequency content do not cause gain reduction. This is necessary in order to prevent the over-all level of a signal from being reduced by a few minor specular reflections or other unimportant white "spikes."

The 22-volt video signal is directly coupled to the triode section of V11 which functions as a cathode follower with fairly low source impedance for properly driving the following rectifier, V10, a 6AL5. The two diodes of this tube are connected in a peak-to-peak rectifier arrangement with a positive delay bias of about 17 volts applied to the input diode cathode to prevent any rectification until the peak-to-peak signal exceeds the bias voltage. Once this occurs, the negative d-c output voltage which is produced across the storage capacitor C21 and applied to the control grids of V2 and V3 is roughly equal to the amount by which the peak-to-peak video exceeds the delay bias, or in this case —5 volts, the difference between 22 volts and 17 volts. The absolute value of the delay bias voltage is variable over a narrow range by means of the "THRESHOLD" potentiometer which permits the level of the gain controlled video appearing at the output of the differential amplifier to be precisely set at 0.5 volt peak to peak.

This regulated 0.5-volt signal is fed to the output and sync-mixing

amplifier, comprised of tubes V5, V6, V7, V8, V12 and V13, through a simple attenuator which has three positions. The loss through the attenuator is 0, 3, or 6 decibels depending upon the tap selected. Since the gain of the negative-feedback output amplifier is exactly 2 and the regulated video at the attenuator input is 0.5 volt, the regulated video at the output of the complete unit may be set to 1, 0.7, or 0.5 volt. This provides composite outputs of 1.4, 1.0, or 0.7 volt after sync has been added in the sync-mixing channel (if desired). The feedback output amplifier section<sup>1</sup> does not influence AGC design.

The sync-mixing channel of the video AGC amplifier is comprised of stages V12, a 6BA6, and V13, a 6BQ7A. The external source of 4-volt sync pulses which have been derived from the incoming composite signal by the stabilizing amplifier is applied to the first section of the 6BQ7A. This section functions as a clipper, eliminating any irregularities or overshoots which may be present on the tips of the sync input. The second half of the 6BQ7A operates in a similar manner so as to remove any irregularities or overshoots from the base-line region of the sync waveform. The base line appears clean and clipped in both directions at its output. This cleaned-up sync signal is fed to the grid of V12, a 6BA6 pentode, which injects it into the cathode circuit of the input tube of the feedback output amplifier. There the sync signal is mixed with the video to produce a composite signal at the output of the AGC amplifier. The amplitude of this sync is adjustable from zero to over 0.5 volt by means of a potentiometer which controls the screen voltage of the 6BA6, control being accomplished in this fashion because it lends itself readily to remote operation.

Since it is desirable for maximum reduction of "bounce" and minimum differential gain distortion that the push-pull amplifiers are fairly well balanced, a switch has been incorporated in the video AGC amplifier which permits the incoming signal to be applied to the control grids of the 6BC5 variable-gain stages in parallel. When this is done, precise circuit balance is achieved by adjusting the potentiometer in the cathode circuit of the 6BC5's for complete cancellation of the signal at the output of the amplifier.

As previously mentioned, it is desirable for maximum flexibility to be able to switch the video AGC system from a remote point so as to handle either composite or non-composite signals. The three-pole double-throw relay whose wiring is shown in the insert makes this possible. In its normal (de-energized) position it feeds the composite signal from the incoming line to the input of the stabilizing amplifier,

---

<sup>1</sup>J. O. Schroeder, "Studio Amplifier Design for Television," *Electronics*, Vol. 28, p. 154, March, 1955.

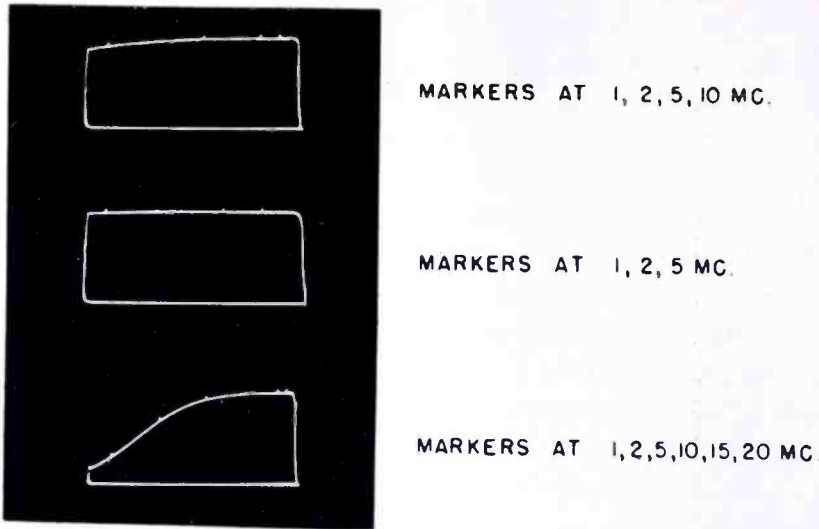


Fig. 4(a)—Frequency response.

feeds the picture signal from the stabilizing-amplifier output to the input of the video AGC amplifier, and energizes the sync-adding channel of the video AGC amplifier by completing the cathode-return circuit of V12. When the relay is energized, the stabilizing amplifier is bypassed and the incoming non-composite signal is fed directly to the AGC amplifier. The sync-adding channel of the AGC amplifier is disabled by opening the cathode-return circuit of V12 to prevent any spurious hum or noise from being mixed with the video signal. Both the sync level and the regulated peak-to-peak video level may be controlled remotely since the "SYNC" potentiometer, P5, and the "THRESHOLD" potentiometer, P4, may be located at a distance from

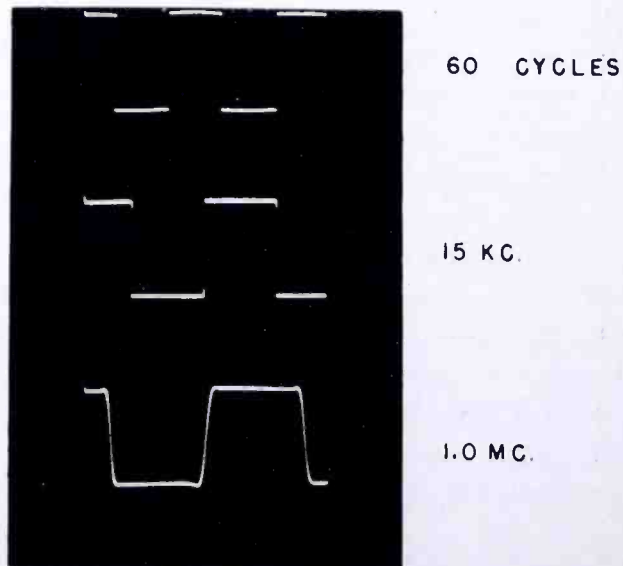
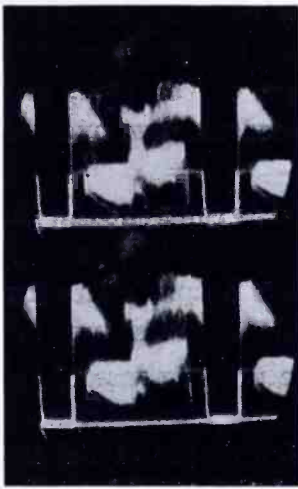
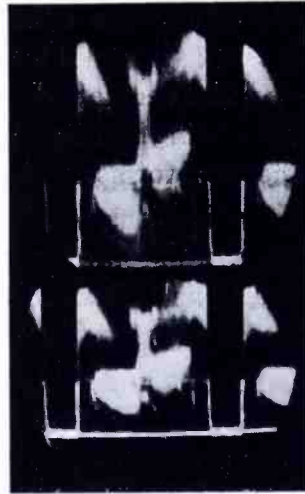


Fig. 4(b)—Square-wave response.



Double input level



Standard input level

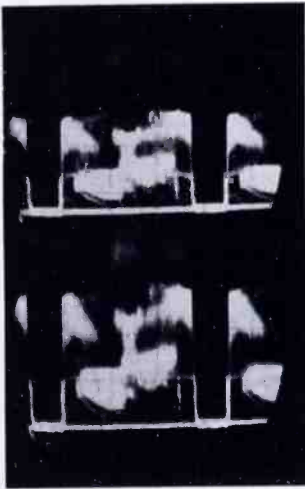
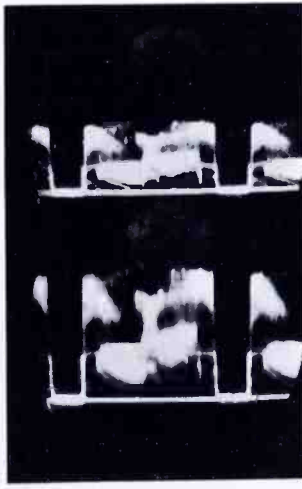
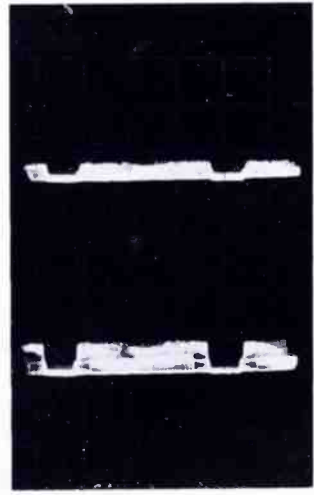
Input 3 decibels below  
standard levelInput 6 decibels below  
standard levelInput 20 decibels below  
standard level

Fig. 5—Output waveforms: upper trace is input and lower trace is output.

the amplifier. To provide complete flexibility, the switch which operates the relay and the sync-clipping level control of the associated stabilizing amplifier should also be at the remote location.

#### OPERATION AND PERFORMANCE

In order to show the performance characteristics of the video AGC amplifier as used on both composite and non-composite signals, a series of photographs was taken of the input and output signals under various conditions.

Figure 4A shows the wide frequency response of the video AGC amplifier by itself (no stabilizing amplifier involved), while Figure 4B shows the excellent square-wave response of the unit, good over-all phase response being indicated by the freedom from over-shoot or tilt on any of the waveforms.

The manner in which the output signal is controlled in the presence of varying non-composite input levels is shown by the waveforms of Figure 5, while the measured input versus output characteristic over a wide range of inputs is indicated by the curve shown in Figure 6.

The photographs in Figure 7 show the performance of the complete video AGC system, including the stabilizing amplifier, when used on composite signals. While the video portion of the signal is controlled to the same degree as indicated by Figure 6, the composite input signal can drop to one-tenth its normal level and the AGC system will still be completely stable and provide normal-level sync out even though video will be down to 20 per cent of normal. Certain modifications to

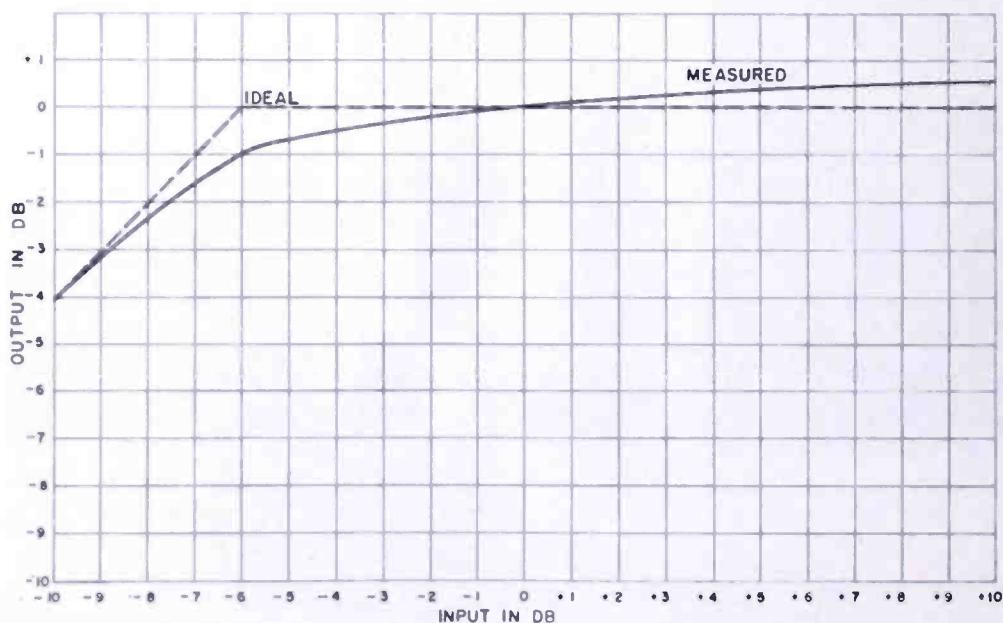
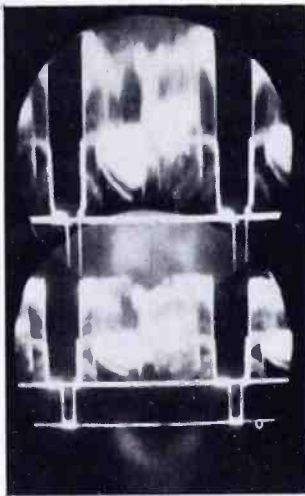


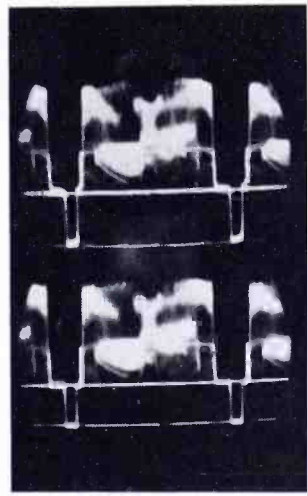
Fig. 6—Input-output characteristic.

the TA-5C stabilizing amplifier have made it possible for this unit to operate over an exceptionally wide range of input signals.

At an input level which produces 6 decibels of gain reduction, the maximum differential gain distortion produced by the AGC amplifier is about 2 per cent for any duty cycle between 10 and 90 per cent, while the differential phase distortion measured under the same conditions amounts to about 1°.



Double input level



Standard input level

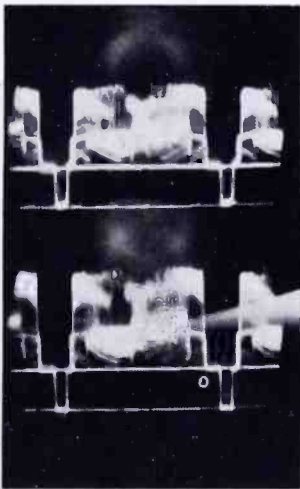
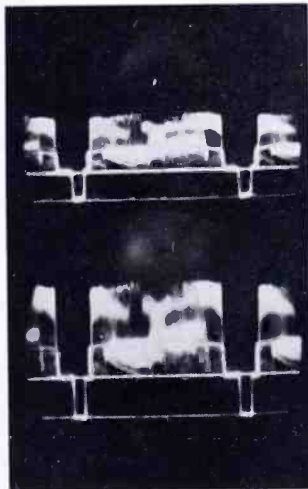
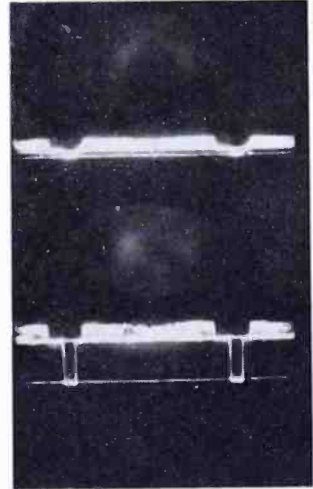
Input 3 decibels below  
standard levelInput 6 decibels below  
standard levelInput 20 decibels below  
standard level

Fig. 7—Over-all performance: upper trace is input and lower trace is output.

### CONCLUSION

The video AGC amplifier described in this paper, pictures of which are shown in Figures 8A and 8B, has been used over a period of several years in the television master control room of the National Broadcasting Company at New York where two complete installations, each capable of handling both composite and non-composite signals have been made.

These devices have proven invaluable for use on television shows containing material originating in various parts of the country or

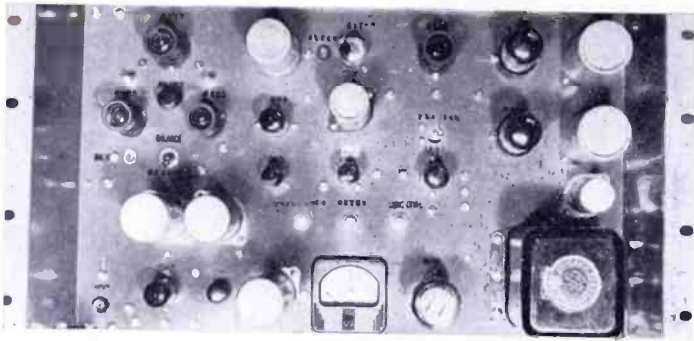


Fig. 8(a)—Amplifier front view.

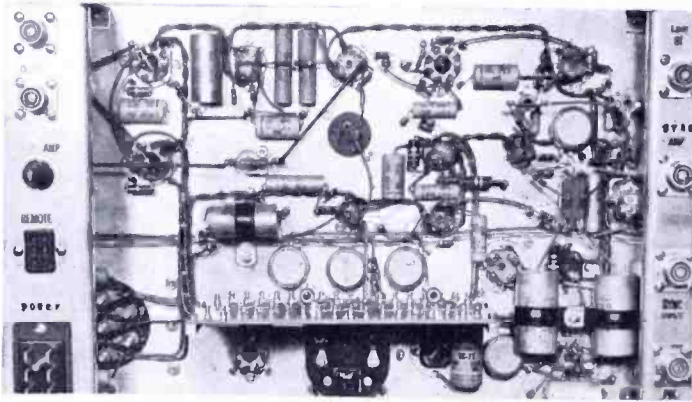


Fig. 8(b)—Amplifier rear view.

which use a considerable amount of newsreel or other film which must sometimes be put on the air without any run-through or rehearsal. Some of the better known programs which have benefited from the use of video AGC are the "Today" show, Camel Newsreel, Cavalcade of Sports, Wide Wide World, and the 1956 political convention coverage.

# A METHOD OF PREDICTING THE COVERAGE OF A TELEVISION STATION

BY

J. EPSTEIN AND D. W. PETERSON

RCA Laboratories,  
Princeton, N. J.

*Summary*—A method is described for estimating television broadcast station field strength coverage for such uses as spectrum utilization studies. The method is simple enough to be applied to studies involving a large number of station locations; an estimate along an entire radial line can be prepared in a few hours. Practical confirmation of the validity of the method is shown in an example of its use.

## INTRODUCTION

ENGINEERS of the Federal Communications Commission have, for allocation purposes, prepared propagation charts<sup>1</sup> which yield the space and time median value of received field strength for UHF and VHF television broadcasting. These empirical propagation charts are a composite of data from many field surveys representing a variety of terrain and surface clutter conditions. It is therefore evident that the FCC charts were not intended to be used to establish a criterion of performance for specific stations.

The nature of the FCC propagation charts has been clearly stated in FCC documents. The "Sixth Report and Order" of the FCC<sup>1</sup> states, with reference to these charts, "It should be stressed again that the service and interference computed by the use of these charts are not expected to prevail for any specific station but rather describe the service and interference which would prevail if the stations involved were all typical ones producing the average field intensities described by the charts." Quoting further from the same document, ". . . no one . . . has proposed a system of prediction of coverage which, while recognizing the differences between rough and smooth terrain, meets the criterion of reasonable simplicity. . . ." A simple method of prediction of the coverage of a television station is desirable and, if available, should enable studies of spectrum utilization and other studies to proceed without costly and time-consuming field surveys.

Two kinds of estimates of received field strength may be made:

---

<sup>1</sup> "Sixth Report and Order" of the FCC (52-294) reprinted by *Television Digest* in TV Allocation Report of April 14, 1952, pp. 201 and 202.

(1) The received field strength at a precisely specified point may be estimated. This requires detailed knowledge about the entire transmission path and the surface clutter surrounding both terminals. This kind of estimate clearly does not meet the "reasonable simplicity" criterion. Except for true line-of-sight conditions, such an estimate is almost impossible to make. (2) The space median field strength at a fixed height along a radial line may be estimated by taking into account the more important terrain features and the effect of average surface clutter at the receiving terminal. Fortunately the latter kind of estimate is applicable to the prediction of television station field performance.

This paper describes a simple method for estimating the median field strength along a radial line. The estimate is based on a plot of the elevation profile along a radial line used in conjunction with theoretical and empirical curves.

#### BACKGROUND FACTS

Before going into the details of the method of estimating field strength several well-known and pertinent facts will be cited. Within the service area of a television station, field strength can be quite accurately computed for the entire VHF and UHF spectrum if the earth's surface is smooth enough. In practice, however, the clutter of houses and trees usually constitutes a serious departure from the "smooth enough" criterion. Such a computation for the service area of a television station makes use of smooth spherical-earth theory. Paths involving broad expanses of water, for example, lend themselves to application of this theory. Free-space theory is applicable under conditions where reflection from the earth contributes negligibly to the received field and is also useful in a limited way. There are situations where a line-of-sight path over rough terrain results in the actual received fields averaging near the free-space theoretical field strength. Another tool for field strength prediction is the knife-edge diffraction theory. The shadows of hills may be predicted with a useful degree of accuracy by application of this theory.<sup>2</sup> A last fact to be mentioned is that the space median received field strength is a function of the surface clutter around a receiving site unless the receiving antenna is high enough above the clutter to "see" the transmitting antenna.

---

<sup>2</sup> Crysedale, Day, Cook, Psutka, and Robillard, "An Experimental Investigation of Electromagnetic Waves by a Dominating Ridge," Defence Research Telecommunications Establishment, Ottawa, Canada, December 30, 1955. This report includes an experimental evaluation of knife-edge diffraction theory applied to a ridge.

## RCA LABORATORIES FIELD SURVEYS

RCA Laboratories conducted field surveys<sup>3</sup> in 1946 and 1947 to learn the variation of coverage as a function of frequency for two quite different elevation profiles. Transmissions from Empire State Building on 67.25, 288, 510, and 910 megacycles were used along a western, hilly profile, and a southwestern, relatively smooth profile. The enhancement of field strength with frequency which was predicted by smooth spherical-earth theory was not in evidence. In fact, even over the quite smooth southwest radial line, field strength fell off with frequency. The plots of measured data showed scattering which increased with frequency. The actual system performance bore little relation to the smooth spherical-earth theory. The disappointing conclusion reached was that television broadcasting would require very much more radiated power for UHF than for VHF.

Another field survey<sup>4</sup> conducted in 1952 was set up to learn what propagation mechanisms were responsible for the observed facts of the earlier surveys. The data from 850-megacycle transmissions at four different heights from the 760-foot WOR tower (located on the Palisades in northern New Jersey) was analyzed in an effort to learn how to predict actual coverage. This analysis has led to the method of estimating field strength which is described in this paper.

## ESTIMATING FIELD STRENGTH

A first approximation to the field strength along a radial line is the free-space field strength reduced by knife-edge diffraction loss wherever hills interrupt the direct ray. This estimate yields values which are generally too high both in shadowed and in non-shadowed areas. Analysis of the 1952 850-megacycle field-survey data for non-shadowed areas revealed that the measured loss below free-space field strength is a function of the angle of arrival,  $\beta$ , of the direct ray at the receiving site.  $\beta$ , as defined in Figure 1, is the angle between the direct ray and a tangent at the receiving site. The loss is attributed to the clutter of buildings and trees and hence will be called "clutter loss." It is reasonable to expect the clutter loss to be related to the angle of arrival since the distance of travel through clutter is inversely proportional to  $\beta$ .

The clutter loss family of curves of Figure 2 has been derived from

---

<sup>3</sup> G. H. Brown, J. Epstein, and D. W. Peterson, "Comparative Propagation Measurements; Television Transmitters at 67.25, 288, 510 and 910 Megacycles," *RCA Review*, Vol. IX, p. 177, June, 1948.

<sup>4</sup> J. Epstein and D. W. Peterson, "An Experimental Study of Wave Propagation at 850 Mc," *Proc. I.R.E.*, Vol. 41, p. 595, May, 1953.

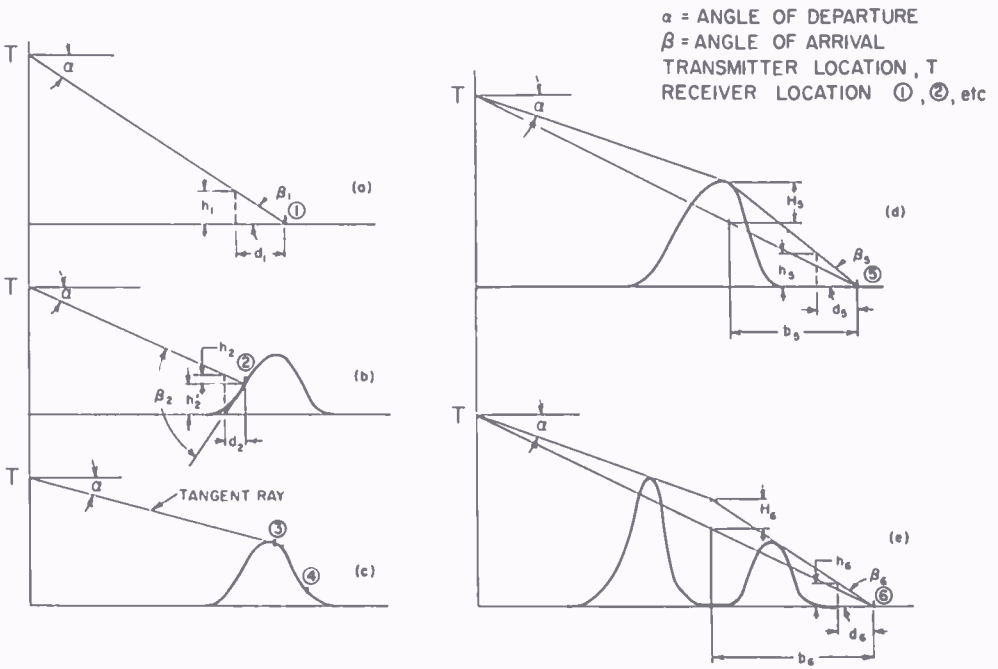


Fig. 1—Angle of arrival and shadow-loss parameters at a variety of receiving locations.

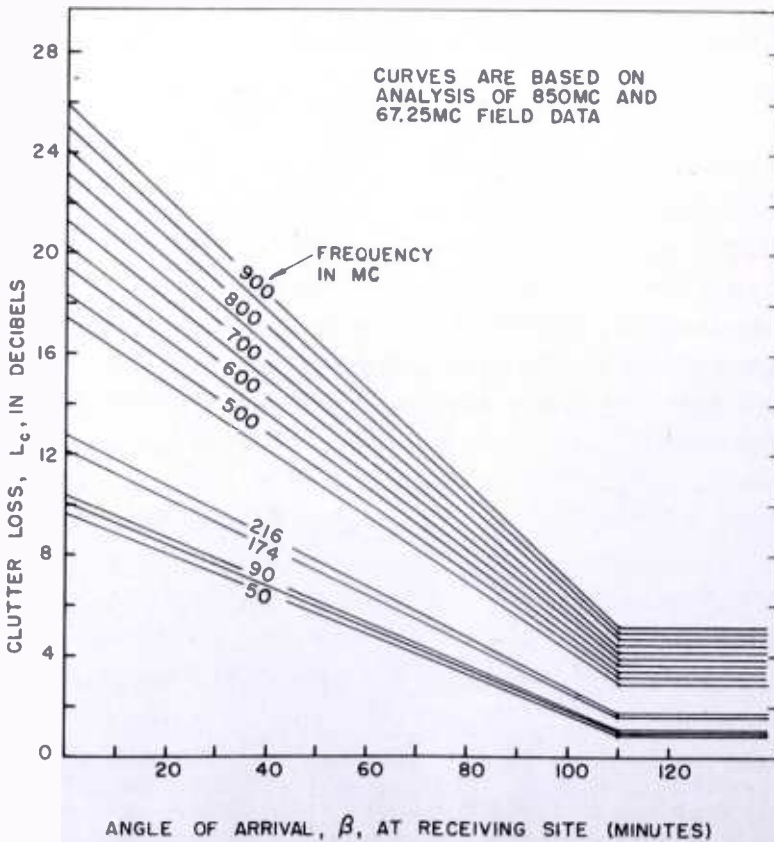


Fig. 2—Clutter loss.

analysis of the data of the 1946 and 1952 surveys. A linear relationship between clutter loss, in decibels, and frequency was assumed. The shadow loss curves of Figure 3 complete the tools required for an estimation of field strength, the usefulness of which will be shown by example.

Receiving antenna height does not appear directly as a parameter in the estimating procedure. In applying the shadow-loss theory, the receiving-antenna height enters into the estimate only as it affects the value of  $H$  as shown in Figure 3.

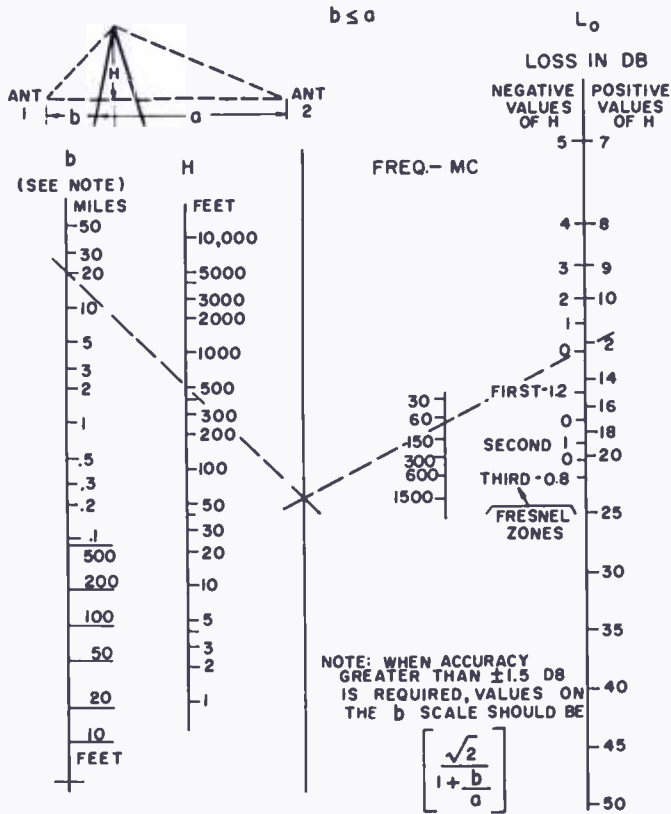


Fig. 3—Shadow loss relative to free-space field strength (knife-edge diffraction theory).

The clutter loss is the consequence of nearby houses and trees. This loss will be affected by the clearance of the receiving antenna with respect to an average height of clutter objects; therefore it is a function of the height of the receiving antenna above the ground. The particular height which is of interest is approximately 5-10 feet above house-top level since this will be the usual location of the receiving antennas which make use of the service rendered by the television station in question. The clutter-loss curves which are used are based upon field survey procedures believed to yield the median of available

field strength at this level. Consequently the prediction is the median value of field strength available at approximately 5-10 feet above average house-top level.

#### PROCEDURE

The basic propagation curve used is theoretical free-space propagation. The free-space propagation law,

$$E_o \text{ (db, } \mu\text{v/m, one kw)} = 102.8 - 20 \log D$$

is shown graphically in Figure 4.  $D$  is the distance from transmitting

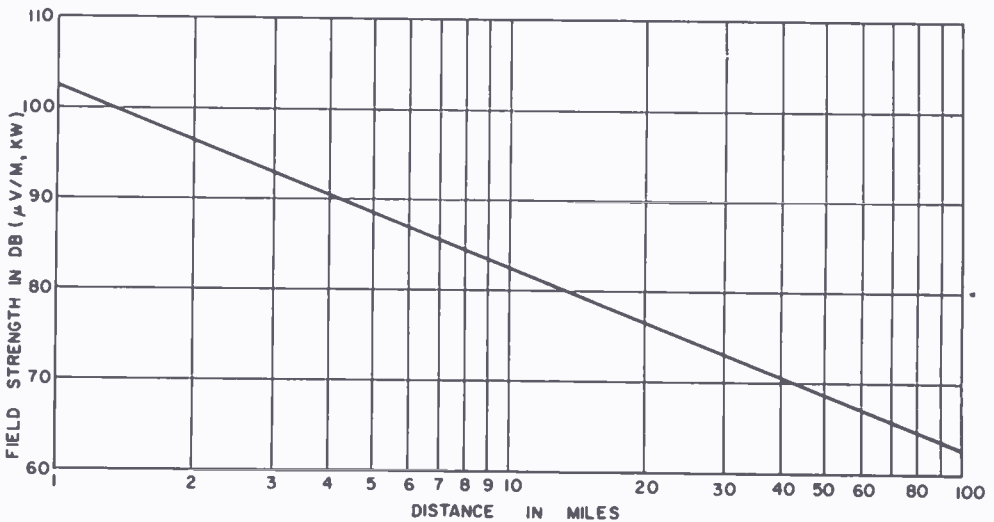


Fig. 4—Free-space field strength.

to receiving antenna in miles, and  $E_o$  is the free-space field strength in decibels referred to one microvolt per meter for one kilowatt of radiated power on the maximum of the transmitting antenna.

The elevation profile along a radial line is plotted on special coordinates. The curvature of the earth is represented by a parabolic approximation.<sup>5</sup> On these coordinates straight lines are true rays. Angles are greatly distorted and cannot be read from the chart, but must be computed.

Several examples of receiving locations are illustrated in Figure 1. Referring to location (1) of Figure 1(a), the angle of arrival is

$$\beta_1 = \tan^{-1} \frac{h_1}{d_1}.$$

<sup>5</sup> The equation of the parabola of the curved coordinates is  $A = 0.500 D^2$  where  $D$  is the distance to the horizon in miles for a point  $A$  feet above the earth. Four thirds of the true earth's radius is used.

The angle of arrival for location (2) of Figure 1(b) is

$$\beta_2 = \tan^{-1} \frac{h_2}{d_2} + \tan^{-1} \frac{h'_2}{d_2}.$$

Location (3) of Figure 1(c) was chosen by drawing a tangent to the hilltop from the transmitting antenna; therefore  $\beta^3 = 0$ . Since the ray arriving at location (4) of Figure 1(c) comes from the hilltop,  $\beta_4 = 0$ . Similarly the ray arriving at location (5) of Figure 1(d) comes from the hilltop so that  $\beta_5 = \tan^{-1} (h_5/d_5)$ . Successive shadowing by two hills is illustrated in Figure 1(e). The angle of arrival,  $\beta_6 = \tan^{-1} (h_6/d_6)$ .

The  $H$  and  $b$  values required for determining the shadow loss of a single or double hill is read directly from Figures 1(d) and (e). The shadow loss nomogram<sup>6</sup> of Figure 3 is entered with  $b$ ,  $H$ , and frequency. The value of shadow loss,  $L_o$ , is read in decibels referred to free-space field strength. By entering Figure 2 with  $\beta$  and frequency, the clutter loss,  $L_c$ , is obtained. The angle of departure,  $\alpha$ , defined in Figure 1, is used with the transmitting antenna vertical pattern to determine  $L_p$ , which is the reduction of field strength resulting from pattern shape.

The estimate of field strength at a point along a radial line is obtained by first plotting the elevation profile. The values of  $E_o$ ,  $L_o$ ,  $L_c$ , and  $L_p$  are then determined as described above. The estimate of median field strength at a point is

$$E \text{ (db, } \mu\text{v/m, kw)} = E_o - (L_o + L_c + L_p),$$

where  $E$  is the median field strength in decibels referred to one microvolt per meter for a kilowatt of radiated power,  $L_o$  is the shadow loss,  $L_c$  is the clutter loss, and  $L_p$  is the loss resulting from vertical pattern shape, all expressed in decibels.

#### EXAMPLE OF FIELD STRENGTH ESTIMATE

The measured data of the previously mentioned 67.25, 288, 510, and 910 megacycle surveys, together with the respective terrain elevation profiles, are reproduced in Figures 5 and 6. The computed points shown were obtained by the method described above. There is a reasonable agreement between the measured and computed points. It is rather difficult to draw any definite conclusions by mere visual

<sup>6</sup> K. Bullington, "Radio Propagation Variations at VHF and UHF," *Proc. I.R.E.*, Vol. 38, p. 27, January, 1950.

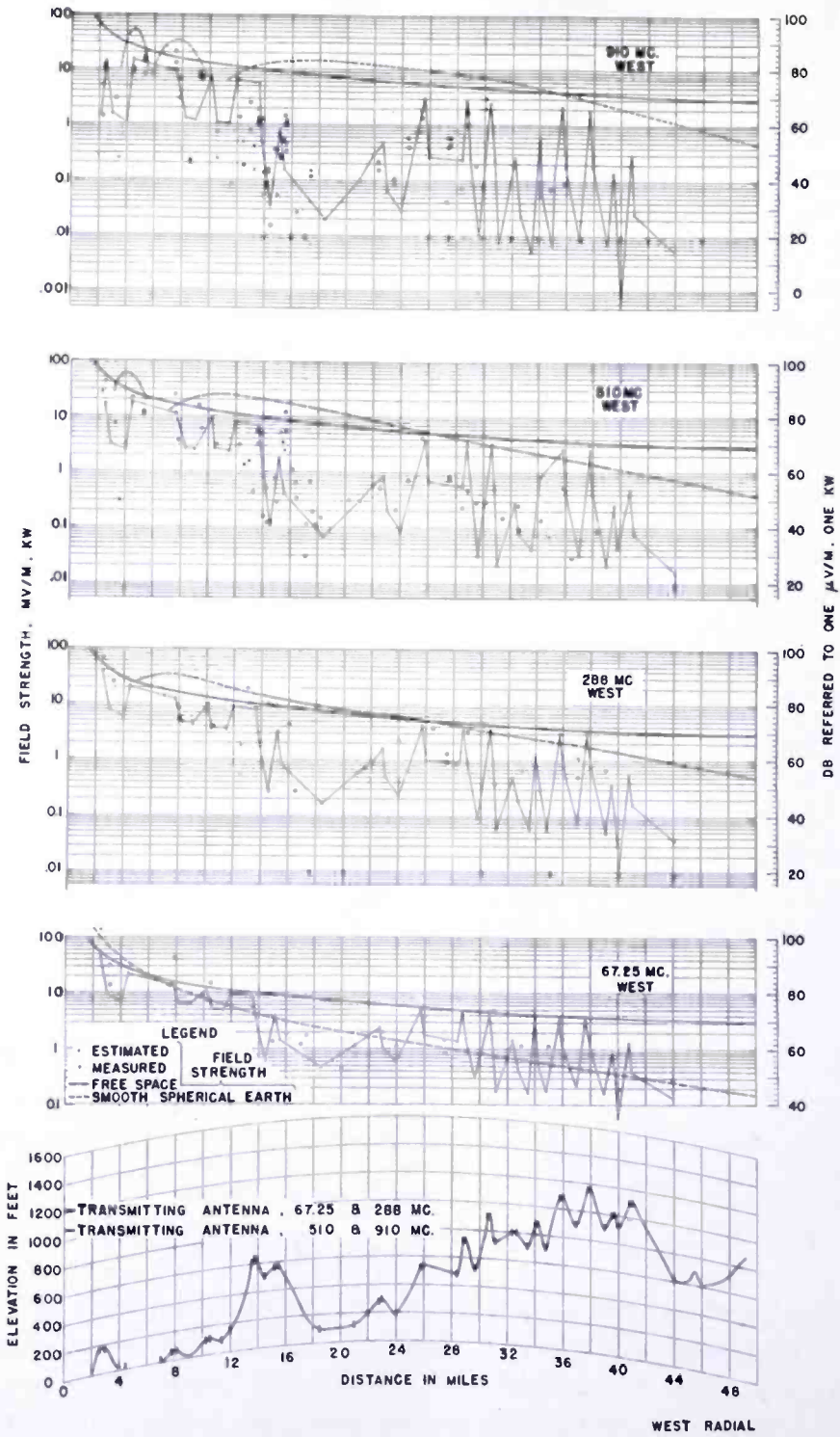


Fig. 5—Comparison of estimated field strength with measured data, west radial.

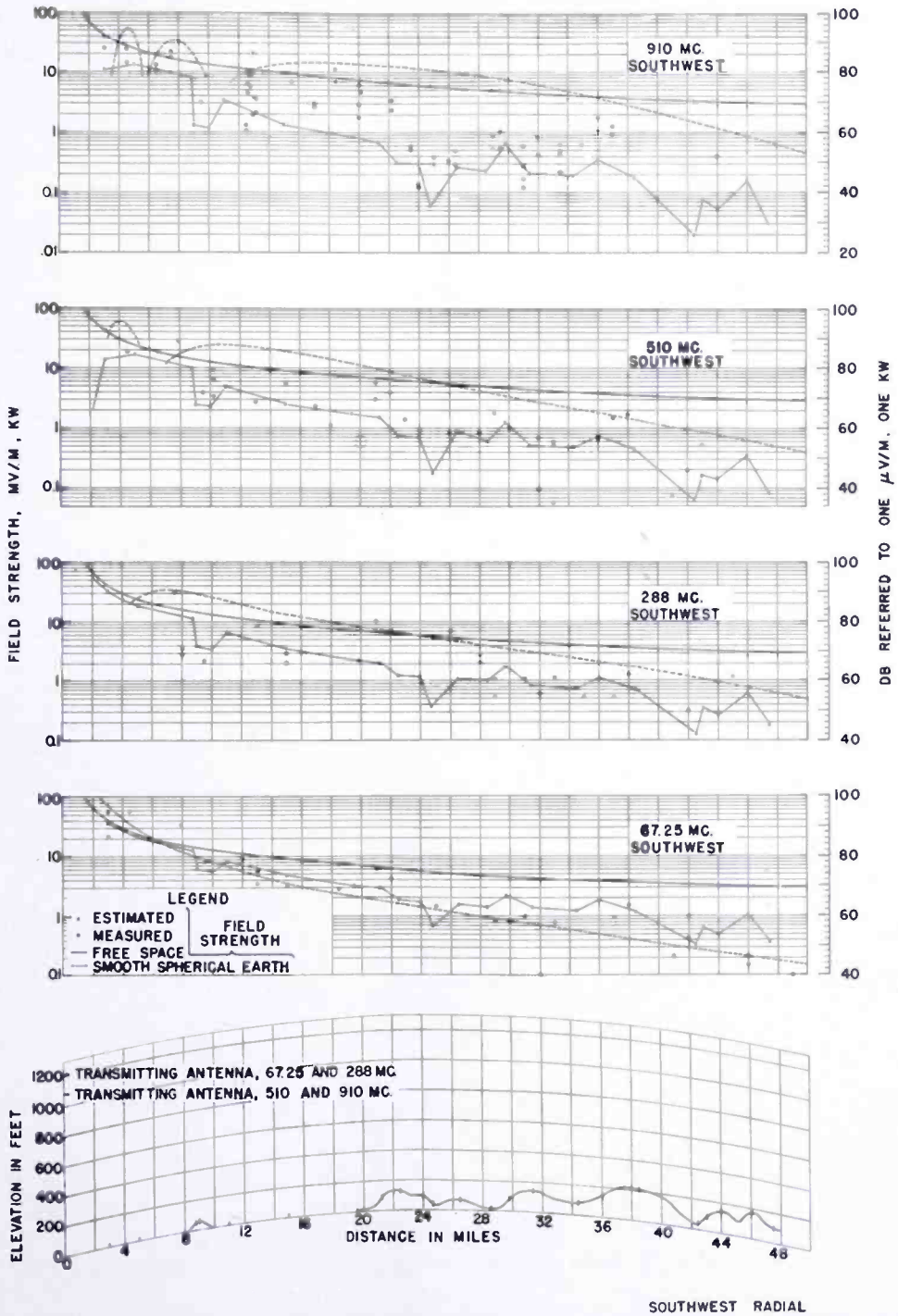


Fig. 6—Comparison of estimated field strength with measured data, southwest radial.

inspection of this data. The error of prediction versus the percentage of locations was established in a previous paper<sup>4</sup> and it is concluded that a useful degree of accuracy is obtained.

Having established the validity of a simple field-strength estimating procedure, it is only natural to use the procedure to prepare a field-strength contour picture of the coverage of a television station. The

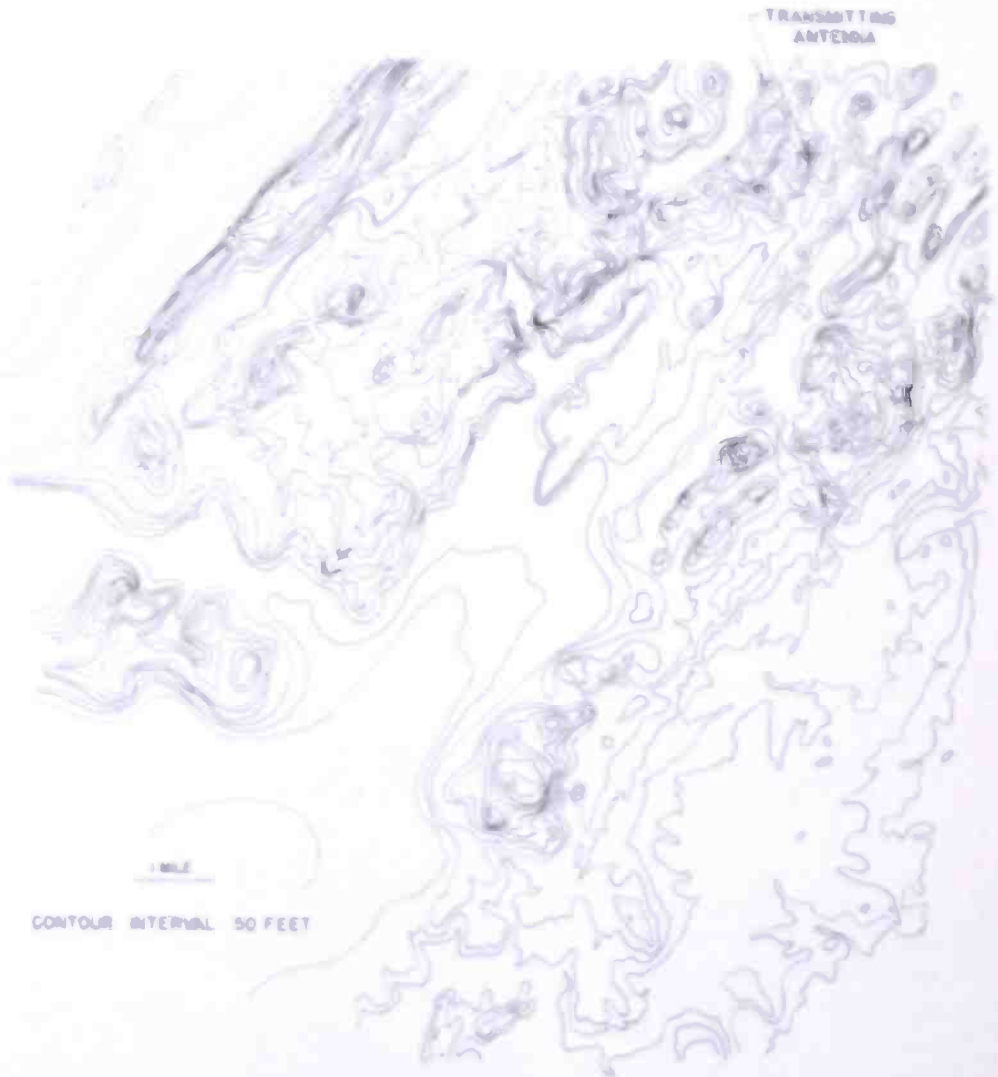


Fig. 7—Topography map for the estimation of field-strength contours.

topography of Figure 7 has been used to produce the field strength estimation contours of Figure 8. A transmitter frequency of 650 megacycles has been chosen. The effective radiated power from the omnidirectional transmitting antenna was one kilowatt. The vertical pattern of the antenna was shaped to yield constant field strength for average conditions out to a radius of 10 miles.

Figure 8 shows three areas designated as I, II, and III. Each of these areas has topography of the sort commonly found in cities. Area I requires transmitter power of one kilowatt to produce field strength of at least 65 decibels (referred to 1 microvolt per meter) in most of the area while areas II and III require respectively 10 kilowatts and 100,000 kilowatts for the same quality of coverage. The character of UHF coverage in hilly topography is well illustrated.

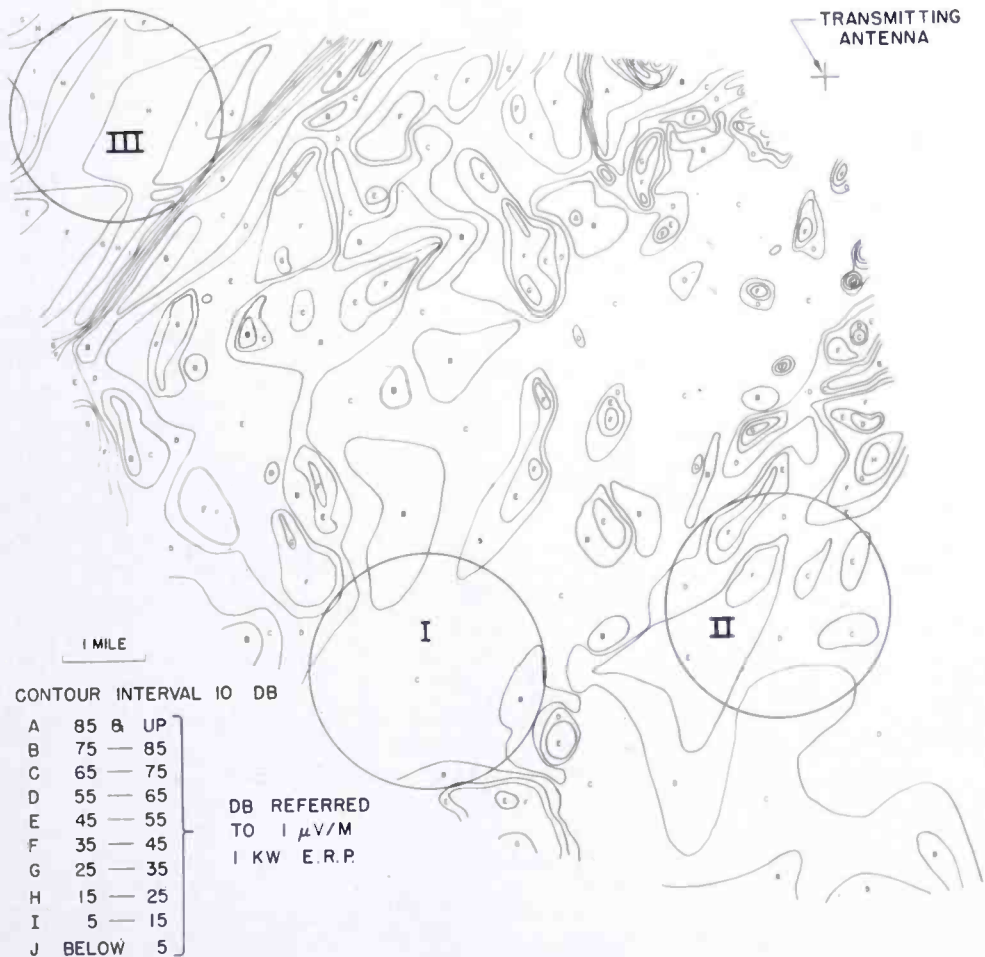


Fig. 8—Field-strength contour map for topography of Figure 7.

### CONCLUSION

A method has been described for estimating television station coverage. The method is based upon carefully planned experiments which required the expenditure of many years of engineering effort. It was possible to confirm the validity of the method with the data from extensive field surveys. The field-survey data is unique in that

it remains the only survey which encompasses the entire VHF and UHF television spectrum and is directly applicable to television station performance. The method is simple enough to be applied to studies involving a large number of television station locations since an estimate of median field strength along an entire radial line can be prepared in a few hours.

As is the case with all methods which make use of empirical data, this method is subject to refinement by improved empirical data and by further theoretical treatment. The clutter-loss empirical curves may be made more precise; the theoretical shadow-loss curves may be replaced by more accurate empirical data or refined theoretical methods. However, a useful degree of accuracy and simplicity has already been achieved and it is unlikely that further refinement will significantly change the results obtained by following the prediction methods described in this paper.

#### ACKNOWLEDGMENT

The authors wish to acknowledge the assistance of J. Bruce Rankin in the preparation of the field strength contour map.

## RCA TECHNICAL PAPERS†

Third Quarter, 1956

Any request for copies of papers listed herein should be addressed to the publication to which credited.

|   |      |
|---|------|
| "Camera Matching and Illumination Control for Color TV," E. P. Bertero, <i>Jour. S.M.P.T.E.</i> (September) .....   | 1956 |
| "Color-Purity and White-Uniformity Adjustment Procedure for the RCA-21AXP22-A Color Kinescope," <i>RCA Application Note AN-167</i> , RCA Tube Division, Harrison, N. J. (September) ..                                  | 1956 |
| "Color Television for Medical and Dental Applications," L. L. Lewis, <i>Broadcast News</i> (August) .....   | 1956 |
| "Color Test Equipment and Test Procedures," J. Wentworth, <i>Broadcast News</i> (August) .....  | 1956 |
| "Color-TV IF Amplifiers," S. Wlasuk, <i>Service</i> (August) .....  | 1956 |
| "Color TV Lighting Survey and Report," G. F. Rester, <i>Jour. S.M.P.T.E.</i> (July) .....   | 1956 |
| "CRT Power Supply Uses Transistor Oscillator," P. M. Toscano and J. B. Heffner, <i>Electronics</i> (September) .....  | 1956 |
| "Effect of Temperature on the Spectral Distribution of Blue Emission Bands of ZnS:I and ZnS:Cu:I Phosphors," R. E. Shrader and S. Larach, <i>Phys. Rev.</i> (September 15) (Letter to the Editor)                       | 1956 |
| "Electronic Control of Noise, Vibration, and Reverberation," H. F. Olson, <i>Jour. Acous. Soc. Amer.</i> (September) .....  | 1956 |
| "Electronic Masking for Improved TV Reproduction of Color Film," H. N. Kozanowski and S. L. Bendell, <i>Broadcast News</i> (August)   | 1956 |
| "Fields in Imperfect Electromagnetic Anechoic Chambers," R. F. Kolar, <i>RCA Review</i> (September) .....   | 1956 |
| "Form and Thickness of Trap-Dominated Space-Charge Layers," A. Rose, <i>Helvetica Physica Acta</i> (July) .....   | 1956 |
| "High-Resolution Flying-Spot Scanner for Graphic Arts Color Applications," L. Shapiro and H. E. Haynes, <i>RCA Review</i> (September) .....   | 1956 |
| "Image Orthicon for Pickup at Low Light Levels," A. A. Rotow, <i>RCA Review</i> (September) .....   | 1956 |
| "Low-Power Binary Counter," W. E. Hostetler and H. J. Wolkstein, <i>Tele-Tech and Electronic Industries</i> (July) .....  | 1956 |
| "A Magnetic Tape System for Recording and Reproducing Standard FCC Color Television Signals," H. F. Olson, W. D. Houghton, A. R. Morgan, M. Artzt, J. A. Zenel, and J. G. Woodward, <i>RCA Review</i> (September) ..... | 1956 |
| "Magnetize for Fun and Utility," R. Samuel, <i>Popular Electronics</i> (August) .....   | 1956 |
| "Magnetron Tester Detects Lost Pulses," P. Koustas and D. D. Mahwinney, <i>Electronics</i> (August) .....   | 1956 |
| "The Make-Your-Own Microphone," G. D. Hanchett, <i>RCA Ham Tips</i> (September) .....   | 1956 |

† Report all corrections or additions to RCA Review, RCA Laboratories, Princeton, N. J.

|  |      |
|--|------|
| "Molecular Ringing," S. Bloom, <i>Jour. Appl. Phys.</i> (July) .....   | 1956 |
| "New Alignment Techniques," J. R. Meagher, <i>PF Reporter</i> (September) .....  | 1956 |
| "Optical and Photoelectric Analog of the Eye," O. H. Schade, Sr., <i>Jour. Opt. Soc. Amer.</i> (September) .....   | 1956 |
| "The Optimum Tapered Transmission Line Matching Section," R. W. Klopfenstein, <i>Proc. I.R.E.</i> (August) (Letter to the Editor) ..   | 1956 |
| "Performance and Design of Low-Noise Guns for Traveling-Wave Tubes," R. C. Knechtli and W. R. Beam, <i>RCA Review</i> (September) .....  | 1956 |
| "Proper Degaussing of the RCA-21AXP22-A Color Kinescope," <i>RCA Application Note AN-166</i> , RCA Tube Division, Harrison, N. J. (September) .....                            | 1956 |
| "'Q' Calculations for High Frequency Inductors," R. J. Schulte, <i>Tele-Tech and Electronic Industries</i> (July) .....  | 1956 |
| "Quasi-Complementary Transistor Amplifier," H. C. Lin, <i>Electronics</i> (September) .....  | 1956 |
| "Simplified Theory of Space-Charge-Limited Currents in an Insulator with Traps," M. A. Lampert, <i>Phys. Rev.</i> (September 15) ....  | 1956 |
| "Some Studies in the Speed of Visual Perception," G. C. Sziklai, <i>Transactions of the I.R.E. Professional Group on Information Theory</i> (September) .....                  | 1956 |
| "The Statistics of Combiner Diversity," H. Staras, <i>Proc. I.R.E.</i> (August) (Letter to the Editor) .....   | 1956 |
| "Television's Expanding Service to the Nation," E. W. Engstrom, <i>Signal</i> (September-October) .....  | 1956 |
| "Theoretical Considerations Governing the Choice of the Optimum Semiconductor for Photovoltaic Solar Energy Conversion," J. J. Loferski, <i>Jour. Appl. Phys.</i> (July) ..... | 1956 |
| "Topological Properties of Telecommunication Networks," Z. Prihar, <i>Proc. I.R.E.</i> (July) .....  | 1956 |
| "21-Inch Color-TV Chassis Featuring Printed-Wiring Boards," J. A. May and W. H. Fulroth, <i>Service</i> (September) .....  | 1956 |
| "Versatile Modulator," P. Koustas, <i>RCA Ham Tips</i> (July-August) ..  | 1956 |
| "11-Tube 90° 8½-Inch RCA Portable TV," W. W. Cook, <i>Service</i> (September) .....  | 1956 |

## AUTHORS



**WILLIAM L. BEHREND** received the B.S. and M.S. degrees from the University of Wisconsin in 1946 and 1947. During 1953-1955, he did graduate work in Systems Engineering at the University of Pennsylvania. He served as an electronic technician in the U. S. Navy from 1944 to 1946. In 1947 he joined the RCA Laboratories Division, Princeton, N. J., where he is now with the Systems Research Laboratory. He has been associated with the development of antennas, experimental UHF television transmitters, and color television. Mr. Behrend is a member of Sigma Xi and a Senior Member of the Institute of Radio Engineers.

**JOHN C. BLEAZEY** (See *RCA Review*, Vol. XVII, No. 1, March 1956, p. 136.)

**DAVID J. CARLSON** served with the Army Signal Corps during World War II. He received the B.S. Degree in E.E. in 1950 from Rensselaer Polytechnic Institute and is currently working for his Master's Degree at the University of Pennsylvania. He joined the Advanced Development Section of the RCA Victor Television Division in 1950, and has been working on projects related to various phases of the ultra high frequencies. Mr. Carlson is a member of Etta Kappa Nu and the Institute of Radio Engineer.



**A. DANFORTH COPE** received the B.A. degree from Colgate University in 1938, later engaging in graduate study in Physics at Yale University. He joined the Radio Corporation of America in 1941 as manufacturing process and development engineer working with special purpose, phototube, and television camera tube types at the Harrison, N. J. and Lancaster, Pa. tube plants. In 1949 Mr. Cope transferred to the RCA Laboratories Division at Princeton, N. J. where he is engaged in research on television camera tubes.

**JESS EPSTEIN** received the E.E. degree and the M.S. degree in Physics from the University of Cincinnati in 1932 and 1934. From 1934 to 1935, he was an instructor in Physics at the Cincinnati College of Pharmacy. In 1935, he joined the research division of RCA Manufacturing Company at Camden, N. J., and was transferred to RCA Laboratories Division at Princeton, N. J., in 1942, where he is now engaged in work on antennas, transmission lines and propagation. Mr. Epstein is a Member of Sigma Xi, and a Senior Member of the Institute of Radio Engineers.





L. E. FLORY received the B.S. degree in Electrical Engineering, University of Kansas in 1930. He was with the research division of RCA Manufacturing Co., Camden, N. J. from 1930 to 1942 during which time he was engaged in research on television tubes and related electronic problems, particularly in the development of the iconoscope. In 1942 he was transferred to the RCA Laboratories Division, Princeton, N. J. From 1949 to 1954 he was in charge of work on storage tubes, and since 1949 he has been in charge of work on industrial television.

More recently he has been concerned with applications of transistors to television circuits and with medical electronics problems. Mr. Flory is a member of Sigma Xi and a Fellow of the Institute of Radio Engineers.

GEORGE W. GRAY attended Princeton University as a civilian and in the Navy V-12 Program until 1943 when he was assigned to active duty in the Navy. After release to inactive duty in 1946, he returned to Princeton University and received the B.A. degree in Physics. In March of 1947 he joined the technical staff of RCA Laboratories Division at Princeton, N. J. He is at present a member of the Electronic Research Laboratory engaged in television research. Mr. Gray is a member of Sigma Xi.



HARVEY O. HOOK received the B.A. degree with Chemistry major from Elon College in 1947, the B.E.E. degree from North Carolina State College in 1949, and the M.S.E.E. degree from North Carolina State College in 1950. Since 1950 he has been with RCA Laboratories Division. Mr. Hook is a Senior Member of the Institute of Radio Engineers and an Associate Member of Sigma Xi.

RALPH C. KENNEDY (See *RCA Review*, Vol. XVII, No. 2, June 1956, p. 308.)

M. KNOLL received the M.S. and Ph.D. degrees in Electrical Engineering in 1922 and 1924 respectively from the Institute of Technology in Munich, Germany. From 1927 to 1945 he was Professor for Vacuum Tube design at the Institute of Technology, Berlin-Charlottenburg, Germany, and from 1932 director of its Vacuum Tube Laboratory. After World War II he became a professor at the University of Munich. He came to the United States in 1947, and joined RCA Laboratories in 1948. In 1955 he returned to Germany where he is now at the Technischen Hochschule in Munich. Dr. Knoll is a Senior Member of the Institute of Radio Engineers, and a Member of Sigma Xi.





HERBERT KROEMER received the degree of a Dr. rer. nat. from the University of Goettingen, Germany, in 1952. From 1952 to 1954 he worked in the Semiconductor Research Laboratory of the German Post Office. Since 1954 he has been with RCA Laboratories in Princeton, N. J. Dr. Kroemer is a member of the American Physical Society and the Institute of Radio Engineers, and Sigma Xi.

JEREMIAH M. MORGAN studied at Drexel Institute. In 1929 he was employed by the Victor Talking Machine Company in Camden, N. J. in the test department. With the absorption into the RCA Manufacturing Co. in 1930, he was transferred to the television laboratory engaged in circuit design. He has continued in this line doing circuit development work on electron microscopes, television and special test equipment, transferring to the RCA Laboratories in Princeton, N. J. in 1942. Since 1948 he has been engaged in the development of industrial television equipment. Mr. Morgan is a Member of the Institute of Radio Engineers and an Associate Member of the Franklin Institute.



HARRY F. OLSON (See *RCA Review*, Vol. XVII, No. 3, September 1956, p. 439.)



WEN YUAN PAN received the E. E. Degree in 1939 and Ph.D. in 1940 from Stanford University. He was engaged as a research associate at the Radio Research Laboratory at Harvard University during World War II. Since 1945 he has been with the RCA Victor Television Division. He is now manager of RF Circuits Development in the Engineering Department. Dr. Pan served in an advisory capacity to the China Defense and Supplies in 1941, the International Civil Aviation Conference in 1944, and the United Nations Telecommunications Committee in 1946.

He is an honorary member of the Veteran Wireless Operators' Association, a member of Sigma Xi, A.O.E., A.A.A.S., A.M.E., and Senior Member of the Institute of Radio Engineers.

DONALD W. PETERSON received the B.S. degree in E.E. from the University of Wisconsin in 1936. In that year, he joined the Service Department of RCA Manufacturing Company, Camden, N. J., shifting to the research division of that company in 1939. In 1942 he was transferred to RCA Laboratories Division in Princeton, N. J., where he is currently engaged in work on antennas, transmission lines and propagation. Mr. Peterson is a Member of Sigma Xi and the Institute of Radio Engineers.





WINTHROP SEELEY PIKE received the B.A. degree in Physics in 1941 from Williams College. He served with U. S. Army Signal Corps during World War II as radar officer and later as project officer in charge of the Signal Corps Moon Radar project. In 1946 he joined the research staff of RCA Laboratories Division at Princeton, N. J., where he has worked on sensory aids for the blind, storage tube applications, color television and industrial television. Mr. Pike is a Member of Sigma Xi and the American Guild of Organists.

JOHN PRESTON (See *RCA Review*, Vol. XVII, No. 1, March 1956, p. 139.)

JOHN O. SCHROEDER was employed in the Receiver and Transmitter Test Department of the Link Radio Corp. from 1940 to 1944. From 1944 to 1946 he was in the U. S. Navy during which time he completed the Radio Material Course at the Naval Research Laboratory and then was sent to Okinawa. On leaving the Navy in 1946 he rejoined the Link Radio Corp. In 1950 he became Assistant Chief Engineer at the Muzak Transcription Studios, and in 1951 he joined the National Broadcasting Company as a Design Engineer in the Engineering Development Group.



R. P. STONE is an Engineering Leader, Advanced Development Display Storage Tubes, RCA Tube Division, Lancaster, Pa. Dr. Stone received the B.E.E. degree in 1940 from the Ohio State University, the M.S. degree in 1941 from Purdue University, and the Ph.D. in Electrical Engineering from Princeton University in 1949. He joined the RCA Laboratories Division in 1941, and worked on various problems in the field of electron tube research. From 1952 to 1955 he was a member of the group at the Laboratories working on Display Storage Tube research. In 1955 Dr. Stone transferred to the

Tube Division, to carry on the advanced development of the Display Storage Tubes, at the Lancaster Plant. He is a senior member of the I.R.E., a member of its professional group on Electron Devices, and a member of Sigma Xi.

# RCA REVIEW

*a technical journal*

RADIO AND ELECTRONICS  
RESEARCH • ENGINEERING

---

## INDEX

---

VOLUME XVII

---

### TABLE OF CONTENTS

#### March

|   | PAGE |
|---|------|
| Surface Treatment of Silicon for Low Recombination Velocity . . . . .<br>H. NELSON AND A. R. MOORE  | 5    |
| The Omniguide Antenna — An Omnidirectional Waveguide Array<br>for UHF-Television Broadcasting . . . . .<br>O. M. WOODWARD, JR. AND J. J. GIBSON | 13   |
| P-N-P Transistors Using High-Emitter-Efficiency Alloy Materials . . .<br>L. D. ARMSTRONG, C. L. CARLSON, AND M. BENTIVEGNA                      | 37   |
| Uniform Planar Alloy Junctions for Germanium Transistors . . . . .<br>C. W. MUELLER AND N. H. DITRICK   | 46   |
| Miniature Loudspeakers for Personal Radio Receivers . . . . .<br>J. C. BLEAZEY, J. PRESTON, AND E. G. MAY                                       | 57   |
| A Variable-Capacitance Germanium Junction Diode for UHF . . . . .<br>J. H. O'CONNELL AND L. J. GIACOLETTO                                       | 68   |
| Phase Angle Distortion in Traveling-Wave Tubes . . . . .<br>W. R. BEAM AND D. J. BLATTNER   | 86   |
| The Electron-Voltaic Effect in Germanium and Silicon P-N Junctions . .<br>P. RAPPAPORT, J. J. LOFERSKI, AND E. G. LINDER                        | 100  |

#### June

|   |     |
|---|-----|
| Recent Improvements in the 21AXP22 Color Kinescope . . . . .<br>R. B. JANES, L. B. HEADRICK, AND J. EVANS | 143 |
| Effect of Magnetic Deflection on Electron Beam Convergence . . . . .<br>P. E. KAUS                        | 168 |
| Electrolytic Transport Phenomena in the Oxide Cathode . . . . .<br>R. H. PLUMLEE                          | 190 |
| The Electron Donor Centers in the Oxide Cathode . . . . .<br>R. H. PLUMLEE                                | 231 |

|   | PAGE |
|---|------|
| Kinescope Electron Guns for Producing Noncircular Spots .....   | 275  |
| R. C. KNECHTLI AND W. R. BEAM   |      |
| Pedestal Processing Amplifier for Television Studio Operation .....   | 297  |
| R. C. KENNEDY   |      |
| September   |      |
| High-Resolution Flying-Spot Scanner for Graphic Arts Color Applications .....                                     | 313  |
| L. SHAPIRO AND H. E. HAYNES   |      |
| A Magnetic Tape System for Recording and Reproducing Standard FCC Color Television Signals .....                  | 330  |
| H. F. OLSON, W. D. HOUGHTON, A. R. MORGAN, M. ARTZT,<br>J. A. ZENEL, AND J. G. WOODWARD                           |      |
| Fields in Imperfect Electromagnetic Anechoic Chambers .....   | 393  |
| R. F. KOLAR   |      |
| Performance and Design of Low-Noise Guns for Traveling-Wave Tubes .....   | 410  |
| R. C. KNECHTLI AND W. R. BEAM   |      |
| Image Orthicon for Pickup at Low Light Levels .....   | 425  |
| A. A. ROTOW   |      |
| December  |      |
| Reduction of Co-Channel Television Interference by Precise Frequency Control of Television Picture Carriers ..... | 443  |
| W. L. BEHREND   |      |
| A Miniature Vidicon of High Sensitivity .....   | 460  |
| A. D. COPE  |      |
| Transistorized Television Cameras Using the Miniature Vidicon ....  | 469  |
| L. E. FLORY, G. W. GRAY, J. M. MORGAN, AND W. S. PIKE   |      |
| Viewing Storage Tubes for Large Displays .....  | 503  |
| H. O. HOOK, M. KNOLL, AND R. P. STONE   |      |
| The Apparent Contact Potential of a Pseudo-Abrupt P-N Junction ..   | 515  |
| H. KROEMER  |      |
| Bigradient Uniaxial Microphone .....  | 522  |
| H. F. OLSON, J. PRESTON, AND J. C. BLEAZEY  |      |
| Analytical Approaches to Local Oscillator Stabilization .....   | 534  |
| W. Y. PAN AND D. J. CARLSON   |      |
| Test Signal for Measuring "On-The-Air" Color-Television System Performance .....                                  | 553  |
| R. C. KENNEDY   |      |
| A Video Automatic-Gain-Control Amplifier .....  | 558  |
| J. O. SCHROEDER   |      |
| A Method of Predicting the Coverage of a Television Station .....   | 571  |
| D. W. PETERSON AND J. EPSTEIN   |      |

## AUTHORS, VOLUME XVII

|  | ISSUE | PAGE |
|--|-------|------|
| Armstrong, L. D. (Coauthor)—“P-N-P Transistors Using High-Emitter-Efficiency Alloy Materials”                                | Mar.  | 37   |
| Artzt, M. (Coauthor)—“A Magnetic Tape System for Recording and Reproducing Standard FCC Color Television Signals”            | Sept. | 330  |
| Beam, W. R. (Coauthor)—“Phase Angle Distortion in Traveling-Wave Tubes”  | Mar.  | 86   |
| “Kinescope Electron Guns for Producing Noncircular Spots”  | June  | 275  |
| “Performance and Design of Low-Noise Guns for Traveling-Wave Tubes”  | Sept. | 410  |
| Behrend, W. L.—“Reduction of Co-Channel Television Interference by Precise Frequency Control of Television Picture Carriers” | Dec.  | 443  |
| Bentivegna, M. (Coauthor)—“P-N-P Transistors Using High-Emitter-Efficiency Alloy Materials”                                  | Mar.  | 37   |
| Blattner, D. J. (Coauthor)—Phase Angle Distortion in Traveling-Wave Tubes”   | Mar.  | 86   |
| Bleazey, J. C. (Coauthor)—“Miniature Loudspeakers for Personal Radio Receivers”  | Mar.  | 57   |
| “Bigradient Uniaxial Microphone”   | Dec.  | 522  |
| Carlson, C. L. (Coauthor)—“P-N-P Transistors Using High-Emitter-Frequency Alloy Materials”                                   | Mar.  | 37   |
| Carlson, D. J. (Coauthor)—“Analytical Approaches to Local Oscillator Stabilization”  | Dec.  | 534  |
| Cope, A. D.—“A Miniature Vidicon of High Sensitivity”  | Dec.  | 460  |
| Ditrick, N. H. (Coauthor)—“Uniform Planar Alloy Junctions for Germanium Transistors”   | Mar.  | 46   |
| Epstein, J. (Coauthor)—“A Method of Predicting the Coverage of a Television Station”   | Dec.  | 571  |
| Evans, J. (Coauthor)—“Recent Improvements in the 21AXP22 Color Kinescope”  | June  | 143  |
| Flory, L. E. (Coauthor)—“Transistorized Television Cameras Using the Miniature Vidicon”                                      | Dec.  | 469  |
| Giacoletto, L. J. (Coauthor)—“A Variable-Capacitance Germanium Junction Diode for UHF”                                       | Mar.  | 68   |
| Gibson, J. J. (Coauthor)—“The Omniguide Antenna—An Omnidirectional Waveguide Array for UHF-Television Broadcasting”          | Mar.  | 13   |
| Gray, G. W. (Coauthor)—“Transistorized Television Cameras Using the Miniature Vidicon”                                       | Dec.  | 469  |
| Haynes, H. E. (Coauthor)—“High-Resolution Flying-Spot Scanner for Graphic Arts Color Applications”                           | Sept. | 313  |
| Headrick, L. B. (Coauthor)—“Recent Improvements in the 21AXP22 Color Kinescope”  | June  | 143  |
| Hook, H. O. (Coauthor)—“Viewing Storage Tubes for Large Displays”  | Dec.  | 503  |
| Houghton, W. D. (Coauthor)—“A Magnetic Tape System for Recording and Reproducing Standard FCC Color Television Signals”      | Sept. | 330  |
| Janes, R. B. (Coauthor)—“Recent Improvements in the 21AXP22 Color Kinescope”   | June  | 143  |
| Kaus, P. E.—“Effect of Magnetic Deflection on Electron Beam Convergence”   | June  | 168  |
| Kennedy, R. C.—“Pedestal Processing Amplifier for Television Studio Operation”   | June  | 297  |
| “Test Signal for Measuring ‘On-The-Air’ Color-Television System Performance”   | Dec.  | 553  |
| Knechtli, R. C. (Coauthor)—“Kinescope Electron Guns for Producing Noncircular Spots”   | June  | 275  |

|  | ISSUE PAGE |
|--|------------|
| Knechtli, R. C. (Coauthor)—“Performance and Design of Low-Noise Guns for Traveling-Wave Tubes”                             | Sept. 410  |
| Knoll, M. (Coauthor)—“Viewing Storage Tubes for Large Displays”  | Dec. 503   |
| Kolar, R. F.—“Fields in Imperfect Electromagnetic Anechoic Chambers”   | Sept. 393  |
| Kroemer, H.—“The Apparent Contact Potential of a Pseudo-Abrupt P-N Junction”   | Dec. 515   |
| Linder, E. G. (Coauthor)—“The Electron-Voltaic Effect in Germanium and Silicon P-N Junctions”                              | Mar. 100   |
| Loferski, J. J. (Coauthor)—“The Electron-Voltaic Effect in Germanium and Silicon P-N Junctions”                            | Mar. 100   |
| May, E. G. (Coauthor)—“Miniature Loudspeakers for Personal Radio Receivers”  | Mar. 57    |
| Moore, A. R. (Coauthor)—“Surface Treatment of Silicon for Low Recombination Velocity”                                      | Mar. 5     |
| Morgan, A. R. (Coauthor)—“A Magnetic Tape System for Recording and Reproducing Standard FCC Color Television Signals”      | Sept. 330  |
| Morgan, J. M. (Coauthor)—“Transistorized Television Cameras Using the Miniature Vidicon”                                   | Dec. 469   |
| Mueller, C. W. (Coauthor)—“Uniform Planar Alloy Junctions for Germanium Transistors”                                       | Mar. 46    |
| Nelson, H. (Coauthor)—“Surface Treatment of Silicon for Low Recombination Velocity”  | Mar. 5     |
| O’Connell, J. H. (Coauthor)—“A Variable-Capacitance Germanium Junction Diode for UHF”                                      | Mar. 68    |
| Olson, H. F. (Coauthor)—“A Magnetic Tape System for Recording and Reproducing Standard FCC Color Television Signals”       | Sept. 330  |
| “Bigradient Uniaxial Microphone”   | Dec. 522   |
| Pan, W. Y. (Coauthor)—“Analytical Approaches to Local Oscillator Stabilization”  | Dec. 534   |
| Peterson, D. W. (Coauthor)—“A Method of Predicting the Coverage of a Television Station”                                   | Dec. 571   |
| Pike, W. S. (Coauthor)—“Transistorized Television Cameras Using the Miniature Vidicon”                                     | Dec. 469   |
| Plumlee, R. H.—“Electrolytic Transport Phenomena in the Oxide Cathode”   | June 190   |
| “The Electron Donor Centers in the Oxide Cathode”  | June 231   |
| Preston, J. (Coauthor)—“Miniature Loudspeakers for Personal Radio Receivers”   | Mar. 57    |
| “Bigradient Uniaxial Microphone”   | Dec. 522   |
| Rappaport, P. (Coauthor)—“The Electron-Voltaic Effect in Germanium and Silicon P-N Junctions”                              | Mar. 100   |
| Rotow, A. A.—“Image Orthicon for Pickup at Low Light Levels”   | Sept. 425  |
| Schroeder, J. O.—“A Video Automatic-Gain-Control Amplifier”  | Dec. 558   |
| Shapiro, L. (Coauthor)—“High-Resolution Flying-Spot Scanner for Graphic Arts Color Applications”                           | Sept. 313  |
| Stone, R. P. (Coauthor)—“Viewing Storage Tubes for Large Displays”   | Dec. 503   |
| Woodward, J. G. (Coauthor)—“A Magnetic Tape System for Recording and Reproducing Standard FCC Color Television Signals”    | Sept. 330  |
| Woodward, O. M., Jr. (Coauthor)—“The Omniguide Antenna—An Omnidirectional Waveguide Array for UHF-Television Broadcasting” | Mar. 13    |
| Zenel, J. A. (Coauthor)—“A Magnetic Tape System for Recording and Reproducing Standard FCC Color Television Signals”       | Sept. 330  |

